

การศึกษาชิ้นส่วนพันทางสำหรับแผ่นรับแรงดัด



นายสุวัฒน์ เสงยศมาก

สถาบันวิทยบริการ
จุฬาลงกรณ์มหาวิทยาลัย

วิทยานิพนธ์ฉบับนี้เป็นส่วนหนึ่งของการศึกษาตามหลักสูตรปริญญาวิศวกรรมศาสตรมหาบัณฑิต

สาขาวิชาวิศวกรรมโยธา ภาควิชาวิศวกรรมโยธา

คณะวิศวกรรมศาสตร์ จุฬาลงกรณ์มหาวิทยาลัย

ปีการศึกษา 2544

ISBN 974-03-1696-4

ลิขสิทธิ์ของจุฬาลงกรณ์มหาวิทยาลัย

A STUDY ON HYBRID FINITE ELEMENTS FOR PLATE BENDING



Mr. Supatana Hengyotmark

สถาบันวิทยบริการ
จุฬาลงกรณ์มหาวิทยาลัย

A Thesis Submitted in Partial Fulfillment of the Requirements
for the Degree of Master of Engineering in Civil Engineering
Department of Civil Engineering
Faculty of Engineering
Chulalongkorn University
Academic Year 2001
ISBN 974-03-1696-4

Thesis Title A Study on Hybrid Finite Elements for Plate Bending
By Mr.Supatana Hengyotmark
Field of Study Civil Engineering
Thesis Advisor Asst. Prof. Dr.Roengdeja Rajatabhothi

Accepted by the Faculty of Engineering, Chulalongkorn University in Partial
Fulfillment of the Requirements for the Master's Degree

_____ Dean of Faculty of Engineering
(Professor Somsak Panyakeow, D.Eng.)

THESIS COMMITTEE

_____ Chairman
(Professor Thaksin Thepchatri, Ph.D.)

_____ Thesis Advisor
(Assistant Professor Roengdeja Rajatabhothi, Ph.D.)

_____ Member
(Assistant Professor Teerapong Senjuntichai, Ph.D.)

สถาบันวิทยบริการ
จุฬาลงกรณ์มหาวิทยาลัย

สุพัฒน์ เสงขมมาก : การศึกษาชิ้นส่วนพันทางสำหรับแผ่นรับแรงดัด (A STUDY ON HYBRID FINITE ELEMENTS FOR PLATE BENDING) อ. ที่ปรึกษา : ผศ. ดร.เรืองเดชา รัชตโพธิ์
77 หน้า. ISBN: 974-03-1696-4.

ในระเบียบวิธีไฟไนต์เอลิเมนต์นั้น นอกจากระเบียบวิธีการกระจัดแล้ว ระเบียบวิธีพันทางถือเป็นระเบียบวิธีหนึ่งที่ทำให้ได้ชิ้นส่วนที่มีประสิทธิภาพ การกระจัดและความเค้นถูกสมมติขึ้นพร้อมกันและเป็นอิสระจากกันเพื่อใช้ในการสร้างชิ้นส่วน วิธีการที่เป็นระบบและมีประสิทธิภาพในการสร้างชิ้นส่วนในระเบียบวิธีไฟไนต์เอลิเมนต์นั้น คือ วิธีที่ใช้หลักการแปรผันของสมการพลังงาน การศึกษานี้ได้ใช้สมการพลังงานของเฮลลิงเกอร์-ไรส์เนอร์ (Hellinger-Reissner Energy Functional) และสมการพลังงานดังกล่าวที่ถูกดัดแปรแล้วในการสร้างชิ้นส่วนพันทาง ชิ้นส่วนพันทางบางชิ้นได้ถูกสร้างขึ้นและเปรียบเทียบประสิทธิภาพกับชิ้นส่วนพันทางอื่นที่ถูกสร้างขึ้นในอดีต

ในการเลือกสนามความเค้นนั้นได้ใช้วิธีการแยกโหมดของความเค้นเป็นแนวทาง ซึ่งจะทำได้ชิ้นส่วนที่ปราศจากโหมดการบิดรูปแบบไร้พลังงาน การสมมติจำนวนของความเค้นสามัญที่มากเกินไปนั้นจะทำให้ได้ชิ้นส่วนที่แข็งแรงเกินไป และยังทำให้เสียเวลาในการคำนวณมากขึ้นด้วย

ในการศึกษานี้ได้ทำการพิสูจน์วิธีการปรับปรุงชิ้นส่วนโดยใช้ทฤษฎีสมดุล (penalty-equilibrium) พบว่า วิธีนี้พยายามกำจัดโหมดของความเค้นที่ไม่สมดุลออกจากกระบวนการสร้างชิ้นส่วน ซึ่งจะเป็นการเปิดโอกาสให้เกิดโหมดการบิดรูปแบบไร้พลังงานขึ้นในชิ้นส่วนได้

ในการทดสอบประสิทธิภาพของชิ้นส่วนนั้น ได้ทำการทดสอบกับแผ่นรับแรงดัดหลายประเภท ได้แก่ แผ่นรับแรงดัดรูปสี่เหลี่ยม แผ่นรับแรงดัดรูปวงกลม และแผ่นรับแรงดัดรูปสี่เหลี่ยมขนมเปียกปูน โดยแต่ละการทดสอบจะขึ้นอยู่กับเงื่อนไขขอบ และชนิดของน้ำหนักบรรทุก ซึ่งในการศึกษานี้ได้ทำการทดสอบประสิทธิภาพของชิ้นส่วนในด้านการลู่เข้าของการกระจัดและแรงดัด การยึดเนื่องจากแรงเฉือน รวมถึงความยืดหยุ่นของชิ้นส่วนด้วย

จากผลของการทดสอบพบว่า ความแม่นยำของการกระจัดมีมากกว่าร้อยละ 95 ในชิ้นส่วนส่วนใหญ่ที่มีการแบ่งชิ้นส่วนละเอียดปานกลาง และจะไม่ขึ้นกับการเปลี่ยนแปลงความหนา หรืออัตราส่วนความกว้างต่อความยาวของชิ้นส่วน ชิ้นส่วนที่ดีบางชิ้นส่วนนั้นสามารถให้ความแม่นยำของการกระจัดมากกว่าร้อยละ 99 แม้ว่าจะเกิดการยึดเนื่องจากแรงเฉือนขึ้น ส่วนความแม่นยำของความเค้นนั้นมีความมากกว่าร้อยละ 90 อย่างไรก็ตามพบว่าชิ้นส่วนทั้งหมดขาดความยืดหยุ่นอยู่บ้าง

จากการเปรียบเทียบประสิทธิภาพโดยรวมแล้ว ในบรรดาชิ้นส่วนที่นำมาเปรียบเทียบทั้งหมดพบว่า ชิ้นส่วน HBP1 และ HBP2 ที่นำเสนอ ให้ประสิทธิภาพที่ดีที่สุดในการทดสอบทุกด้าน โดยเฉพาะด้านการยึดเนื่องจากแรงเฉือน

ภาควิชา _____ วิศวกรรมโยธา _____ ลายมือชื่อนิสิต _____
สาขาวิชา _____ วิศวกรรมโยธา _____ ลายมือชื่ออาจารย์ที่ปรึกษา _____
ปีการศึกษา _____ 2544 _____

4270611221 : MAJOR CIVIL ENGINEERING

KEY WORD : HYBRID FINITE ELEMENT / PLATE BENDING

SUPATANA HENGYOTMARK : A STUDY ON HYBRID FINITE ELEMENTS FOR PLATE BENDING. THESIS ADVISOR: ASST. PROF. ROENGDEJA RAJATABHOTHI, Ph.D. 77 pp. ISBN: 974-03-1696-4

Alternative to the conventional finite element method, there is another version named hybrid finite element in which the displacement fields and the stress fields are assumed independently and simultaneously for the element stiffness formulation. The method regarded as systematic and efficient in formulating the stiffness is the variation of the energy functional. The Hellinger-Reissner energy functional and its modified version are employed in the present study. Numerous hybrid plate elements based on these energy functionals have been proposed in the past. Some four-node quadrilateral elements with interior displacement assumptions were formulated.

The stress classification method was used as a guideline in order to obtain the stress matrix. The stress matrix, which is free from kinematic deformation modes in the element stiffness, can easily be obtained. Numerical studies confirmed that using too many stress parameters in the assumed stresses would result in an overstiff model and more computational effort.

Proof of the optimization method through the penalty-equilibrium matrix showed that a penalty constant tends to eliminate the stress modes which do not satisfy the equilibrium equations from the element stiffness formulation - as if those stress modes are not present in the stress matrix. Therefore, kinematic deformation modes may be introduced into an element this way.

Various types of plates with different boundary conditions and loading such as square plates, circular plates and thin rhombic plates were tested. Tests were concentrated on convergence of displacement and moment, shear-locking as well as invariance property.

Tests on accuracy of displacement showed that most of the elements gave more than 95 percent accuracy regardless of variation in thickness and aspect ratio for moderate mesh refinement. Some good elements gave more than 99 percent accuracy despite some shear-locking. Accuracy of moments averaged more than 90 percent. All elements, however, lack invariance to some degree.

Comparison of the overall performance of the hybrid elements studied indicates that the element HBP1 and HBP2 are the most efficient among those elements compared. These versatile elements perform very well in all tests, especially, the shear-locking test.

Department Civil Engineering
 Field of study Civil Engineering
 Academic year 2001

Student's signature _____
 Advisor's signature _____

Acknowledgements

I would like to express my deepest appreciation to Dr.Roengdeja Rajatabhothi for his continuous guidance and generous help throughout this study. I also want to extend my gratitude to Dr.Thaksin Thepchatri and Dr.Teerapong Senjuntichai for their assistance while serving on the thesis committee.

Special thanks are due to Rachid Touzani for the valuable OFELI, an Object Finite Element Library, used in the HybridFE program.

Finally, I would like to express my deep gratitude to my beloved parents for their endless support and love. Thanks are also extended to my friends for their continued encouragement.



สถาบันวิทยบริการ
จุฬาลงกรณ์มหาวิทยาลัย

Table of Contents

	Page
Abstract in Thai	iv
Abstract in English	v
Acknowledgements	vi
Table of Contents	vii
List of Tables	ix
List of Figures	x
Chapter I : Introduction	
1.1 General	1
1.2 Literature Review	2
1.3 Objectives of Present Study	9
1.4 Scope of Present Study	9
Chapter II : Theoretical Considerations	
2.1 Bending of Flat Plates	10
2.1.1 Kirchhoff Plate Theory	12
2.1.2 Mindlin Plate Theory	13
2.2 Multifield Variational Principles	16
2.3 Hybrid Finite Element Formulation	19
Chapter III : Hybrid Plate Elements	
3.1 Determination of Desirable Stress Matrix	22
3.2 Optimization with Penalty-Equilibrium Approach	24
3.3 Hybrid Plate Elements Considered	25
3.3.1 Spilker Elements	25
3.3.2 Dong Element	27
3.3.3 Henshell Element	28
3.3.4 Hamhim Elements	28
3.3.5 Proposed Elements	29
3.4 Evaluation of Element Stiffness Matrix	31
Chapter IV : Efficiency of Hybrid Plate Elements	
4.1 Shortcomings and Limitations of Optimization Method	32
4.2 Test for Convergence	37
4.2.1 Rectangular Plate	37
4.2.2 Circular Plate	42
4.2.3 Thin Rhombic Plate	46
4.2.4 Cantilever Plate	47
4.3 Test for Shear-Locking Effect	49
4.4 Test on Element Aspect Ratio	53
4.5 Test for Invariance	55
Chapter V : Conclusions	56
References	58

Table of Contents *(continued)*

	Page
Appendix A : Details of Element Stiffness Formulation	
A.1 Stress-Strain Approach _____	62
A.2 Moment-Curvature Approach _____	68
Appendix B : Program HybridFE	
B.1 Input File Format _____	70
B.2 Element Stiffness Matrix Subroutine _____	71
B.3 Main Fragment of Code in Analysis Task _____	75
Biography _____	77



สถาบันวิทยบริการ
จุฬาลงกรณ์มหาวิทยาลัย

List of Tables

		Page
Table 1.2-1	Stress parameters and corresponding deformation modes for 4-node quadrilateral element _____	7
Table 1.2-2	Stress modes after classification into mode groups _____	8
Table 2.1-1	Governing equations used in plate theories : Kirchhoff and Mindlin Plate theories _____	15
Table 2.2-1	Flow diagram for variational principles in small displacement theory of elastostatics _____	17
Table 3.3.1-1	Mode groups for Spilker's assumed stresses after classification _____	27
Table 3.3.5-1	Mode groups for proposed assumed stresses after classification _____	30
Table 4.2.1-1	Corresponding constraints of forces and displacements with respect to various edge conditions _____	38

List of Figures

	Page
Figure 1.2-1 Small perturbation applied to element geometry _____	4
Figure 2.1-1a Stresses acting on a differential element of a homogeneous, linearly elastic plate _____	10
Figure 2.1-1b The same differential element viewed normal to the plate _____	10
Figure 2.1-2a Differential element of a thin plate before loading _____	12
Figure 2.1-2b After loading: deformations associated with Kirchhoff plate theory _____	12
Figure 2.1-3 Differential plate element after loading, analogous to Fig. 2.1-2b, but with transverse shear deformation allowed _____	13
Figure 4.2.1-1 A square plate for convergent tests _____	38
Figure 4.2.1-2 Convergence of central deflections of square plate with SS2-UL _	39
Figure 4.2.1-3 Convergence of central deflections of square plate with SS2-CL _	39
Figure 4.2.1-4 Convergence of central deflections of square plate with C-UL __	40
Figure 4.2.1-5 Convergence of central deflections of square plate with C-CL __	40
Figure 4.2.1-6 Convergence of central moments of square plate with SS2-UL __	41
Figure 4.2.1-7 Convergence of central moments of square plate with C-UL ____	41
Figure 4.2.2-1 Three meshes for quadrant of a circular plate _____	42
Figure 4.2.2-2 Convergence of central deflections of circular plate with SS1-UL 43	43
Figure 4.2.2-3 Convergence of central deflections of circular plate with SS1-CL 43	43
Figure 4.2.2-4 Convergence of central deflections of circular plate with C-UL __ 44	44
Figure 4.2.2-5 Convergence of central deflections of circular plate with C-CL __ 44	44
Figure 4.2.2-6 Convergence of central moments of circular plate with SS1-UL _ 45	45
Figure 4.2.2-7 Convergence of central moments of circular plate with C-CL ____ 45	45
Figure 4.2.3-1 Simply supported thin rhombic plate _____	46
Figure 4.2.3-2 Convergence of central deflections of rhombic plate with SS1-UL 46	46
Figure 4.2.3-3 Convergence of central moments of rhombic plate with C-UL __ 47	47

List of Figures (continued)

	Page
Figure 4.2.4-1a Cantilever plate (beam) subjected to moment _____	47
Figure 4.2.4-1b Cantilever plate (beam) subjected to tip load _____	47
Figure 4.2.4-2 Convergence of tip deflection of cantilever plate subjected to point load _____	48
Figure 4.2.4-3 Convergence of tip deflection of cantilever plate subjected to end moment _____	48
Figure 4.3-1 Effect of plate thickness on center deflection of square plate with SS2-UL ($N_{el} = 4$) _____	49
Figure 4.3-2 Effect of plate thickness on center deflection of square plate with SS2-CL ($N_{el} = 4$) _____	50
Figure 4.3-3 Effect of plate thickness on center deflection of square plate with C-UL ($N_{el} = 4$) _____	50
Figure 4.3-4 Effect of plate thickness on center deflection of square plate with C-CL ($N_{el} = 4$) _____	51
Figure 4.3-5 Effect of plate thickness on center deflection of circular plate with SS2-UL ($N_{el} = 48$) _____	51
Figure 4.3-6 Effect of plate thickness on center deflection of circular plate with SS2-CL ($N_{el} = 48$) _____	52
Figure 4.3-7 Effect of plate thickness on center deflection of circular plate with C-UL ($N_{el} = 48$) _____	52
Figure 4.3-8 Effect of plate thickness on center deflection of circular plate with C-CL ($N_{el} = 48$) _____	53
Figure 4.4-1 Square plate for testing on element aspect ratio ($N_{el} = 4$) _____	53
Figure 4.4-2 Effect of aspect ratio on center deflection of square plate with SS2-UL ($N_{el} = 4$) _____	54
Figure 4.4-3 Effect of aspect ratio on center deflection of square plate with SS2-CL ($N_{el} = 4$) _____	54
Figure 4.5-1 Mesh for testing invariance of SS2-UL element _____	55
Figure 4.5-2 Effect on mesh orientation with SS1-UL _____	55

Chapter I

Introduction

1.1 General

In the early 1960s, there were two types of rationally constructed finite elements in structural and solid mechanics. These may be formulated by using methods based, respectively, on the principles of stationary potential energy and complementary energy. The resulting elements are the so-called *compatible elements* for which the assumed displacements are compatible both within each element and along the interelement boundary and the *equilibrium elements* for which the assumed stresses are equilibrated within each element and the tractions reciprocated along the interelement boundary.

Obviously, one of the most popular and efficient methods in finite element formulation is to employ the *Variational Principles*. Due to the wide use of the finite element method along with the elaborate development of the variational principles, the finite element method can be then formulated by relaxing the continuity requirements along the interelement boundaries.

The combination of different variational principles and different boundary continuity conditions yields numerous types of approximate models^[1]. Such *multifield* variational principles were treated in a text by Washisu^[2]. A model in which compatible displacement functions are assumed along the interelement boundary in addition to equilibrating stress fields assumed within each element is the *Hybrid Model*. However, in later development using *Lagrange multipliers*^[2], compatibility of displacement functions or equilibrium of the assumed stress fields may not be satisfied anymore.

In comparing elements, Pian and Tong^[1] concluded that the equilibrium and compatible elements will provide, respectively, the upper and lower bounds for the strain energy. Also, the assumed stress hybrid element will yield a structure which is more flexible than the compatible element of the same boundary displacement approximation and more rigid than the equilibrium element of the same interior stress approximation. Results have shown that several hybrid elements can provide more accurate results than both the compatible and equilibrium elements.

The desirable characteristics of an ideal finite element^[9] are that it should be free from zero-energy or kinematic deformation modes, invariant with respect to the reference coordinates, efficient in computer implementation, not overly rigid, as well as accurate with regard to stress calculation. The conventional assumed displacement methods generally satisfy the first three items listed above but usually not the last two. For hybrid elements several conditions for the assumed stress terms may be considered in order to meet all or some of the items.

This present study will develop an efficient hybrid finite element satisfying most of the characteristics of an ideal element. The selection of the assumed displacement and stress fields will aim at improving the element properties and avoiding some undesirable locking problems.

1.2 Literature Review

The term ‘*hybrid element*’ in this study means a *hybrid stress element* for which the displacement and stress fields are assumed independently. Such an element was first developed by Pian^[4]. This element was formulated based on assumed equilibrating stresses within the element and compatible displacements along the interelement boundary instead of displacement within the element. It was found that the results converge more rapidly than using a compatible element. Initially, it was recognized by its advantage of constructing plate elements because it is not an easy task to construct, within an element, a compatible displacement field in terms of nodal displacements while it is simple to express boundary displacements in terms of nodal displacements. However, there is another version of the hybrid element named the *hybrid displacement element*^[5]. This element is based on independently assumed displacements in the interior and along the boundary of the element. It is interesting to note that only displacement fields are involved in the formulation.

In its formulation the first hybrid element constructed by Pian^[4] employs the complementary energy functional of the form

$$\Pi_C = \int_V \frac{1}{2} \boldsymbol{\sigma}^T \mathbf{S} \boldsymbol{\sigma} dV - \int_{S_u} \mathbf{T}^T \bar{\mathbf{u}} dS \quad (1.2-1)$$

The assumed stress $\boldsymbol{\sigma}$ are expressed in the form

$$\boldsymbol{\sigma} = \mathbf{P} \boldsymbol{\beta} \quad (1.2-2)$$

where \mathbf{P} is the stress matrix and $\boldsymbol{\beta}$ are stress parameters. The boundary tractions \mathbf{T} are the stresses evaluated along the boundary. The displacements along the boundary are

$$\bar{\mathbf{u}} = \mathbf{L} \mathbf{q} \quad (1.2-3)$$

where \mathbf{L} are the interpolation functions along the boundary of an element and \mathbf{q} the nodal displacements.

According to the constraint of the principle of complementary energy, the stresses in an element must be in equilibrium. Thus

$$\partial \boldsymbol{\sigma} = \mathbf{0} \quad (1.2-4)$$

where ∂ is a differential operator matrix.

One of the criteria, and only the one at that time, to obtain the assumed stresses is utilizing the equilibrium constraint shown in Eq. 1.2-4. The possible stress matrices the satisfy that constraint are, for example,

$$\mathbf{P} = \begin{bmatrix} 1 & \cdot & \cdot & y & \cdot \\ \cdot & 1 & \cdot & \cdot & \cdot \\ \cdot & \cdot & 1 & \cdot & x \end{bmatrix}, \mathbf{P} = \begin{bmatrix} 1 & \cdot & \cdot & y & \cdot & x & \cdot \\ \cdot & 1 & \cdot & \cdot & x & \cdot & y \\ \cdot & \cdot & 1 & \cdot & \cdot & -y & -x \end{bmatrix}, \text{ and so on.} \quad (1.2-5)$$

Substitution of Eqs. 1.2-2, 1.2-3 into Eq. 1.2-1, yields

$$\Pi_C = \frac{1}{2} \boldsymbol{\beta}^T \mathbf{H} \boldsymbol{\beta} - \boldsymbol{\beta}^T \mathbf{G} \mathbf{q} \quad (1.2-6)$$

where

$$\mathbf{H} = \int_V \mathbf{P}^T \mathbf{S} \mathbf{P} dV, \quad \mathbf{G} = \int_{S_u} \mathbf{P}^T \mathbf{L} dS \quad (1.2-7)$$

From variation with respect to $\boldsymbol{\beta}$, within the element level,

$$\begin{aligned} \mathbf{H} \boldsymbol{\beta} &= \mathbf{G} \mathbf{q} \\ \text{or} \quad \boldsymbol{\beta} &= \mathbf{H}^{-1} \mathbf{G} \mathbf{q} \end{aligned} \quad (1.2-8)$$

Thus, the strain energy term of Eq. 1.2-6 becomes

$$U = \frac{1}{2} \mathbf{q}^T (\mathbf{G}^T \mathbf{H}^{-1} \mathbf{G}) \mathbf{q} \quad (1.2-9)$$

We also know that the strain energy in an element is in the form

$$U = \frac{1}{2} \mathbf{q}^T \mathbf{k} \mathbf{q} \quad (1.2-10)$$

where \mathbf{k} is the element stiffness matrix. Hence, from Eq. 1.2-9, the element stiffness matrix obtained from the hybrid approach is

$$\mathbf{k} = \mathbf{G}^T \mathbf{H}^{-1} \mathbf{G} \quad (1.2-11)$$

Tong and Pian^[7] suggested that for better accuracy, the stress and displacement approximations must be improved properly and simultaneously. Besides, the total number of stress parameters must be greater than or equal to the total number of degrees of freedom in order to guarantee the existence of solutions.

Since the development of the various variational principles, several assumed stress hybrid elements have been constructed by using the Hellinger-Reissner principle or its derived versions. Equilibrium of the assumed stresses and compatibility of the assumed displacements are no longer satisfied. Pian and Chen^[8,9] proposed a new and more general method for formulating the assumed stress hybrid element. An extended Hellinger-Reissner principle is taken into consideration.

$$\Pi_R = \int_V \left[-\frac{1}{2} \boldsymbol{\sigma}^T \mathbf{S} \boldsymbol{\sigma} - \boldsymbol{\sigma}^T (\mathbf{D} \mathbf{u}_q) - (\mathbf{D}^T \boldsymbol{\sigma})^T \mathbf{u}_\lambda \right] dV \quad (1.2-12)$$

The stress equilibrium conditions, the third term on the right-hand side of the above equation, are then introduced through the application of constraint conditions with internal displacements as *Lagrange multipliers*. Therefore, the stresses are not necessarily equilibrated. Incompatible displacements are used and the internal displacements are separated into two parts – compatible part \mathbf{u}_q and additional part \mathbf{u}_λ .

$$\mathbf{u} = \mathbf{u}_q + \mathbf{u}_\lambda \quad (1.2-13)$$

This new method opens up the possibility of using natural coordinates for the assumed stresses. This is because it is impossible to express the assumed stresses in natural coordinates which exactly satisfy equilibrium conditions pointwise. The accuracy of such an element will not be affected very much when the element shape is distorted from regular geometry.

Similar to the assumed displacement finite element formulation, the displacements for the hybrid element can be uniquely defined when the nodal displacements for the element are chosen. But the choice of assumed stresses was left open in this method. At first, assumed stress hybrid elements evolved under a strict condition of equilibrium. Later, stress relaxation under certain conditions such as the satisfaction of equilibrium conditions in a variational or integral sense within each element was allowed^[8]. A suggested scheme^[10,11] is based on the initial choice of stress terms to be unrestrained with complete polynomials expressed in natural coordinates,

$$\begin{Bmatrix} \sigma_x \\ \sigma_y \\ \tau_{xy} \end{Bmatrix} = \begin{bmatrix} 1 & \xi & \eta & \cdot & \cdot & \cdot & \cdot & \cdot & \cdot \\ \cdot & \cdot & \cdot & 1 & \xi & \eta & \cdot & \cdot & \cdot \\ \cdot & \cdot & \cdot & \cdot & \cdot & \cdot & 1 & \xi & \eta \end{bmatrix} \begin{Bmatrix} \beta_1 \\ \vdots \\ \beta_9 \end{Bmatrix} \quad (1.2-14)$$

and on adding internal displacements such that the corresponding strain terms are also complete and consistent with the assumed stresses,

$$\mathbf{u} = \mathbf{u}_q + \mathbf{u}_\lambda \quad (1.2-13)$$

where

$$\mathbf{u}_q = \sum_{i=1}^4 (1 + \xi_i \xi)(1 + \eta_i \eta) \begin{Bmatrix} u_i \\ v_i \end{Bmatrix}, \quad \mathbf{u}_\lambda = \begin{bmatrix} 1 - \xi^2 & 1 - \eta^2 & \cdot & \cdot \\ \cdot & \cdot & 1 - \xi^2 & 1 - \eta^2 \end{bmatrix} \begin{Bmatrix} \lambda_1 \\ \vdots \\ \lambda_4 \end{Bmatrix} \quad (1.2-14)$$

The additional displacements are used as Lagrange multipliers to enforce the stress equilibrium constraint. This scheme utilizes a stress equilibrium constraint of Eq. 1.2-12 to obtain the stress matrix which condenses out the dependent stress parameters. The condition in doing this is

$$I = \int_V (\mathbf{D}^T \boldsymbol{\sigma})^T \mathbf{u}_\lambda dV \quad (1.2-15)$$

After taking the first variation with respect to λ_i , only two independent relations are obtained. To obtain the other two remaining relations, for the sake of mathematics, a small perturbation method is used.

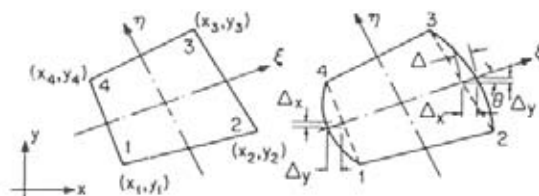


Figure 1.2-1 Small perturbation applied to element geometry.

The stresses after condensation become

$$\begin{Bmatrix} \sigma_x \\ \sigma_y \\ \tau_{xy} \end{Bmatrix} = \begin{bmatrix} 1 & \cdot & \cdot & a_1^2 \eta & a_3^2 \xi \\ \cdot & 1 & \cdot & b_1^2 \eta & b_3^2 \xi \\ \cdot & \cdot & 1 & a_1 b_1 \eta & a_3 b_3 \xi \end{bmatrix} \begin{Bmatrix} \beta_1 \\ \vdots \\ \beta_5 \end{Bmatrix} \quad (1.2-16)$$

This element has been shown to have desirable properties. By using natural coordinates, the resulting elements can be made less sensitive to geometrical distortion and by using complete polynomials for the stress terms, the element can be made basically invariant.

Because of the complexity in such a scheme with a small perturbation of the element geometry, Pian and Wu^[12] proposed a new concept to determine the constraint conditions for the assumed stresses in the hybrid formulation. Consequently, any geometrical perturbation is no longer needed. Internal incompatible displacements are added within each element in order to maintain completeness and internal stresses are interpolated in isoparametric coordinates. The stress distribution is obtained through a so-called *optimization condition (OPC)*,

$$\oint_{\partial V^e} \sigma_h^T \mathbf{n}^T \delta \mathbf{u}_\lambda dS = 0 \quad (1.2-17)$$

which requires a vanishing virtual work along the element boundary due to linear and higher order stress terms and the additional incompatible displacements. It has been shown that the resulting stress terms based on such a condition will lead to better element properties. For the 4-node plane problem if the incompatible displacements are the same as that used by Pian and Sumihara^[10], then this would result in the same element.

Recently, Wu and Cheung^[13] classified the method to obtain an optimal hybrid stress element into two approaches: the pre- and post-treatment. In the pre-treatment approach, the improvement of the element performance is realized by using the optimal stress fields that satisfied the optimization conditions (OPC).^[12] In the post-treatment approach, the penalty-equilibrating approach has been suggested, in which neither the modification of the initial stresses nor the introduction of the additional displacements is required for the improvement of many existing hybrid elements. Ignoring the effect of distributed loads within an element, the equilibrium equation can be written as

$$\partial \sigma = \mathbf{0} \quad (1.2-4)$$

The element energy functional Π_R^e after introducing a penalty-equilibrium becomes

$$\Pi_R^e(\sigma, \mathbf{u}) = \Pi_R^e - \alpha \int_{V^e} (\partial \sigma)^T (\partial \sigma) dV \quad (1.2-18)$$

where α is a penalty factor of large positive number. The equilibrium constraints will be satisfied when $\alpha \rightarrow \infty$

The Mindlin-Reissner plate theory has been used to develop efficient and reliable plate bending elements. Only C^0 -continuity of displacement is required. However, in developing Mindlin-Reissner plate elements, the well-known shear locking effect is often encountered. As plate thickness is decreased, the element overstiffens rapidly.

To demonstrate the shear locking effect^[14], for simplicity, the potential energy functional Π_p of simple beam can be written as

$$\Pi_p = \frac{1}{2} \frac{Et^3}{L} \left[\int_0^1 \frac{1}{12} \left(\frac{d\phi}{dx} \right)^2 dx + \frac{G\beta}{E} \left(\frac{L}{t} \right)^2 \int_0^1 \left(\phi + \frac{dw}{dx} \right)^2 dx \right] - W \quad (1.2-19)$$

The first and second integrals represent the bending and the transverse shear strain energy, respectively. As the beam becomes thinner, the magnitude of the transverse shear strain energy is dominant. This in turn causes an over stiff element.

In displacement models, many approaches have been proposed to overcome shear-locking effects such as using discrete Kirchhoff assumption and uniform or selective reduced integration. This scheme causes less contribution of the shear strain energy term in the element stiffness formulation because of using improper quadrature rules. However, the application of uniform or selective reduced integration very often results in the development of kinematic deformation modes.

By contrast, hybrid approach appears to be more attractive in developing thin and moderate thick plate elements without shear locking effects. In the early hybrid elements^[14-16] this was achieved by using appropriate assumed stress fields. Lee and Pian^[14] have shown that hybrid elements are identical to the reduced integration elements and the results are reliable and not sensitive to thickness reduction. Spilker and Munir^[15] presented a rationale for the selection of assumed stress fields. Such a rationale was suggested, motivated by the form of the Euler equations in the thin plate limit, to avoid locking in the thin plate limit and to avoid kinematic deformation modes. Various 4-node quadrilateral hybrid elements^[15] were constructed as well as 8-node hybrid elements.^[16] Note that all the hybrid plate elements above require the stress equilibrium conditions to be satisfied locally at the element level.

The stress equilibrium constraints, however, seem to limit the development of hybrid or hybrid plate elements. By introducing internal incompatibles and relaxing the stress equilibrium constraints within the element as well as using natural coordinates, an efficient hybrid plate element can be formulated^[8-10].

Wanji and Cheung^[17] proposed a new functional which includes stresses, strains and displacements. The displacements and stresses were further decoupled into two parts. This approach could construct not only hybrid elements, but also displacement-based elements. This reveals the relationship between these two element types as pointed out by Pian and Tong^[18].

Cheung and Wanji^[19] applied a new functional^[17] to Mindlin-Reissner plate elements. The locking phenomenon was eliminated by introducing internal

displacement parameters and by adopting a method for constraining the shear strains. Invariant elements free from kinematic deformation modes were obtained.

Dong and his associates^[20] utilized a stress optimization condition (OPC)^[12] to develop an efficient and reliable 8-node serendipity Mindlin-Reissner plate element. The stress optimization condition was used to select the appropriate stress interpolations. Internal incompatible displacements were used to eliminate shear locking in the thin plate limit as well. The resulting element was accurate in displacements and stresses, and insensitive to mesh distortion. A similar scheme was also used in developing an efficient 4-node quadrilateral Mindlin-Reissner plate element^[21].

Ever since the development of the assumed stress hybrid model, some mathematical basis for the stability of the numerical solution of the finite element model has been established and a number of approaches for obtaining the optimal stress modes have been proposed. Pian and Tong^[1] presented a *necessary condition* to avoid kinematic deformation modes,

$$m' \geq n - r \quad (1.2-20)$$

in which m' is the total number of independent β -stress parameters, n the total number of nodal displacements, and r the number of rigid-body modes. A rank deficiency of the element stiffness matrix is a sign of the appearance of a kinematic deformation mode in the element. Pian and Chen^[22] proposed a systematic procedure for the choice of the necessary assumed stresses such that kinematic deformation modes will not appear by matching one stress mode individually with one strain mode. For a 4-node quadrilateral element, the displacements u and v are expressed in terms of five basic displacement modes

$$\begin{aligned} u &= \alpha_1 x + \alpha_3 y + \alpha_4 xy \\ v &= \alpha_3 x + \alpha_2 y + \alpha_5 xy \end{aligned} \quad (1.2-21)$$

The deformation energy due to the assumed stresses and displacements is given by

$$I_i = \int_{-1}^1 \int_{-1}^1 \sigma_i \varepsilon_i dx dy \quad (1.2-22)$$

To guarantee that I_i does not vanish, the integrand must produce an even function. Thus the stress modes corresponding to the displacement modes are shown in Table 1.2-1

Table 1.2-1 Stress parameters and corresponding deformation modes for 4-node quadrilateral element.

	Const.	x	y
σ_x	β_1 $u = \alpha_1 x$		β_4 $u = \alpha_4 xy$
σ_y	β_2 $v = \alpha_2 y$	β_5 $v = \alpha_5 xy$	
τ_{xy}	β_3 $u = \frac{\alpha_3}{2} y, v = \frac{\alpha_3}{2} x$		

The stresses in Table 1.2-1 can be written in matrix form as

$$\begin{Bmatrix} \sigma_x \\ \sigma_y \\ \tau_{xy} \end{Bmatrix} = \begin{bmatrix} 1 & \cdot & \cdot & y & \cdot \\ \cdot & 1 & \cdot & \cdot & x \\ \cdot & \cdot & 1 & \cdot & \cdot \end{bmatrix} \begin{Bmatrix} \beta_1 \\ \vdots \\ \beta_5 \end{Bmatrix} \quad (1.2-23)$$

This procedure does not address the question of good or bad properties of the resulting element. It just only yields an element that is free from kinematic deformation modes.

However, even when a necessary condition is satisfied, it does not guarantee that all kinematic deformation modes will be suppressed. An efficient method which gives the necessary and sufficient condition for avoiding kinematic deformation modes was proposed by Feng et. al.^[23] In this work, it is assumed that there are m ($=n-r$) natural deformation modes for an element which has n degrees of freedom and r rigid-body modes. For any type of hybrid element, all stress modes in various stress matrices derived by different methods can be classified into m stress mode groups corresponding to m natural deformation modes and a zero-energy mode group corresponding to r rigid-body modes. For a plane stress problem, a 4-node quadrilateral element gives $n=8$, $r=3$ and hence $m=5$. By applying the procedure suggested, an initial stress matrix

$$\begin{aligned} \mathbf{P}_0 &= \begin{bmatrix} 1 & \cdot & \cdot & x & y & \cdot & \cdot & \cdot & \cdot \\ \cdot & 1 & \cdot & \cdot & \cdot & x & y & \cdot & \cdot \\ \cdot & \cdot & 1 & \cdot & \cdot & \cdot & \cdot & x & y \end{bmatrix} \\ &= [\sigma_1 \quad \sigma_2 \quad \sigma_3 \quad \sigma_4 \quad \sigma_5 \quad \sigma_6 \quad \sigma_7 \quad \sigma_8 \quad \sigma_9] \end{aligned} \quad (1.2-24)$$

can be classified into six mode groups shown in Table 1.2-2

Table 1.2-2 Stress modes after classification into mode groups.

Mode group	1	σ_1
	2	σ_2
	3	σ_3
	4	σ_5, σ_8
	5	σ_6, σ_9
Zero-energy mode group	σ_4, σ_7	

The *necessary and sufficient condition* for avoiding kinematic deformation modes is that an assumed stress matrix must contain m stress modes chosen from m different stress mode groups, except the zero-energy mode group. The reason for the existence of kinematic deformation modes when the condition ($m > n - r$) is satisfied is that the stress modes in the assumed stress matrix are not chosen from m different stress mode groups corresponding to m natural deformation modes.

Hamhim^[24] applied a method of classification of stress modes^[23] to obtain a desirable stress field free from kinematic deformation modes. Some hybrid plate bending elements were constructed. Most of these elements performed acceptably.

1.3 Objectives of Present Study

- 1). To study an efficient way for hybrid finite element formulation.
- 2). To develop some efficient hybrid plate bending elements.
- 3). To compare the results of such developed hybrid plate bending elements with existing hybrid elements.

1.4 Scope of Present Study

- 1). Thickness of the plate is small in comparison with the lateral dimension.
- 2). Lateral displacement of the plate is considered small compared with the plate thickness.
- 3). Neglect the effects of membrane forces.
- 4). Materials are linearly elastic and isotropic.
- 5). Only static analysis is considered.



สถาบันวิทยบริการ
จุฬาลงกรณ์มหาวิทยาลัย

Chapter II

Theoretical Considerations

The pertinent theories presented in this chapter are the basic theory of plate bending and the variational principles serve as a basis for finite element formulation. Only the fundamental concepts and equations related to the bending of plates are reviewed. Also, energy functionals based on several variational principles developed in the past will be summarized and an element stiffness matrix will be formulated as an example.

2.1 Bending of Flat Plates

Consider an infinitesimal plate in Cartesian coordinates (x, y, z) subjected to stresses acting on cross sections as shown in Fig. 2.1-1a. The material is considered to be linearly elastic and homogeneous. Normal stresses σ_x and σ_y vary linearly with z and are associated with bending moments M_x and M_y . Shear stress τ_{xy} also varies linearly with z and is associated with twisting moment M_{xy} . Normal stress σ_z is considered negligible in comparison with σ_x , σ_y , and τ_{xy} by employing the assumption of small plate thickness t in comparison with the lateral dimension. The transverse shear stresses τ_{yz} and τ_{zx} vary quadratically with z .

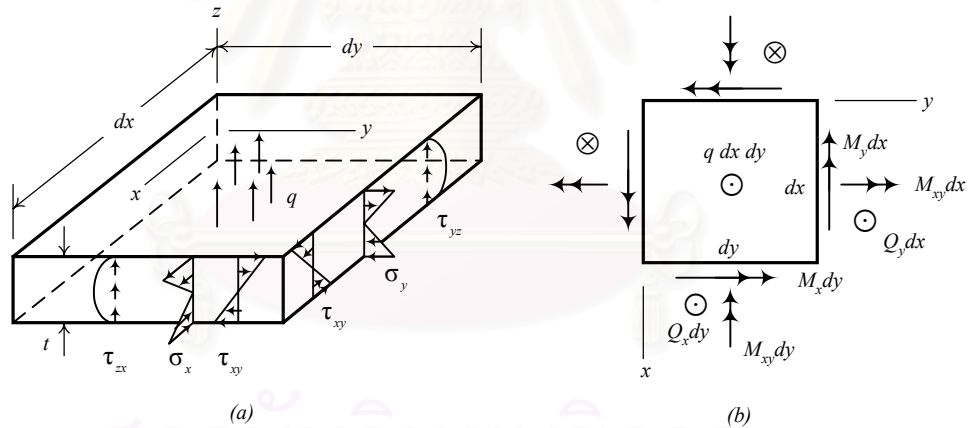


Figure 2.1-1 (a) Stresses acting on a differential element of a homogeneous, linearly elastic plate. The distributed transverse load is q (force per unit area). (b) The same differential element viewed normal to the plate. Forces \odot and \otimes act in the positive and negative z directions, respectively.

The transverse load q includes surface load and body force, both in the z direction. By disregarding the effects of membrane forces, $\sigma_x = \sigma_y = \tau_{xy} = 0$ on the midsurface $z=0$.

The stresses in Fig. 2.1-1 provide the following moments M and transverse shear forces Q :

$$M_x = \int_{-t/2}^{t/2} \sigma_x z dz, \quad M_y = \int_{-t/2}^{t/2} \sigma_y z dz, \quad M_{xy} = \int_{-t/2}^{t/2} \tau_{xy} z dz \quad (2.1-1a)$$

$$Q_x = \int_{-t/2}^{t/2} \tau_{xz} dz, \quad Q_y = \int_{-t/2}^{t/2} \tau_{yz} dz \quad (2.1-1b)$$

where

M_x and M_y are the bending moments *per unit length* on sections perpendicular to the x - and y -axis respectively, positive when producing tensile stress on portion of the positive z direction.

$M_{xy} = -M_{yx}$ are the twisting moments *per unit length* on sections perpendicular to the x - and y -axis respectively, following the positive right-hand rule.

Q_x and Q_y are the transverse shear forces on sections perpendicular to the x - and y -axis respectively.

Fig. 2.1-1b shows differential total moments and forces such as $M_x dy$, $Q_x dy$, and so on. Stresses σ_x , σ_y , and τ_{xy} are largest at the surfaces $z = \pm t/2$, where they have the magnitudes of $6M_x/t^2$, $6M_y/t^2$, and $6M_{xy}/t^2$, respectively. At arbitrary values of z ,

$$\sigma_x = \frac{M_x z}{t^3/12}, \quad \sigma_y = \frac{M_y z}{t^3/12}, \quad \tau_{xy} = \frac{M_{xy} z}{t^3/12} \quad (2.1-2)$$

as may be verified by substituting Eqs. 2.1-2 into Eqs. 2.1-1a. Transverse shear stresses are usually small in comparison with σ_x , σ_y , and τ_{xy} . They have the greatest magnitude at $z = 0$, where $\tau_{yz} = 1.5Q_y/t$ and $\tau_{zx} = 1.5Q_x/t$.

Consider the equilibrium of moments and shears acting on a differential element above. One may prove that the equilibrium of those forces are

$$\begin{aligned} \frac{\partial M_x}{\partial x} + \frac{\partial M_{xy}}{\partial y} &= Q_x \\ \frac{\partial M_{xy}}{\partial x} + \frac{\partial M_y}{\partial y} &= Q_y \\ \frac{\partial Q_x}{\partial x} + \frac{\partial Q_y}{\partial y} &= -q \end{aligned} \quad (2.1-3)$$

Rewrite into matrix form as

$$\begin{bmatrix} \frac{\partial}{\partial x} & \cdot & \frac{\partial}{\partial y} & -1 & \cdot \\ \cdot & \frac{\partial}{\partial y} & \frac{\partial}{\partial x} & \cdot & -1 \\ \cdot & \cdot & \cdot & \frac{\partial}{\partial x} & \frac{\partial}{\partial y} \end{bmatrix} \begin{Bmatrix} M_x \\ M_y \\ M_{xy} \\ Q_x \\ Q_y \end{Bmatrix} = \begin{Bmatrix} \cdot \\ \cdot \\ \cdot \\ -q \end{Bmatrix} \quad (2.1-4)$$

On account of deformations in plate bending there are two theories involved : Kirchhoff and Mindlin plate theories. Both plate theories depend on the transverse shear deformation - whether it exists or not. This will cause the deformed shape of the plate to be different.

2.1.1 Kirchhoff Plate Theory

Points on the midsurface $z = 0$ move in only the z -direction as the plate deforms in bending. A line straight and normal to the midsurface before loading is assumed to remain straight and normal to the midsurface after loading as illustrated by line OP in Fig. 2.1-2. This assumption is justifiable if the transverse shear deformation is disregarded. A point not on the midsurface has displacement components u and v in the x - and y -directions, Fig. 2.1-2, with $w_{,x}$ and $w_{,y}$ as small angles of rotation.

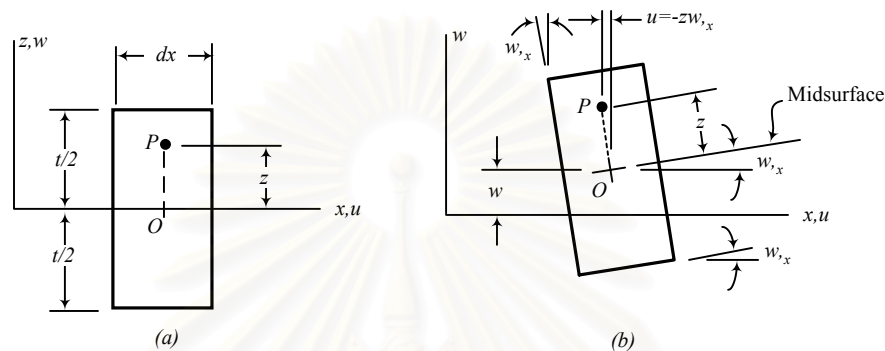


Figure 2.1-2. (a) Differential element of a thin plate before loading. (b) After loading: deformations associated with Kirchhoff plate theory. Point P displaces w units up and $zw_{,x}$ units leftward because of midsurface displacement w and small rotation $w_{,x}$.

The displacement components u and v may be related to $w_{,x}$ and $w_{,y}$ as

$$u = -zw_{,x} \quad (2.1-5)$$

$$v = -zw_{,y}$$

From mechanics of solids, the strains can be obtained as

$$\epsilon_x = u_{,x} = -zw_{,xx}$$

$$\epsilon_y = v_{,y} = -zw_{,yy} \quad (2.1-6)$$

$$\gamma_{xy} = u_{,y} + v_{,x} = -2zw_{,xy}$$

which may be rewritten in matrix form as

$$\begin{Bmatrix} \epsilon_x \\ \epsilon_y \\ \gamma_{xy} \end{Bmatrix} = -z \begin{Bmatrix} w_{,xx} \\ w_{,yy} \\ 2w_{,xy} \end{Bmatrix} \quad (2.1-7)$$

or

$$\boldsymbol{\epsilon} = -z\boldsymbol{\kappa}$$

where $\boldsymbol{\epsilon}$ denotes the bending strains and $\boldsymbol{\kappa}$ the curvatures.

These are the strain-displacement relations for Kirchhoff plate bending which is applicable to a thin plate.

For an isotropic material, with E = elastic modulus and ν = Poisson's ratio, the stress-strain relations are

$$\begin{Bmatrix} \sigma_x \\ \sigma_y \\ \tau_{xy} \end{Bmatrix} = \frac{E}{1-\nu^2} \begin{bmatrix} 1 & \nu & \cdot \\ \nu & 1 & \cdot \\ \cdot & \cdot & (1-\nu)/2 \end{bmatrix} \begin{Bmatrix} \epsilon_x \\ \epsilon_y \\ \gamma_{xy} \end{Bmatrix} \quad (2.1-8)$$

The moment-curvature relations are obtained by substitution of Eqs. 2.1-6 into Eqs. 2.1-8 and the result into Eqs. 2.1-1a. This process yields

$$\begin{Bmatrix} M_x \\ M_y \\ M_{xy} \end{Bmatrix} = -D \begin{bmatrix} 1 & \nu & \cdot \\ \nu & 1 & \cdot \\ \cdot & \cdot & (1-\nu)/2 \end{bmatrix} \begin{Bmatrix} w_{,xx} \\ w_{,yy} \\ 2w_{,xy} \end{Bmatrix} \quad (2.1-9)$$

or

$$\mathbf{M} = -\mathbf{D}_k \boldsymbol{\kappa}$$

where $D = \frac{Et^3}{12(1-\nu^2)}$ is known as “flexural rigidity” or “plate rigidity” and is analogous to bending stiffness EI of a beam. Indeed, if a plate has a unit width and $\nu = 0$, then $D = EI = Et^3/12$.

2.1.2 Mindlin Plate Theory

A line that is straight and normal to the midsurface before loading is assumed to remain straight but not necessarily normal to the midsurface after loading. Thus, transverse shear deformation is allowed. The motion of a point not on the midsurface is not governed by the slopes $w_{,x}$ and $w_{,y}$ as in the Kirchhoff theory. Rather, the motion depends on the rotations θ_x and θ_y of lines that were normal to the midsurface of the undeformed plate shown in Fig. 2.1-3 below

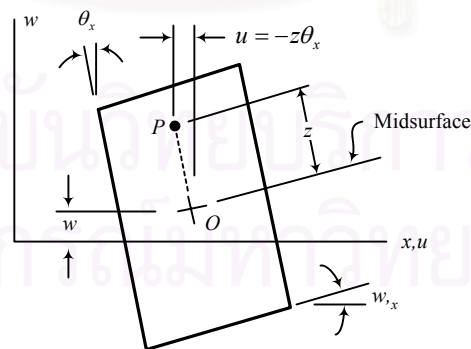


Figure 2.1-3. Differential plate element after loading, analogous to Fig. 2.1-2b, but with transverse shear deformation allowed ($w_{,x} \neq \theta_x$, so that $\gamma_{xz} = w_{,x} - \theta_x \neq 0$).

Thus, with θ_x and θ_y as small angles of rotation,

$$\begin{aligned} u &= -z\theta_x \\ v &= -z\theta_y \end{aligned} \quad (2.1-10)$$

and the strain-displacement relations for the Mindlin plate theory are

$$\begin{aligned} \varepsilon_x &= -z\theta_{x,y} \\ \varepsilon_y &= -z\theta_{y,y} \\ \gamma_{xy} &= -z(\theta_{x,y} + \theta_{y,x}) \\ \gamma_{yz} &= w_{,y} - \theta_y \\ \gamma_{zx} &= w_{,x} - \theta_x \end{aligned} \quad (2.1-11)$$

This theory accounts for transverse shear deformation and is therefore especially suited to the analysis of thick plates and sandwich plates.

By considering uncoupling between shears and moments in an isotropic plate, $\tau_{yz} = G\gamma_{yz}$ and $\tau_{zx} = G\gamma_{zx}$ where $G = E/2(1+\nu)$ is the shear modulus, therefore, the stress-strain relations for the Mindlin plate are

$$\begin{Bmatrix} \sigma_x \\ \sigma_y \\ \tau_{xy} \end{Bmatrix} = \frac{E}{1-\nu^2} \begin{bmatrix} 1 & \nu & \cdot \\ \nu & 1 & \cdot \\ \cdot & \cdot & (1-\nu)/2 \end{bmatrix} \begin{Bmatrix} \varepsilon_x \\ \varepsilon_y \\ \gamma_{xy} \end{Bmatrix} \quad (2.1-12)$$

and

$$\begin{Bmatrix} \tau_{zx} \\ \tau_{yz} \end{Bmatrix} = \begin{bmatrix} G & \cdot \\ \cdot & G \end{bmatrix} \begin{Bmatrix} \gamma_{zx} \\ \gamma_{yz} \end{Bmatrix}$$

The moment-curvature relations for the Mindlin plate theory are obtained by essentially the same procedure used to obtain Eqs. 2.1-9. However, Eqs. 2.1-11 must be used instead of Eqs. 2.1-6 including the shear stress-strain relations. The resulting moment-curvature relations are

$$\begin{Bmatrix} M_x \\ M_y \\ M_{xy} \\ Q_x \\ Q_y \end{Bmatrix} = - \begin{bmatrix} \cdot & \cdot & \cdot & \cdot & \cdot \\ \mathbf{D}_K & \cdot & \cdot & \cdot & \cdot \\ 3 \times 3 & \cdot & \cdot & \cdot & \cdot \\ \cdot & \cdot & \cdot & Gt & \cdot \\ \cdot & \cdot & \cdot & \cdot & Gt \end{bmatrix} \begin{Bmatrix} \theta_{x,y} \\ \theta_{y,y} \\ \theta_{x,y} + \theta_{y,x} \\ \theta_x - w_{,x} \\ \theta_y - w_{,y} \end{Bmatrix} \quad (2.1-13)$$

or abbreviated as

$$\mathbf{M} = -\mathbf{D}_M \boldsymbol{\kappa}$$

where \mathbf{D}_M is the same as in Eqs. 2.1-9.

Note that the transverse shear stresses τ_{yz} and τ_{zx} as shown in Fig. 2.1-1 vary quadratically with z while, in the Mindlin plate, uniform distributions are taken into account. Therefore, the shear modulus G in Eqs. 2.1-12 may be replaced by $G/1.2$ to permit the parabolic distribution of τ_{yz} and τ_{zx} to be replaced by uniform

distributions. To do so the shear strain energy terms due to both distributions must be equal.

In summary, all relations are tabulated in Table 2.1-1 as follows :

Table 2.1-1 Governing equations used in plate theories : Kirchhoff and Mindlin Plate theories

Kirchhoff Plate theory	Mindlin Plate theory
Displacements	
$u = -zw_{,x}$ $v = -zw_{,y}$	$u = -z\theta_x$ $v = -z\theta_y$
Strain-Displacement Relations	
$\epsilon_x = u_{,x} = -zw_{,xx}$ $\epsilon_y = v_{,y} = -zw_{,yy}$ $\gamma_{xy} = u_{,y} + v_{,x} = -2zw_{,xy}$	$\epsilon_x = -z\theta_{x,x}$ $\epsilon_y = -z\theta_{y,y}$ $\gamma_{xy} = -z(\theta_{x,y} + \theta_{y,x})$ $\gamma_{zx} = w_{,x} - \theta_x$ $\gamma_{yz} = w_{,y} - \theta_y$
Stress-Strain Relations	
$\begin{Bmatrix} \sigma_x \\ \sigma_y \\ \tau_{xy} \end{Bmatrix} = \frac{E}{1-\nu^2} \begin{bmatrix} 1 & \nu & \cdot \\ \nu & 1 & \cdot \\ \cdot & \cdot & (1-\nu)/2 \end{bmatrix} \begin{Bmatrix} \epsilon_x \\ \epsilon_y \\ \gamma_{xy} \end{Bmatrix}$	<p>Because of uncoupling between shears and moments,</p> $\begin{Bmatrix} \sigma_x \\ \sigma_y \\ \tau_{xy} \end{Bmatrix} = \frac{E}{1-\nu^2} \begin{bmatrix} 1 & \nu & \cdot \\ \nu & 1 & \cdot \\ \cdot & \cdot & (1-\nu)/2 \end{bmatrix} \begin{Bmatrix} \epsilon_x \\ \epsilon_y \\ \gamma_{xy} \end{Bmatrix}$ $\begin{Bmatrix} \tau_{zx} \\ \tau_{yz} \end{Bmatrix} = \frac{E}{1-\nu^2} \begin{bmatrix} (1-\nu)/2 & \cdot \\ \cdot & (1-\nu)/2 \end{bmatrix} \begin{Bmatrix} \gamma_{zx} \\ \gamma_{yz} \end{Bmatrix}$ <p>where $G = E/2(1+\nu)$</p>
Moment-Curvature Relations	
$\begin{Bmatrix} M_x \\ M_y \\ M_{xy} \end{Bmatrix} = -D \begin{bmatrix} 1 & \nu & \cdot \\ \nu & 1 & \cdot \\ \cdot & \cdot & (1-\nu)/2 \end{bmatrix} \begin{Bmatrix} w_{,xx} \\ w_{,yy} \\ 2w_{,xy} \end{Bmatrix}$ $\mathbf{M} = -\mathbf{D}_K \boldsymbol{\kappa}$ <p>where $D = \frac{Et^3}{12(1-\nu^2)}$</p>	$\begin{Bmatrix} M_x \\ M_y \\ M_{xy} \\ Q_x \\ Q_y \end{Bmatrix} = - \begin{bmatrix} \cdot & \cdot & \cdot & \cdot & \cdot \\ \mathbf{D}_K & \cdot & \cdot & \cdot & \cdot \\ 3 \times 3 & \cdot & \cdot & \cdot & \cdot \\ \cdot & \cdot & \cdot & Gt & \cdot \\ \cdot & \cdot & \cdot & \cdot & Gt \end{bmatrix} \begin{Bmatrix} \theta_{x,x} \\ \theta_{y,y} \\ \theta_{x,y} + \theta_{y,x} \\ \theta_x - w_{,x} \\ \theta_y - w_{,y} \end{Bmatrix}$ $\mathbf{M} = -\mathbf{D}_M \boldsymbol{\kappa}$ <p>where $D = \frac{Et^3}{12(1-\nu^2)}$</p>
Equilibrium Equations	
$\begin{bmatrix} \partial/\partial x & \cdot & \partial/\partial y & -1 & \cdot \\ \cdot & \partial/\partial y & \partial/\partial x & \cdot & -1 \\ \cdot & \cdot & \cdot & \partial/\partial x & \partial/\partial y \end{bmatrix} \begin{Bmatrix} M_x \\ M_y \\ M_{xy} \\ Q_x \\ Q_y \end{Bmatrix} = \begin{Bmatrix} \cdot \\ \cdot \\ \cdot \\ -q \end{Bmatrix}$	

2.2 Multifield Variational Principles

The finite element methods for problems that are governed by self-adjoint differential equations can be formulated most conveniently by variational methods. The construction of the conventional finite elements for structural and solid mechanics is based on the stationary condition of the potential energy functional. The strain energy is expressed in terms of the strain vector $\boldsymbol{\varepsilon}$, which, in turn, is expressed in terms of the displacement vector \mathbf{u} through the constraining strain-displacement relations, $\boldsymbol{\varepsilon} = \mathbf{D}\mathbf{u}$. This primal variational principle, which contains the displacements \mathbf{u} as the only field, is,

$$\Pi_p(\mathbf{u}) = \int_V [\frac{1}{2}(\mathbf{D}\mathbf{u})^T \mathbf{C}(\mathbf{D}\mathbf{u}) - \bar{\mathbf{F}}^T \mathbf{u}] dV - \int_{S_\sigma} \bar{\mathbf{T}}^T \mathbf{u} dS \quad (2.2-1)$$

where \mathbf{C} is the elastic stiffness matrix, and $\bar{\mathbf{F}}$ and $\bar{\mathbf{T}}$ are, respectively, the prescribed body force and boundary traction vectors. Note that the potential energy, Π_p , is subjected to the constrained conditions or subsidiary conditions $\mathbf{u} = \bar{\mathbf{u}}$ on S_u . However, finite element methods can be formulated by relaxing the requirement of constraints within the element and/or along the interelement boundaries.

Generally, the equations governing the mechanics of solids consist of the equilibrium equations, strain-displacement relations, constitutive relations, compatibility equations and the boundary conditions. Some or all of these constraint conditions can be relaxed. One systematic procedure for the derivation of the multifield variational principles is to impose the constraint conditions through the application of Lagrange multipliers^[2]. By relaxing the strain-displacement relation and the displacement boundary conditions on Π_p using the Lagrangian multipliers which are, physically, the stresses $\boldsymbol{\sigma}$ and boundary tractions $\bar{\mathbf{T}}$, a three-field variational principle results. It is the following Hu-Washizu variational principle:

$$\Pi_G(\boldsymbol{\varepsilon}, \boldsymbol{\sigma}, \mathbf{u}) = \int_V [\frac{1}{2}\boldsymbol{\varepsilon}^T \mathbf{C}\boldsymbol{\varepsilon} - \boldsymbol{\sigma}^T (\boldsymbol{\varepsilon} - \mathbf{D}\mathbf{u}) - \bar{\mathbf{F}}^T \mathbf{u}] dV - \int_{S_\sigma} \bar{\mathbf{T}}^T \mathbf{u} dS - \int_{S_u} \mathbf{T}^T (\mathbf{u} - \bar{\mathbf{u}}) dS, \quad (2.2-2)$$

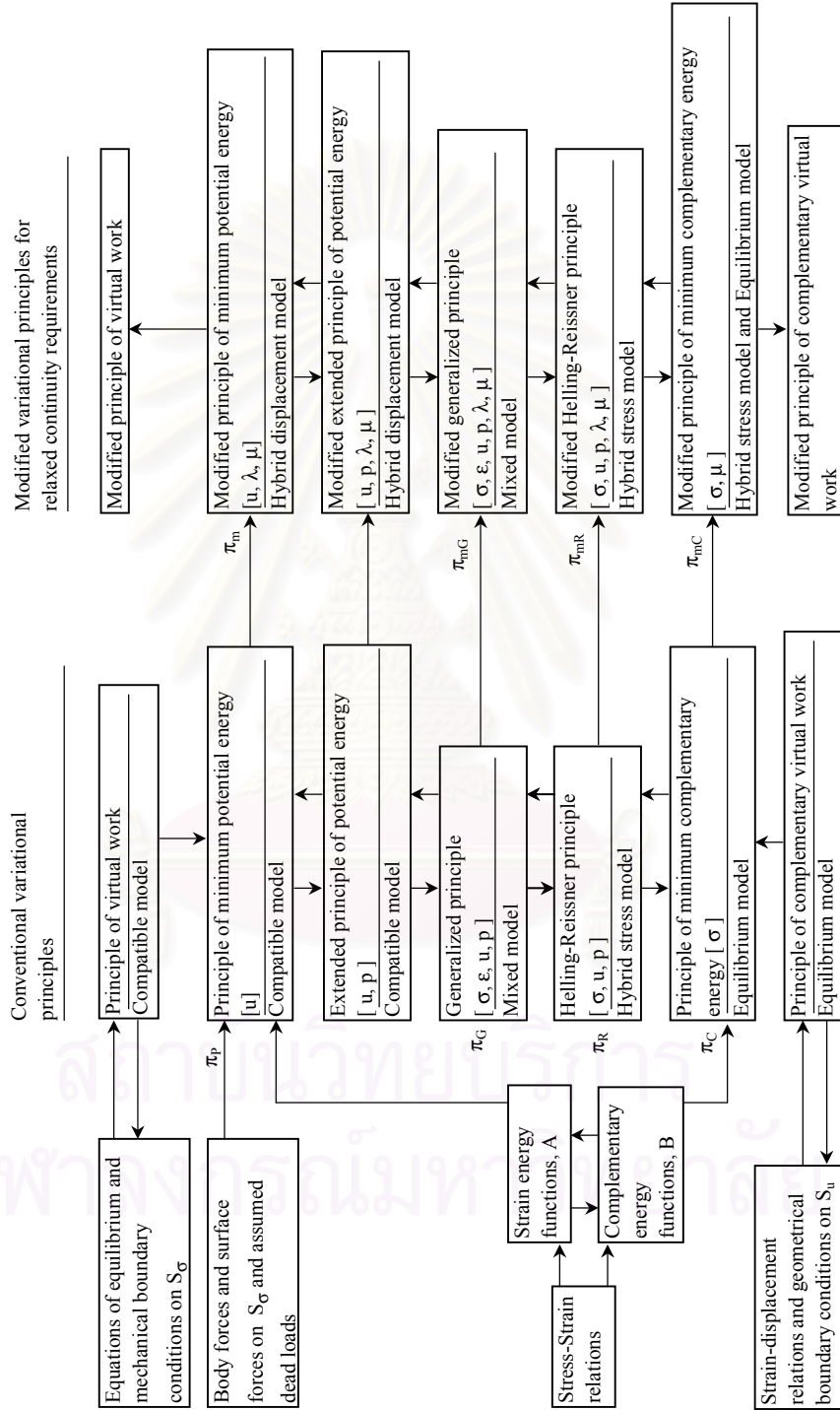
where \mathbf{T} is the boundary traction vector expressed in terms of $\boldsymbol{\sigma} (= \mathbf{v}\boldsymbol{\sigma})$, \mathbf{v} is the directional cosines of surface normals, and $\bar{\mathbf{u}}$ is the vector of prescribed boundary displacements. The Hu-Washizu variational principle is subjected to independent variables $\boldsymbol{\sigma}$, $\boldsymbol{\varepsilon}$, and \mathbf{u} with no constraint conditions. By eliminating the strain variables and the stress variables respectively, through the introduction of the constitutive relations, two 2-field variational principles result:

$$\Pi_R(\boldsymbol{\sigma}, \mathbf{u}) = \int_V [-\frac{1}{2}\boldsymbol{\sigma}^T \mathbf{S}\boldsymbol{\sigma} - \boldsymbol{\sigma}^T (\mathbf{D}\mathbf{u}) - \bar{\mathbf{F}}^T \mathbf{u}] dV - \int_{S_\sigma} \bar{\mathbf{T}}^T \mathbf{u} dS - \int_{S_u} \mathbf{T}^T (\mathbf{u} - \bar{\mathbf{u}}) dS, \quad (2.2-3)$$

$$\Pi_R(\boldsymbol{\varepsilon}, \mathbf{u}) = \int_V [-\frac{1}{2}\boldsymbol{\varepsilon}^T \mathbf{C}\boldsymbol{\varepsilon} - \mathbf{C}\boldsymbol{\varepsilon}^T (\mathbf{D}\mathbf{u}) - \bar{\mathbf{F}}^T \mathbf{u}] dV - \int_{S_\sigma} \bar{\mathbf{T}}^T \mathbf{u} dS - \int_{S_u} \mathbf{T}^T (\mathbf{u} - \bar{\mathbf{u}}) dS, \quad (2.2-4)$$

where \mathbf{S} is the compliance matrix. Eq. 2.2-3 is the original Hellinger-Reissner principle.

Table 2.2-1 Flow Diagram for Variational Principles in the Small
Displacement Theory of Elastostatics^[2]



By applying the divergence theorem, Eq. 2.2-3 can be transformed to

$$\Pi_R = \int_V [\frac{1}{2} \boldsymbol{\sigma}^T \mathbf{S} \boldsymbol{\sigma} - (\mathbf{D}^T \boldsymbol{\sigma})^T \mathbf{u} - \bar{\mathbf{F}}^T \mathbf{u}] dV - \int_{S_\sigma} (\mathbf{T} - \bar{\mathbf{T}})^T \mathbf{u} dS - \int_{S_u} \mathbf{T}^T \bar{\mathbf{u}} dS, \quad (2.2-5)$$

When the equilibrating stress and prescribed tractions along the boundary are satisfied, Eq. 2.2-5 is reduced to another primal principle, the principle of stationary complementary energy, with stresses $\boldsymbol{\sigma}$ as the only field variable:

$$\Pi_C = \int_V \frac{1}{2} \boldsymbol{\sigma}^T \mathbf{S} \boldsymbol{\sigma} dV - \int_{S_u} \mathbf{T}^T \bar{\mathbf{u}} dS \quad (2.2-6)$$

For these energy functionals, details of the modification may be found in the text by Washizu^[2]. Table 2.2-1 shows routes in the derivation of multifield variational principles. Arrows in the diagram show transformation direction from one principle to another.

Corresponding to the foregoing energy functionals, Eqs. 2.2-1 to 2.2-6, numerous types of finite element formulations can be obtained^[1]. Descriptions of the features of various formulations are summarized in Table 2.2-2

Table 2.2-2 Classification of Finite Element Methods in Solid Mechanics^[1]

Model	Variational Principle	Assumed inside Each element	Along Interelement Boundary	Unknowns in Final Equations
Compatible	Minimum Potential Energy	Smooth Displacement Distribution	Continuous Displacement	Nodal Displacements
Equilibrium	Minimum Complementary Energy	Smooth and Equilibrating Stress Distribution	Equilibrium of Boundary Traction	(a) Generalized Nodal Displacements (b) Stress Function Parameters
Hybrid	Hellinger-Reissner Variational Principle	Stress & Displacement Distribution	Displacement	Nodal Displacements
Mixed	Hu-Washizu Variational Principle	Stress, Displacement and Strain Distribution	Displacement	Nodal Displacements

For the finite element formulation, the entire continuum is discretized into a number of fictitious elements of finite magnitude, called finite elements, and the corresponding variational functional is the sum of those for the individual elements. Such functionals for the individual elements are expressed in the same form as Eqs. 2.2-1 to 2.2-6. The element displacements \mathbf{u} , stresses $\boldsymbol{\sigma}$, and strains $\boldsymbol{\varepsilon}$ can all be expressed in terms of internal parameters which are *independent* from one element to another. When they are statically condensed in the element level, the strain energy U can be expressed in terms of the nodal displacements \mathbf{q} , and eventually, the element stiffness matrix can be obtained.

2.3 Hybrid Finite Element Formulation

One attractive element corresponding to the Hellinger-Reissner principle is considered. As stated in Section 1.1, hybrid elements are more preferred than either compatible elements or equilibrium elements because more desirable and accurate results are obtained. The variational method for the formulation of the original version of the hybrid stress finite element is based on the complementary energy principle. But, recently, Pian^[27] revealed that the original hybrid stress element is actually developed based on the Hellinger-Reissner principle and not on the complementary energy principle as indicated in the earlier paper^[4]. This is because when the assumed stress fields satisfy exactly the homogeneous equilibrium conditions the Hellinger-Reissner principle become the complementary energy principle.

To derive the element stiffness matrix, it is only necessary to express the boundary displacements $\bar{\mathbf{u}}$ in terms of the nodal displacements \mathbf{q} in the form

$$U = \frac{1}{2} \mathbf{q}^T \mathbf{k} \mathbf{q} \quad (2.3-1)$$

Then \mathbf{k} is the element stiffness matrix.

When the displacements \mathbf{u} in an element are not compatible with the boundary displacements $\bar{\mathbf{u}}$, the Hellinger-Reissner principle including body forces and boundary tractions then takes the form

$$\Pi_R(\boldsymbol{\sigma}, \mathbf{u}) = \int_V \left[-\frac{1}{2} \boldsymbol{\sigma}^T \mathbf{S} \boldsymbol{\sigma} - \boldsymbol{\sigma}^T (\mathbf{D}\mathbf{u}) - \bar{\mathbf{F}}^T \mathbf{u} \right] dV - \int_{S_\sigma} \bar{\mathbf{T}}^T \mathbf{u} dS - \int_{\partial V} \mathbf{T}^T (\mathbf{u} - \bar{\mathbf{u}}) dS \quad (2.3-2)$$

where $\boldsymbol{\sigma}$ = stresses, \mathbf{S} = elastic compliance, \mathbf{T} = boundary traction related to $\boldsymbol{\sigma}$, V = volume of the element, and ∂V = entire boundary of the element, and the strain-displacement relations are expressed as

$$\boldsymbol{\varepsilon} = \mathbf{D}\mathbf{u} \quad (2.3-3)$$

In the finite element formulation we separate element displacements \mathbf{u} into two parts: the compatible part \mathbf{u}_q which is expressed in terms of \mathbf{q} and the additional part \mathbf{u}_λ which is expressed in terms of internal displacement parameters λ that can be statically condensed at the element level. Here, \mathbf{u}_λ may be incompatible along the boundary or it may be bubble functions which are zero along the boundary. If \mathbf{u}_λ is incompatible, Eq. 2.3-2 should be used in the formulation. By realizing that

$$\int_V \boldsymbol{\sigma}^T (\mathbf{D}\mathbf{u}_\lambda) dV = - \int_V (\mathbf{D}^T \boldsymbol{\sigma})^T \mathbf{u}_\lambda dV + \int_{\partial V} \mathbf{T}^T \mathbf{u}_\lambda dS$$

and $\mathbf{u}_\lambda = \mathbf{u} - \bar{\mathbf{u}}$ on ∂V , we have the modified Hellinger-Reissner principle

$$\Pi_{mR} = \int_V \left[-\frac{1}{2} \boldsymbol{\sigma}^T \mathbf{S} \boldsymbol{\sigma} + \boldsymbol{\sigma}^T (\mathbf{D}\mathbf{u}_q) - (\mathbf{D}^T \boldsymbol{\sigma})^T \mathbf{u}_\lambda \right] dV - \int_V \bar{\mathbf{F}}^T \mathbf{u} dV - \int_{S_\sigma} \bar{\mathbf{T}}^T \mathbf{u} dS \quad (2.3-4)$$

We also note that when \mathbf{u}_λ are bubble functions for which $\mathbf{u}_\lambda = 0$ on ∂V , the boundary integral term in Eq. 2.3-2 no longer appears, so Eq. 2.3-4 still holds. Since the equation

$$\mathbf{D}^T \boldsymbol{\sigma} = 0 \quad (2.3-5)$$

represents the stress equilibrium conditions, the last term in the integral in Eq. 2.3-4 actually plays the role of the conditions of constraint with the corresponding Lagrange multipliers.

In the finite element implementation, we assume

$$\boldsymbol{\sigma} = \mathbf{P}\boldsymbol{\beta} \quad (2.3-6)$$

Also

$$\mathbf{u}_q = \mathbf{N}_q \mathbf{q} \quad (2.3-7)$$

and

$$\mathbf{u}_\lambda = \mathbf{N}_\lambda \boldsymbol{\lambda} \quad (2.3-8)$$

from which

$$\mathbf{D}\mathbf{u}_q = \mathbf{B}\mathbf{q} \quad (2.3-9)$$

and

$$\mathbf{D}^T \boldsymbol{\sigma} = (\mathbf{D}^T \mathbf{P})\boldsymbol{\beta} \quad (2.3-10)$$

Let

$$\mathbf{F}^T = -\int_V \bar{\mathbf{F}}^T \mathbf{u} dV - \int_{S_\sigma} \bar{\mathbf{T}}^T \mathbf{u} dS \quad (2.3-11)$$

serve as an equivalent nodal force.

The functional Π_R thus takes the form

$$\Pi_{mR} = -\frac{1}{2} \boldsymbol{\beta}^T \mathbf{H}\boldsymbol{\beta} + \boldsymbol{\beta}^T \mathbf{G}\mathbf{q} - \boldsymbol{\beta}^T \mathbf{R}\boldsymbol{\lambda} - \mathbf{F}^T \mathbf{q} \quad (2.3-12)$$

where

$$\begin{aligned} \mathbf{H} &= \int_V \mathbf{P}^T \mathbf{S} \mathbf{P} dV \\ \mathbf{G} &= \int_V \mathbf{P}^T \mathbf{B} dV \\ \mathbf{R} &= \int_V (\mathbf{D}^T \mathbf{P})^T \mathbf{N}_\lambda dV \end{aligned} \quad (2.3-13)$$

From the first variation of Π_{mR} with respect to $\boldsymbol{\beta}$, $\boldsymbol{\lambda}$ and \mathbf{q} , we then obtain

$$\begin{aligned} \mathbf{G}\mathbf{q} - \mathbf{R}\boldsymbol{\lambda} - \mathbf{H}\boldsymbol{\beta} &= \mathbf{0}, \\ -\mathbf{R}^T \boldsymbol{\beta} &= \mathbf{0}, \end{aligned} \quad (2.3-14)$$

and

$$\mathbf{G}^T \boldsymbol{\beta} = \mathbf{F},$$

respectively.

By eliminating $\boldsymbol{\lambda}$ and substituting $\boldsymbol{\beta}$ into Π_{mR} , the strain energy term of functional becomes

$$U = \frac{1}{2} \boldsymbol{\beta}^T \mathbf{H}\boldsymbol{\beta} \quad (2.3-15)$$

and in view of Eq. 2.3-1, then

$$\mathbf{k} = \mathbf{G}^T \mathbf{H}^{-1} \mathbf{G} - (\mathbf{G}^T \mathbf{H}^{-1} \mathbf{R})(\mathbf{R}^T \mathbf{H}^{-1} \mathbf{R})^{-1} (\mathbf{R}^T \mathbf{H}^{-1} \mathbf{G}) \quad (2.3-16)$$

This element stiffness is thus named the "*Hybrid Stress Element*"

Instead of evaluating an element stiffness matrix above explicitly by matrix operation, the method of Gauss elimination technique^[28] is preferred. To do this the stationary conditions of Π_{mR} in Eq. 2.3-14 are successively substituted in order to eliminate unwanted parameters. For systematic elimination, all of stationary conditions are put together into matrix form. The partitioned matrix containing these conditions is written as

$$\begin{bmatrix} \cdot & \cdot & \mathbf{G}^T \\ \cdot & \cdot & -\mathbf{R}^T \\ \mathbf{G} & -\mathbf{R} & -\mathbf{H} \end{bmatrix} \begin{Bmatrix} \mathbf{q} \\ \lambda \\ \beta \end{Bmatrix} = \begin{Bmatrix} \mathbf{F} \\ \cdot \\ \cdot \end{Bmatrix} \quad (2.3-17)$$

Then applying reverse Gauss elimination method, we obtain

$$\begin{bmatrix} \mathbf{G}^T \mathbf{H}^{-1} \mathbf{G} & -\mathbf{G}^T \mathbf{H}^{-1} \mathbf{R} & \cdot \\ -\mathbf{R}^T \mathbf{H}^{-1} \mathbf{G} & \mathbf{R}^T \mathbf{H}^{-1} \mathbf{R} & \cdot \\ \mathbf{G} & -\mathbf{R} & -\mathbf{H} \end{bmatrix} \begin{Bmatrix} \mathbf{q} \\ \lambda \\ \beta \end{Bmatrix} = \begin{Bmatrix} \mathbf{F} \\ \cdot \\ \cdot \end{Bmatrix} \quad (2.3-18)$$

and then,

$$\begin{bmatrix} \mathbf{G}^T \mathbf{H}^{-1} \mathbf{G} - (\mathbf{G}^T \mathbf{H}^{-1} \mathbf{R})(\mathbf{R}^T \mathbf{H}^{-1} \mathbf{R})^{-1} (\mathbf{R}^T \mathbf{H}^{-1} \mathbf{G}) & \cdot & \cdot \\ -\mathbf{R}^T \mathbf{H}^{-1} \mathbf{G} & \mathbf{R}^T \mathbf{H}^{-1} \mathbf{R} & \cdot \\ \mathbf{G} & -\mathbf{R} & -\mathbf{H} \end{bmatrix} \begin{Bmatrix} \mathbf{q} \\ \lambda \\ \beta \end{Bmatrix} = \begin{Bmatrix} \mathbf{F} \\ \cdot \\ \cdot \end{Bmatrix} \quad (2.3-19)$$

Eventually, the first equation is reduced to the form

$$\mathbf{kq} = \mathbf{F} \quad (2.3-20)$$

where \mathbf{k} is the element stiffness matrix. Obviously, the element stiffness matrix is the same as that obtained in Eq. 2.3-16.

Chapter III

Hybrid Plate Elements

In the present study, some hybrid plate bending elements will be constructed. These elements should be free from kinematic deformation modes, invariant with respect to the reference coordinates and accurate with regard to stress and displacement calculation. Four-node quadrilateral elements are considered. With the aim of obtaining well-behaved elements, at first, the stress matrix \mathbf{P} of Eq. 2.3-6 should be chosen so as to avoid all the unwanted kinematic deformation modes and to make it contain a minimal number of stress parameters. These requirements are achieved by applying the method of classification of stress modes. After that, the element stiffness matrix will be formulated. The formulation may take the additional displacement parameters into consideration. This study also accounts for the optimization of equilibrium in plate elements. Furthermore, a penalty-equilibrium matrix is included in the formulation of the element stiffness matrix. Lastly, some elements are reviewed and used for comparison with the new hybrid elements proposed in this study.

3.1 Determination of Desirable Stress Matrix

Since the day of the first hybrid finite element constructed, the question on how to obtain the stress matrix has arisen. The equilibrium equations were first used as a guideline to obtain the assumed stresses and also the condition to ensure the existence of solutions in Eq. 1.2-20. The stress matrix must be expressed in Cartesian coordinates in order to satisfy the equilibrium equations. After the modification of governing energy functionals in the finite element method, equilibrium of the stress matrix may be relaxed. This opens the way to express the stress matrix in natural coordinates so that the element is less sensitive to distortion of geometry.

The method of classification of stress modes is chosen in this study to obtain the stress matrix. This method is considered to be a reasonable one. All stress modes are classified into individual mode groups no matter how those stress modes are obtained. The initial assumed stresses may be complete polynomials of any order. A postulate in the classification of stress modes is cited in Reference 23 and may be rewritten as

"There exists and only exists $m (=n-r)$ natural deformation modes in a hybrid element. All stress modes in the assumed stress matrices can be classified into m stress mode groups corresponding to m natural deformation modes and a zero energy mode group corresponding rigid-body modes of the element which has n degrees of freedom and r rigid-body modes".

Based on this postulate, a procedure to classify stress modes was proposed. This procedure is summarized as in the following.

Step 1: Derive an initial stress matrix by whichever methods. One may extract some stress modes from the existing stress matrices. The important point to note here is the number of stress modes must not be less than $m(=n-r)$ because there are m mode groups, excluding the zero-energy mode group, into which these stress modes are classified. Rearrange the stress modes in ascending order terms.

Step 2: Pick out the zero-energy stress modes by selecting one stress mode from the initial stress matrix to form an assumed stress matrix \mathbf{P}_0 . Note that \mathbf{P}_0 contains only one stress mode. Then, the element stiffness matrix corresponding to a stress matrix \mathbf{P}_0 can be formulated by using Eqs. 2.3-13 and 2.3-16. If the element stiffness gives a non-zero eigenvalue, the selected stress mode is not a zero-energy mode. Repeat this examination for the next stress mode. After all stress modes in the initial stress matrix are examined, remove all stress modes that give zero eigenvalues and put them into a zero-energy stress mode group.

Step 3: Take a non-zero-energy stress mode to form an assumed stress matrix \mathbf{P}_1 . The first stress mode σ_1 is the representative of a stress mode in stress mode group 1.

Step 4: Select another stress mode next in order from the initial stress matrix and add it into the assumed stress matrix \mathbf{P}_1 . Then, a new stress matrix \mathbf{P}_2 is obtained.

$$\mathbf{P}_2 = [\sigma_1 \quad \sigma_2] \quad (3.1-1)$$

Apply eigenvalue examination to the element stiffness matrix corresponding to \mathbf{P}_2 . If this gives only one non-zero eigenvalue, stress mode σ_2 belongs to the stress mode group 1. Then, repeat this step by selecting the next stress mode and put it into the stress matrix \mathbf{P}_2 in place of stress mode σ_2 . Until two non-zero eigenvalues are obtained from the eigenvalue examination, stress matrix σ_2 is the representative of a stress mode in group 2 of stress modes.

Step 5: Select another stress mode and append that stress mode to the stress matrix \mathbf{P}_2 to form a new stress matrix \mathbf{P}_3 ,

$$\mathbf{P}_3 = [\sigma_1 \quad \sigma_2 \quad \sigma_3] \quad (3.1-2)$$

If three non-zero eigenvalues are obtained, stress matrix σ_3 is the representative of a stress mode in group 3 of stress modes, then go to step 6. If only two non-zero eigenvalues are obtained, stress matrix σ_3 may belong to group 1 or group 2 of stress modes. To determine which stress mode group to which the new stress mode belongs, this stress mode is paired with the existing stress modes. The following new stress matrices are formed:

$$\mathbf{P}'_2 = [\sigma_1 \quad \sigma_3] \quad \text{and} \quad \mathbf{P}''_2 = [\sigma_2 \quad \sigma_3] \quad (3.1-3)$$

So whichever pair gives only one non-zero eigenvalue, all stress modes of that pair belong to the same stress mode group. For example, if the element stiffness corresponding to stress matrix \mathbf{P}'_2 gives one non-zero eigenvalue, stress mode σ_3 is in the same stress mode group as stress mode σ_1 , that is, stress mode group 1.

Step 6: Add one more stress mode into stress matrix \mathbf{P}_3 , and form a new stress matrix \mathbf{P}_4 ,

$$\mathbf{P}_4 = [\sigma_1 \quad \sigma_2 \quad \sigma_3 \quad \sigma_4] \quad (3.1-4)$$

and so on. Repeating the same process until m representatives stress modes that represent m stress mode groups are obtained. These m stress modes are formed into an optimal stress matrix \mathbf{P}_{opt} .

Step 7: In this step, there remains stress modes in the initial stress matrix that have not yet been classified. Any remaining stress mode can be classified by using it to replace each and every stress mode in the stress matrix \mathbf{P}_{opt} in regular order. Once m eigenvalues are obtained, that representative stress mode which is replaced and the remaining stress mode which replaces the stress mode in matrix \mathbf{P}_{opt} belongs to the same stress mode group. Repeat the same process until all remaining stress modes are classified.

Many stress modes derived by different methods can also be classified into m stress mode groups corresponding to m natural deformation modes and the zero-energy mode group corresponding rigid-body modes

For a hybrid element to be free from kinematic deformation modes, the assumed stress matrix should appropriately be constructed by employing the necessary and sufficient condition^[23] stated as follows:

“The number of stress modes in an assumed stress matrix must be equal to or more than $m (=n-r)$ and at least m stress modes in the stress matrix \mathbf{P} must be chosen from m different stress mode groups corresponding to m natural deformation modes of an element which has n degrees of freedom and r rigid-body modes”.

3.2 Optimization with Penalty-Equilibrium Approach

This technique was proposed by Wu and Cheung^[13]. The method can be applied to any assumed stresses to optimize the hybrid element. No modification of the initially assumed stresses is needed.

By ignoring the effect of distributed loads within element, the equilibrium equations can be written as

$$\partial\boldsymbol{\sigma} = \mathbf{0} \quad \text{in } V^e \quad (1.2-4)$$

The introduction of a penalty-equilibrium term into the element energy functional will produce a generalized one of the form

$$\Pi_{R^*}^e(\boldsymbol{\sigma}, \mathbf{u}) = \Pi_R^e - \alpha \int_{V^e} (\partial\boldsymbol{\sigma})^T (\partial\boldsymbol{\sigma}) dV \quad (1.2-18)$$

where α is a penalty factor of large positive number. From the stationary condition $\delta\Pi_{R^*}^e = 0$, when $\alpha \rightarrow \infty$, the last term of Eq. 1.2-18 becomes

$$\int_{V^e} (\partial\boldsymbol{\sigma})^T \delta(\partial\boldsymbol{\sigma}) dV = 0 \quad \text{or} \quad \int_{V^e} (\partial\boldsymbol{\sigma})^T (\partial\boldsymbol{\sigma}) dV = \text{minimize} \quad (3.2-1)$$

This means that the stress equilibrium constraints are imposed on the element in a least-square sense. Substituting Eqs. 2.3-6, 2.3-7 and 2.3-9 into the energy functional $\Pi_{R^*}^e$, we obtain

$$\Pi_{R^*}^e = \boldsymbol{\beta}^T \mathbf{G} \mathbf{q} - \frac{1}{2} \boldsymbol{\beta}^T \mathbf{H} \boldsymbol{\beta} - \alpha \boldsymbol{\beta}^T \mathbf{H}_p \boldsymbol{\beta} \quad (3.2-2)$$

where \mathbf{G} and \mathbf{H} are the same as defined in Eq. 2.3-13 and

$$\mathbf{H}_p = \int_V (\partial \mathbf{P})^T (\partial \mathbf{P}) dV \quad (3.2-3)$$

which is the penalty-equilibrium matrix. By letting $\alpha = \alpha/2$, the energy functional $\Pi_{R^*}^e$ can be rewritten in the form

$$\Pi_{R^*}^e = \boldsymbol{\beta}^T \mathbf{G} \mathbf{q} - \frac{1}{2} \boldsymbol{\beta}^T (\mathbf{H} + \alpha \mathbf{H}_p) \boldsymbol{\beta} \quad (3.2-4)$$

Hence, the element stiffness matrix becomes

$$\mathbf{k} = \mathbf{G}^T (\mathbf{H} + \alpha \mathbf{H}_p)^{-1} \mathbf{G} \quad (3.2-5)$$

3.3 Hybrid Plate Elements Considered

All elements in this study are four-node quadrilateral elements. The displacement field is assumed within an element. Two approaches of formulation are involved. One is in terms of stresses and strains and the other in terms of moments and curvatures. Some elements by other researchers are chosen in order to compare the efficiency among the elements. See Appendix A for more information on element formulation.

In a four-node quadrilateral element, each node contains 3 degrees of freedom or in other words 12 degrees of freedom in an element. It can be shown that there are 3 rigid-body displacement modes in a four-node quadrilateral plate element. Therefore, the minimum number of stress modes to be chosen must not less than 9 (=12-3) in order to guarantee the existence of a solution^[1].

The differences among the elements depend on the stress matrix, the reference coordinates system and the additional displacements used in the element stiffness formulations.

3.3.1 Spilker Elements

Elements LH3, LH4, LH5 and LH11 proposed by Spilker^[15] are the hybrid elements with the Mindlin-type displacement assumption including all components of stresses. The assumed stresses for these elements were chosen so as to satisfy the condition of equilibrium within an element. Only the stress components σ_x , σ_y and τ_{xy} were assumed with completely linear terms and the other components can be obtained by making all stress components in equilibrium. Only elements LH3 and LH4 are considered in this study because elements LH5 and LH11 seem to cause an undesirable element property, that is, shear-locking. The numerical results are shown in Reference 15.

The initially assumed stresses proposed by Spilker has 13 stress parameters that may be written in matrix form as in Eq. 2.3-6 where

$$\mathbf{P} = \begin{bmatrix} 1 & x & y & \cdot & \cdot & \cdot & \cdot & \cdot & \cdot & xy & \cdot & \cdot & \frac{1}{2}x^2 \\ \cdot & \cdot & \cdot & 1 & x & y & \cdot & \cdot & \cdot & \cdot & xy & \cdot & -\frac{1}{2}y^2 \\ \cdot & \cdot & \cdot & \cdot & \cdot & \cdot & \cdot & \cdot & \cdot & \cdot & \cdot & 2 & \cdot \\ \cdot & \cdot & \cdot & \cdot & \cdot & \cdot & 1 & x & y & \cdot & \cdot & xy & \cdot \\ \cdot & 1 & \cdot & \cdot & \cdot & \cdot & \cdot & \cdot & 1 & y & \cdot & x & x \\ \cdot & \cdot & \cdot & \cdot & \cdot & 1 & \cdot & 1 & \cdot & \cdot & x & y & -y \end{bmatrix}_{6 \times 13} \quad (3.3.1-1)$$

$$= [\sigma_1 \quad \sigma_2 \quad \sigma_3 \quad \sigma_4 \quad \sigma_5 \quad \sigma_6 \quad \sigma_7 \quad \sigma_8 \quad \sigma_9 \quad \sigma_{10} \quad \sigma_{11} \quad \sigma_{12} \quad \sigma_{13}]$$

which can be shown to satisfy the homogeneous equilibrium equations.

Element LH3 is a 9- β element obtained by setting $\beta_{10}=\beta_{11}=\beta_{12}=\beta_{13}=0$. Therefore the stress matrix for LH3 becomes

$$\mathbf{P}_{\text{LH3}} = \begin{bmatrix} 1 & x & y & \cdot & \cdot & \cdot & \cdot & \cdot & \cdot \\ \cdot & \cdot & \cdot & 1 & x & y & \cdot & \cdot & \cdot \\ \cdot & \cdot & \cdot & \cdot & \cdot & \cdot & \cdot & \cdot & \cdot \\ \cdot & \cdot & \cdot & \cdot & \cdot & \cdot & 1 & x & y \\ \cdot & 1 & \cdot & \cdot & \cdot & \cdot & \cdot & \cdot & 1 \\ \cdot & \cdot & \cdot & \cdot & \cdot & 1 & \cdot & 1 & \cdot \end{bmatrix}_{6 \times 9} \quad (3.3.1-2)$$

$$= [\sigma_1 \quad \sigma_2 \quad \sigma_3 \quad \sigma_4 \quad \sigma_5 \quad \sigma_6 \quad \sigma_7 \quad \sigma_8 \quad \sigma_9]$$

Element LH4 is a 11- β element obtained by setting $\beta_{12}=\beta_{13}=0$. The stress matrix thus becomes

$$\mathbf{P}_{\text{LH4}} = \begin{bmatrix} 1 & x & y & \cdot & \cdot & \cdot & \cdot & \cdot & \cdot & xy & \cdot \\ \cdot & \cdot & \cdot & 1 & x & y & \cdot & \cdot & \cdot & \cdot & xy \\ \cdot & \cdot & \cdot & \cdot & \cdot & \cdot & \cdot & \cdot & \cdot & \cdot & \cdot \\ \cdot & \cdot & \cdot & \cdot & \cdot & \cdot & 1 & x & y & \cdot & \cdot \\ \cdot & 1 & \cdot & \cdot & \cdot & \cdot & \cdot & \cdot & 1 & y & \cdot \\ \cdot & \cdot & \cdot & \cdot & 1 & \cdot & 1 & \cdot & \cdot & \cdot & x \end{bmatrix}_{6 \times 11} \quad (3.3.1-3)$$

$$= [\sigma_1 \quad \sigma_2 \quad \sigma_3 \quad \sigma_4 \quad \sigma_5 \quad \sigma_6 \quad \sigma_7 \quad \sigma_8 \quad \sigma_9 \quad \sigma_{10} \quad \sigma_{11}]$$

By applying the method of stress classification to the stress matrix shown in Eq. 3.3.1-1, all 13 stress modes can be classified into 9 stress mode groups. The result of the classification is shown in Table 3.3.1-1

Table 3.3.1-1 Stress mode groups of Spilker's assumed stresses after classification.

Mode group	1	$\sigma_1, \sigma_{12}, \sigma_{13}$
	2	σ_2, σ_9
	3	σ_3, σ_8
	4	σ_4
	5	σ_5
	6	σ_6
	7	σ_7
	8	σ_{10}
	9	σ_{11}
Zero-energy mode group	-	

From Table 3.3.1-1, it can be seen that element LH3 contains stress modes belonging to only 7 different stress mode groups rather than 9 stress mode groups. Thus, element LH3 will introduce 2 kinematic deformation modes. However, these two stress modes are generally eliminated by boundary conditions or constrained by element assembly.

Element LH4 was chosen from stress modes belonging to 9 different stress mode groups. Hence, the element stiffness matrix has no spurious kinematic deformation mode.

3.3.2 Dong Element^[21]

Element QHMID: The assumed stresses are

$$\begin{Bmatrix} M_x \\ M_y \\ M_{xy} \\ Q_x \\ Q_y \end{Bmatrix} = \begin{bmatrix} 1 & \cdot & \cdot & \xi & \eta & \cdot & \cdot & \cdot & \cdot & \cdot & \cdot & \cdot & \cdot \\ \cdot & 1 & \cdot & \cdot & \cdot & \xi & \eta & \cdot & \cdot & \cdot & \cdot & \cdot & \cdot \\ \cdot & \cdot & 1 & \cdot & \cdot & \cdot & \xi & \eta & \cdot & \cdot & \cdot & \cdot & \cdot \\ \cdot & \cdot & \cdot & \cdot & \cdot & \cdot & \cdot & \cdot & 1 & \cdot & a_1\eta & a_3\xi & \cdot \\ \cdot & \cdot & \cdot & \cdot & \cdot & \cdot & \cdot & \cdot & \cdot & 1 & b_1\eta & b_3\xi & \cdot \end{bmatrix} \begin{Bmatrix} \beta_1 \\ \beta_2 \\ \vdots \\ \vdots \\ \beta_{13} \end{Bmatrix} \quad (3.3.2-1)$$

And the additional displacements are

$$\begin{Bmatrix} \theta_{x\lambda} \\ \theta_{y\lambda} \\ w_\lambda \end{Bmatrix} = \begin{bmatrix} \xi^2 & \eta^2 & \cdot & \cdot \\ \cdot & \cdot & \xi^2 & \eta^2 \\ \cdot & \cdot & \cdot & \cdot \end{bmatrix} \begin{Bmatrix} \lambda_1 \\ \vdots \\ \lambda_4 \end{Bmatrix} \quad (3.3.2-2)$$

where a_1 , a_3 , b_1 and b_3 are the same as that in Eq. A1-10 in Appendix A.

3.3.3 Henshell Element

Element QRDH : The assumed stresses are

$$\begin{Bmatrix} M_x \\ M_y \\ M_{xy} \\ Q_x \\ Q_y \end{Bmatrix} = \begin{bmatrix} 1 & x & y & \cdot & \cdot & \cdot & \cdot & \cdot & \cdot & xy & \cdot \\ \cdot & \cdot & \cdot & 1 & x & y & \cdot & \cdot & \cdot & \cdot & xy \\ \cdot & \cdot & \cdot & \cdot & \cdot & \cdot & 1 & x & y & \cdot & \cdot \\ \cdot & 1 & \cdot & \cdot & \cdot & \cdot & \cdot & \cdot & -1 & y & \cdot \\ \cdot & \cdot & \cdot & \cdot & 1 & 1 & \cdot & -1 & \cdot & \cdot & x \end{bmatrix} \begin{Bmatrix} \beta_1 \\ \beta_2 \\ \vdots \\ \vdots \\ \beta_{11} \end{Bmatrix} \quad (3.3.3-1)$$

with no additional displacements.

3.3.4 Hamhim Elements

Hamhim^[24] proposed many hybrid plate elements, namely, LH-OP, HSC1-OP, HSC2-OP, QHMID-OP and QRDH-OP. The stress matrices for these elements were chosen from existing elements by utilizing the method of stress classification. Since Hamhim's stress matrices are extracted from the existing elements, no variety of stress modes are offered by the choices. The QHMID-OP element, modified from Dong QHMID element and the QRDH-OP element, modified from Henshell QRDH element were considered to be efficient. Thus, only the QHMID-OP and QRDH-OP elements are considered in this study.

Element QHMID-OP : The assumed stresses are

$$\begin{Bmatrix} M_x \\ M_y \\ M_{xy} \\ Q_x \\ Q_y \end{Bmatrix} = \begin{bmatrix} 1 & \cdot & \cdot & \xi & \cdot & \cdot & \cdot & \cdot & \cdot \\ \cdot & 1 & \cdot & \cdot & \xi & \cdot & \cdot & \cdot & \cdot \\ \cdot & \cdot & 1 & \cdot & \cdot & \cdot & \cdot & \cdot & \eta \\ \cdot & \cdot & \cdot & \cdot & \cdot & 1 & \cdot & a_1\eta & a_3\xi \\ \cdot & \cdot & \cdot & \cdot & \cdot & \cdot & 1 & b_1\eta & b_3\xi \end{bmatrix} \begin{Bmatrix} \beta_1 \\ \beta_2 \\ \vdots \\ \vdots \\ \beta_9 \end{Bmatrix} \quad (3.3.4-1)$$

where a_1 , a_3 , b_1 and b_3 are the same as that in Eq. A1-10 on Appendix A.

This element contains one kinematic deformation mode because the fourth stress mode is in a zero-energy mode group when the element shape is irregular.

Element QRDH-OP : The assumed stresses are

$$\begin{Bmatrix} M_x \\ M_y \\ M_{xy} \\ Q_x \\ Q_y \end{Bmatrix} = \begin{bmatrix} 1 & x & y & \cdot & \cdot & \cdot & \cdot & xy & \cdot \\ \cdot & \cdot & \cdot & 1 & x & y & \cdot & \cdot & xy \\ \cdot & \cdot & \cdot & \cdot & \cdot & \cdot & 1 & \cdot & \cdot \\ \cdot & 1 & \cdot & \cdot & \cdot & \cdot & \cdot & y & \cdot \\ \cdot & \cdot & \cdot & \cdot & 1 & 1 & \cdot & \cdot & x \end{bmatrix} \begin{Bmatrix} \beta_1 \\ \beta_2 \\ \vdots \\ \vdots \\ \beta_9 \end{Bmatrix} \quad (3.3.4-2)$$

3.3.5 Proposed Elements

In present study, the stress matrix is assumed initially as being complete polynomials. All stress components are uncoupled. The initial 50- β stress matrix complete to third-order polynomials is

$$\mathbf{P} = \begin{matrix}
 \begin{matrix} 1 & 2 & 3 & 4 & 5 & 6 & 7 & 8 & 9 & 10 & 11 & 12 & 13 & 14 & 15 \\
 \left[\begin{array}{cccccccccccccc}
 1 & x & y & \cdot & \cdot & \cdot & \cdot & \cdot & \cdot & \cdot & \cdot & \cdot & \cdot & \cdot & \cdot \\
 \cdot & \cdot & \cdot & 1 & x & y & \cdot & \cdot & \cdot & \cdot & \cdot & \cdot & \cdot & \cdot & \cdot \\
 \cdot & \cdot & \cdot & \cdot & \cdot & \cdot & \cdot & \cdot & \cdot & \cdot & \cdot & \cdot & \cdot & \cdot & \cdot \\
 \cdot & \cdot & \cdot & \cdot & \cdot & \cdot & 1 & x & y & \cdot & \cdot & \cdot & \cdot & \cdot & \cdot \\
 \cdot & \cdot & \cdot & \cdot & \cdot & \cdot & \cdot & \cdot & \cdot & 1 & x & y & \cdot & \cdot & \cdot \\
 \cdot & \cdot & \cdot & \cdot & \cdot & \cdot & \cdot & \cdot & \cdot & \cdot & \cdot & \cdot & 1 & x & y
 \end{array} \right. \\
 \\
 \begin{matrix} 16 & 17 & 18 & 19 & 20 & 21 & 22 & 23 & 24 & 25 & 26 & 27 & 28 & 29 & 30 \\
 \left[\begin{array}{cccccccccccccc}
 x^2 & xy & y^2 & \cdot & \cdot & \cdot & \cdot & \cdot & \cdot & \cdot & \cdot & \cdot & \cdot & \cdot & \cdot \\
 \cdot & \cdot & \cdot & x^2 & xy & y^2 & \cdot & \cdot & \cdot & \cdot & \cdot & \cdot & \cdot & \cdot & \cdot \\
 \cdot & \cdot & \cdot & \cdot & \cdot & \cdot & \cdot & \cdot & \cdot & \cdot & \cdot & \cdot & \cdot & \cdot & \cdot \\
 \cdot & \cdot & \cdot & \cdot & \cdot & \cdot & x^2 & xy & y^2 & \cdot & \cdot & \cdot & \cdot & \cdot & \cdot \\
 \cdot & \cdot & \cdot & \cdot & \cdot & \cdot & \cdot & \cdot & \cdot & x^2 & xy & y^2 & \cdot & \cdot & \cdot \\
 \cdot & \cdot & \cdot & \cdot & \cdot & \cdot & \cdot & \cdot & \cdot & \cdot & \cdot & \cdot & x^2 & xy & y^2
 \end{array} \right. \\
 \\
 \begin{matrix} 31 & 32 & 33 & 34 & 35 & 36 & 37 & 38 & 39 & 40 & 41 & 42 \\
 \left[\begin{array}{cccccccccccc}
 x^3 & x^2y & x^2y & y^3 & \cdot & \cdot & \cdot & \cdot & \cdot & \cdot & \cdot & \cdot \\
 \cdot & \cdot & \cdot & \cdot & x^3 & x^2y & xy^2 & y^3 & \cdot & \cdot & \cdot & \cdot \\
 \cdot & \cdot & \cdot & \cdot & \cdot & \cdot & \cdot & \cdot & \cdot & \cdot & \cdot & \cdot \\
 \cdot & \cdot & \cdot & \cdot & \cdot & \cdot & \cdot & \cdot & \cdot & x^3 & x^2y & xy^2 & y^3 \\
 \cdot & \cdot & \cdot & \cdot & \cdot & \cdot & \cdot & \cdot & \cdot & \cdot & \cdot & \cdot
 \end{array} \right. \\
 \\
 \begin{matrix} 43 & 44 & 45 & 46 & 47 & 48 & 49 & 50 \\
 \left[\begin{array}{cccccc}
 \cdot & \cdot & \cdot & \cdot & \cdot & \cdot \\
 \cdot & \cdot & \cdot & \cdot & \cdot & \cdot \\
 \cdot & \cdot & \cdot & \cdot & \cdot & \cdot \\
 x^3 & x^2y & x^2y & y^3 & \cdot & \cdot \\
 \cdot & \cdot & \cdot & \cdot & x^3 & x^2y & x^2y & y^3
 \end{array} \right]_{6 \times 50}
 \end{matrix}
 \end{matrix}
 \end{matrix} \tag{3.3.5-1}$$

All 50-stress modes can be classified into 9 stress mode groups plus an additional zero-energy mode group. The classification is tabulated in Table 3.3.5-1.

Table 3.3.5-1 Stress mode groups of proposed assumed stresses after classification.

Mode group	1	$\sigma_1, \sigma_{11}, \sigma_{16}, \sigma_{18}, \sigma_{43}, \sigma_{45}$
	2	$\sigma_3, \sigma_8, \sigma_{26}, \sigma_{32}, \sigma_{34}, \sigma_{39}, \sigma_{41}$
	3	$\sigma_4, \sigma_{15}, \sigma_{19}, \sigma_{21}, \sigma_{48}, \sigma_{50}$
	4	$\sigma_5, \sigma_9, \sigma_{29}, \sigma_{35}, \sigma_{37}, \sigma_{40}, \sigma_{42}$
	5	$\sigma_7, \sigma_{22}, \sigma_{24}$
	6	$\sigma_{10}, \sigma_{25}, \sigma_{27}$
	7	$\sigma_{12}, \sigma_{44}, \sigma_{46}$
	8	$\sigma_{13}, \sigma_{28}, \sigma_{30}$
	9	$\sigma_{14}, \sigma_{47}, \sigma_{49}$
Zero-energy mode group		$\sigma_2, \sigma_6, \sigma_{17}, \sigma_{20}, \sigma_{23}, \sigma_{31}, \sigma_{33}, \sigma_{36}, \sigma_{38}$

From the necessary and sufficient conditions given in Sec. 3.1, the stress matrix, which is free from kinematic deformation modes, can be obtained as

$$\mathbf{P} = \begin{bmatrix} 1 & \cdot & \cdot & \cdot & \cdot & y & \cdot & \cdot & \cdot \\ \cdot & 1 & \cdot & \cdot & \cdot & \cdot & x & \cdot & \cdot \\ \cdot & \cdot & \cdot & \cdot & \cdot & \cdot & \cdot & \cdot & \cdot \\ \cdot & \cdot & 1 & \cdot & \cdot & \cdot & \cdot & \cdot & \cdot \\ \cdot & \cdot & \cdot & 1 & \cdot & \cdot & \cdot & y & \cdot \\ \cdot & \cdot & \cdot & \cdot & 1 & \cdot & \cdot & \cdot & x \end{bmatrix}_{6 \times 9} \quad (3.3.5-1)$$

$$= [\sigma_1 \quad \sigma_4 \quad \sigma_7 \quad \sigma_{10} \quad \sigma_{13} \quad \sigma_3 \quad \sigma_5 \quad \sigma_{12} \quad \sigma_{14}]$$

After some observations on the results using well-behaved hybrid plate elements, the stress matrix in Eq. 3.3.5-1 may be expressed in natural reference coordinates with some constants accounting for distortion of element geometry. Eventually, the element HBP1 is proposed. The stress matrix for this element is

$$\mathbf{P}_{\text{HBP1}} = \begin{bmatrix} 1 & \cdot & \cdot & \cdot & \cdot & a_1\eta & a_3\xi & \cdot & \cdot \\ \cdot & 1 & \cdot & \cdot & \cdot & b_1\eta & b_3\xi & \cdot & \cdot \\ \cdot & \cdot & \cdot & \cdot & \cdot & \cdot & \cdot & \cdot & \cdot \\ \cdot & \cdot & 1 & \cdot & \cdot & \cdot & b_1\eta & a_3\xi & \cdot \\ \cdot & \cdot & \cdot & 1 & \cdot & \cdot & a_1\eta & a_3\xi & \cdot \\ \cdot & \cdot & \cdot & \cdot & 1 & \cdot & b_1\eta & b_3\xi \end{bmatrix}_{6 \times 9} \quad (3.3.5-2)$$

where a_1 , a_3 , b_1 and b_3 are the same as that in Eq. A1-10 on Appendix A.

Note that when the element is rectangular in shape, a_3 and b_1 vanish. Thus, the stress matrix in Eq. 3.3.5-2 is the same as that in Eq. 3.3.5-1.

The additional displacements are taken into consideration to construct element HBP2. The element has the same stress matrix as the element HBP1. From Eq. A.1-19 in Appendix A, the additional displacements are added to the lateral displacements only. The other two rotational degrees of freedom obviously have no effects on the formulation. Hence, the additional displacements for element HBP2 are

$$\mathbf{N}_\lambda = \begin{bmatrix} \cdot & \cdot \\ \cdot & \cdot \\ \xi^2 & \eta^2 \end{bmatrix} \quad (3.3.5-3)$$

3.4 Evaluation of Element Stiffness Matrix

After obtaining the stress matrix and the additional displacements, the element stiffness matrix can be formulated. At first the matrices

$$\begin{aligned} \mathbf{H} &= \int_V \mathbf{P}^T \mathbf{S} \mathbf{P} dV \\ \mathbf{G} &= \int_V \mathbf{P}^T \mathbf{B} dV \\ \mathbf{R} &= \int_V (\mathbf{D}^T \mathbf{P})^T \mathbf{N}_\lambda dV \end{aligned} \quad (2.3-13)$$

are evaluated by employing the stress matrix and the additional displacements obtained previously. After this all matrices in Eq.2.3-13 are put together into the partitioned matrix

$$\begin{bmatrix} \cdot & \cdot & \mathbf{G}^T \\ \cdot & \cdot & -\mathbf{R}^T \\ \mathbf{G} & -\mathbf{R} & -\mathbf{H} \end{bmatrix}$$

Applying reverse Gauss elimination to the first partition, we obtain

$$\begin{bmatrix} \mathbf{G}^T \mathbf{H}^{-1} \mathbf{G} - (\mathbf{G}^T \mathbf{H}^{-1} \mathbf{R})(\mathbf{R}^T \mathbf{H}^{-1} \mathbf{R})^{-1} (\mathbf{R}^T \mathbf{H}^{-1} \mathbf{G}) & \cdot & \cdot \\ -\mathbf{R}^T \mathbf{H}^{-1} \mathbf{G} & \mathbf{R}^T \mathbf{H}^{-1} \mathbf{R} & \cdot \\ \mathbf{G} & -\mathbf{R} & -\mathbf{H} \end{bmatrix}$$

Therefore, the topleftmost partition after elimination is the element stiffness matrix.

After analysis, the nodal displacements in each element are required to compute the stress parameters from the relation

$$\boldsymbol{\beta} = (\mathbf{H}^{-1} \mathbf{G} - \mathbf{H}^{-1} \mathbf{R} (\mathbf{R}^T \mathbf{H}^{-1} \mathbf{R})^{-1} (\mathbf{R}^T \mathbf{H}^{-1} \mathbf{G})) \mathbf{q} \quad (3.4-1)$$

In practice, the stress parameters can be evaluated by forward substitution instead of explicit multiplication and inversion. Finally, all stress components in each element are calculated from

$$\boldsymbol{\sigma} = \mathbf{P} \boldsymbol{\beta} \quad (2.3-6)$$

by specifying the coordinates to the stress matrix.

Chapter IV

Efficiency of Hybrid Plate Elements

All hybrid plate elements considered were tested and compared with respect to accuracy of displacement and force. Mesh refinement was performed to test for convergence of results. Shear-locking effects were tested by varying the plate thickness. Locking occurred when plate thickness becomes small. The sensitivity of element properties with regard to the aspect ratio was also examined. In addition, invariance property of all elements was tested.

The method of optimization employed in the present study to improve the results has some shortcomings and limitations. The proof of this is shown in the next section. However, this method is still applicable if some conditions are imposed.

In all tests, the results are normalized by using analytical solutions from thin-plate theory^[31].

4.1 Shortcomings and Limitations of Optimization Method

The optimization used in this study was carried out through the penalty-equilibrium matrix, \mathbf{H}_p . Instead of obtaining better results, this method tends to cause unstable element stiffness matrix in some elements. For the sake of simplicity, the proof is shown for a plane stress problem.

The homogeneous equilibrium equations can be expressed as

$$\partial \boldsymbol{\sigma} = \mathbf{0} \quad (1.2-4)$$

or, in matrix form,

$$\begin{bmatrix} \frac{\partial}{\partial x} & \cdot & \frac{\partial}{\partial y} \\ \cdot & \frac{\partial}{\partial y} & \frac{\partial}{\partial x} \end{bmatrix} \begin{Bmatrix} \sigma_x \\ \sigma_y \\ \tau_{xy} \end{Bmatrix} = \mathbf{0} \quad (4.1-1)$$

From the relation $\boldsymbol{\sigma} = \mathbf{P}\boldsymbol{\beta}$, Eq. 1.2-4 becomes

$$(\partial \mathbf{P})\boldsymbol{\beta} = \mathbf{0}$$

Let

$$\mathbf{P} = \begin{bmatrix} P_{11} & P_{12} & \cdots & P_{1i} & \cdots & P_{1\beta} \\ P_{21} & P_{22} & \cdots & P_{2i} & \cdots & P_{2\beta} \\ P_{31} & P_{32} & \cdots & P_{3i} & \cdots & P_{3\beta} \end{bmatrix}_{3 \times \beta} \quad (4.1-2)$$

where β is the number of stress parameters or stress modes.

Performing matrix multiplication of $\partial \mathbf{P}$ explicitly, we obtain

$$\begin{aligned} \partial \mathbf{P} &= \begin{bmatrix} \frac{\partial}{\partial x} & \cdot & \frac{\partial}{\partial y} \\ \cdot & \frac{\partial}{\partial y} & \frac{\partial}{\partial x} \end{bmatrix} \begin{bmatrix} P_{11} & P_{12} & \cdots & P_{1i} & \cdots & P_{1\beta} \\ P_{21} & P_{22} & \cdots & P_{2i} & \cdots & P_{2\beta} \\ P_{31} & P_{32} & \cdots & P_{3i} & \cdots & P_{3\beta} \end{bmatrix}_{3 \times \beta} \\ &= \begin{bmatrix} \frac{\partial P_{11}}{\partial x} + \frac{\partial P_{31}}{\partial y} & \frac{\partial P_{12}}{\partial x} + \frac{\partial P_{32}}{\partial y} & \cdots & \frac{\partial P_{1i}}{\partial x} + \frac{\partial P_{3i}}{\partial y} & \cdots & \frac{\partial P_{1\beta}}{\partial x} + \frac{\partial P_{3\beta}}{\partial y} \\ \frac{\partial P_{21}}{\partial y} + \frac{\partial P_{31}}{\partial x} & \frac{\partial P_{22}}{\partial y} + \frac{\partial P_{32}}{\partial x} & \cdots & \frac{\partial P_{2i}}{\partial y} + \frac{\partial P_{3i}}{\partial x} & \cdots & \frac{\partial P_{2\beta}}{\partial y} + \frac{\partial P_{3\beta}}{\partial x} \end{bmatrix}_{2 \times \beta} \end{aligned}$$

If stress mode i does not satisfy Eq. 1.2-4, all entries of $\partial \mathbf{P}$ vanish except that on column i . The matrix $\partial \mathbf{P}$ then becomes

$$= \begin{bmatrix} \cdot & \cdot & \cdots & \frac{\partial P_{1i}}{\partial x} + \frac{\partial P_{3i}}{\partial y} & \cdots & \cdot \\ \cdot & \cdot & \cdots & \frac{\partial P_{2i}}{\partial y} + \frac{\partial P_{3i}}{\partial x} & \cdots & \cdot \end{bmatrix}_{2 \times \beta}$$

For this step, the penalty-equilibrium matrix is

$$\mathbf{H}_p = \int_V (\partial \mathbf{P})^T (\partial \mathbf{P}) dV \quad (4.1-3)$$

$$= \begin{bmatrix} \cdot & \cdot & \cdots & \cdot & \cdots & \cdot \\ \cdot & \cdot & \cdots & \cdot & \cdots & \cdot \\ \vdots & \vdots & \ddots & \vdots & \ddots & \vdots \\ \text{Row } i & \cdot & \cdot & \int_V \left(\frac{\partial P_{1i}}{\partial x} + \frac{\partial P_{3i}}{\partial y} \right)^2 + \left(\frac{\partial P_{2i}}{\partial y} + \frac{\partial P_{3i}}{\partial x} \right)^2 dV & \cdot & \cdot \\ \vdots & \vdots & \ddots & \vdots & \ddots & \vdots \\ \cdot & \cdot & \cdots & \cdot & \cdots & \cdot \end{bmatrix}_{\beta \times \beta}$$

Obviously, only matrix entry (i,i) does not vanish. If this entry vanishes through the integration, it is worthless to employ this optimization method.

Let us take a look at the matrix multiplication for matrix \mathbf{H} in Eq. 2.3-13,

$$\mathbf{H} = \int_V \mathbf{P}^T \mathbf{S} \mathbf{P} dV$$

We then obtain

$$\begin{aligned}
\mathbf{H} &= \int_V \begin{bmatrix} P_{11} & P_{21} & P_{31} \\ P_{12} & P_{22} & P_{32} \\ \vdots & \vdots & \vdots \\ P_{1i} & P_{2i} & P_{3i} \\ \vdots & \vdots & \vdots \\ P_{1\beta} & P_{2\beta} & P_{3\beta} \end{bmatrix} \begin{bmatrix} S_{11} & S_{13} & S_{31} \\ S_{21} & S_{22} & S_{32} \\ S_{31} & S_{32} & S_{33} \end{bmatrix} \begin{bmatrix} P_{11} & P_{12} & \cdots & P_{1i} & \cdots & P_{1\beta} \\ P_{21} & P_{22} & \cdots & P_{2i} & \cdots & P_{2\beta} \\ P_{31} & P_{32} & \cdots & P_{3i} & \cdots & P_{3\beta} \end{bmatrix} dV \\
&= \int_V \begin{bmatrix} \sum_{l=1}^3 \left(\sum_{k=1}^3 P_{k1} S_{kl} \right) P_{l1} & \sum_{l=1}^3 \left(\sum_{k=1}^3 P_{k1} S_{kl} \right) P_{l2} & \cdots & \sum_{l=1}^3 \left(\sum_{k=1}^3 P_{k1} S_{kl} \right) P_{li} & \cdots & \sum_{l=1}^3 \left(\sum_{k=1}^3 P_{k1} S_{kl} \right) P_{l\beta} \\ \sum_{l=1}^3 \left(\sum_{k=1}^3 P_{k2} S_{kl} \right) P_{l1} & \sum_{l=1}^3 \left(\sum_{k=1}^3 P_{k2} S_{kl} \right) P_{l2} & \cdots & \sum_{l=1}^3 \left(\sum_{k=1}^3 P_{k2} S_{kl} \right) P_{li} & \cdots & \sum_{l=1}^3 \left(\sum_{k=1}^3 P_{k2} S_{kl} \right) P_{l\beta} \\ \vdots & \vdots & \ddots & \vdots & \ddots & \vdots \\ \sum_{l=1}^3 \left(\sum_{k=1}^3 P_{ki} S_{kl} \right) P_{l1} & \sum_{l=1}^3 \left(\sum_{k=1}^3 P_{ki} S_{kl} \right) P_{l2} & \cdots & \sum_{l=1}^3 \left(\sum_{k=1}^3 P_{ki} S_{kl} \right) P_{li} & \cdots & \sum_{l=1}^3 \left(\sum_{k=1}^3 P_{ki} S_{kl} \right) P_{l\beta} \\ \vdots & \vdots & \ddots & \vdots & \ddots & \vdots \\ \sum_{l=1}^3 \left(\sum_{k=1}^3 P_{k\beta} S_{kl} \right) P_{l1} & \sum_{l=1}^3 \left(\sum_{k=1}^3 P_{k\beta} S_{kl} \right) P_{l2} & \cdots & \sum_{l=1}^3 \left(\sum_{k=1}^3 P_{k\beta} S_{kl} \right) P_{li} & \cdots & \sum_{l=1}^3 \left(\sum_{k=1}^3 P_{k\beta} S_{kl} \right) P_{l\beta} \end{bmatrix} dV \quad (4.1-4)
\end{aligned}$$

Note that stress mode i contributes to only row i and column i of matrix \mathbf{H} .

From Eq. 4.1-3 and 4.1-4, let $\alpha \rightarrow \infty$, then

$$\mathbf{H} + \alpha \mathbf{H}_p = \begin{bmatrix} \oplus & \oplus & \cdots & \oplus & \cdots & \oplus \\ \oplus & \oplus & \cdots & \oplus & \cdots & \oplus \\ \vdots & \vdots & \ddots & \vdots & \ddots & \vdots \\ \oplus & \oplus & \cdots & \infty & \cdots & \oplus \\ \vdots & \vdots & \ddots & \vdots & \ddots & \vdots \\ \oplus & \oplus & \cdots & \oplus & \cdots & \oplus \end{bmatrix} \quad \begin{array}{l} \text{Col. } i \\ \text{Row } i \\ \beta \times \beta \end{array}$$

And the inversion of above matrix gives

$$(\mathbf{H} + \alpha \mathbf{H}_p)^{-1} = \begin{bmatrix} \otimes & \otimes & \cdots & 0 & \cdots & \otimes \\ \otimes & \otimes & \cdots & 0 & \cdots & \otimes \\ \vdots & \vdots & \ddots & \vdots & \ddots & \vdots \\ 0 & 0 & \cdots & 0 & \cdots & 0 \\ \vdots & \vdots & \ddots & \vdots & \ddots & \vdots \\ \otimes & \otimes & \cdots & 0 & \cdots & \otimes \end{bmatrix} \quad \begin{array}{l} \text{Col. } i \\ \text{Row } i \\ \beta \times \beta \end{array} \quad (4.1-5)$$

where \oplus and \otimes are generally non-zero values.

Note: Stress mode i does not make a contribution in matrix $(\mathbf{H} + \alpha \mathbf{H}_p)^{-1}$.

Now take a look at the matrix multiplication for matrix \mathbf{G} in Eq. 2.3-13,

$$\begin{aligned}
 \mathbf{G} &= \int_V \mathbf{P}^T \mathbf{B} dV \\
 &= \int_V \begin{bmatrix} P_{11} & P_{21} & P_{31} \\ P_{12} & P_{22} & P_{32} \\ \vdots & \vdots & \vdots \\ P_{1i} & P_{2i} & P_{3i} \\ \vdots & \vdots & \vdots \\ P_{1\beta} & P_{2\beta} & P_{3\beta} \end{bmatrix} \begin{bmatrix} B_{11} & B_{12} & \cdots & B_{1q} \\ B_{21} & B_{22} & \cdots & B_{2q} \\ B_{31} & B_{32} & \cdots & B_{3q} \end{bmatrix}_{3 \times q} dV \\
 &= \int_V \begin{bmatrix} \sum_{k=1}^3 P_{k1} B_{k1} & \sum_{k=1}^3 P_{k1} B_{k2} & \cdots & \sum_{k=1}^3 P_{k1} B_{kq} \\ \sum_{k=1}^3 P_{k2} B_{k1} & \sum_{k=1}^3 P_{k2} B_{k2} & \cdots & \sum_{k=1}^3 P_{k2} B_{kq} \\ \vdots & \vdots & \ddots & \vdots \\ \sum_{k=1}^3 P_{ki} B_{k1} & \sum_{k=1}^3 P_{ki} B_{k2} & \cdots & \sum_{k=1}^3 P_{ki} B_{kq} \text{ Row } \hat{i} \\ \vdots & \vdots & \ddots & \vdots \\ \sum_{k=1}^3 P_{k\beta} B_{k1} & \sum_{k=1}^3 P_{k\beta} B_{k2} & \cdots & \sum_{k=1}^3 P_{k\beta} B_{kq} \end{bmatrix} dV \\
 &= \begin{bmatrix} G_{11} & G_{12} & \cdots & G_{1q} \\ G_{21} & G_{22} & \cdots & G_{2q} \\ \vdots & \vdots & \ddots & \vdots \\ G_{i1} & G_{i2} & \cdots & G_{iq} \text{ Row } \hat{i} \\ \vdots & \vdots & \ddots & \vdots \\ G_{\beta 1} & G_{\beta 2} & \cdots & G_{\beta q} \end{bmatrix}_{\beta \times q} \quad (4.1-6)
 \end{aligned}$$

where q is the number of degrees of freedom in the element.

It can be seen that stress mode i contributes to only row i of matrix \mathbf{G} .

From Eqs. 4.1-5 and 4.1-6, the element stiffness matrix can be obtained from

$$\mathbf{k} = \mathbf{G}^T (\mathbf{H} + \alpha \mathbf{H}_p)^{-1} \mathbf{G} \quad (3.2-5)$$

$$\begin{aligned}
&= \begin{bmatrix} G_{11} & G_{21} & \cdots & G_{i1} & \cdots & G_{\beta 1} \\ G_{12} & G_{22} & \cdots & G_{i2} & \cdots & G_{\beta 2} \\ \vdots & \vdots & \ddots & \vdots & \ddots & \vdots \\ G_{1q} & G_{2q} & \cdots & G_{iq} & \cdots & G_{\beta q} \end{bmatrix} \begin{bmatrix} \otimes & \otimes & \cdots & 0 & \cdots & \otimes \\ \otimes & \otimes & \cdots & 0 & \cdots & \otimes \\ \vdots & \vdots & \ddots & \vdots & \ddots & \vdots \\ 0 & 0 & \cdots & 0 & \cdots & 0 \\ \vdots & \vdots & \ddots & \vdots & \ddots & \vdots \\ \otimes & \otimes & \cdots & 0 & \cdots & \otimes \end{bmatrix} \begin{bmatrix} G_{11} & G_{12} & \cdots & G_{1q} \\ G_{21} & G_{22} & \cdots & G_{2q} \\ \vdots & \vdots & \ddots & \vdots \\ G_{i1} & G_{i2} & \cdots & G_{iq} \\ \vdots & \vdots & \ddots & \vdots \\ G_{\beta 1} & G_{\beta 2} & \cdots & G_{\beta q} \end{bmatrix} \\
&= \begin{bmatrix} \Delta & \Delta & \cdots & 0 & \cdots & \Delta \\ \Delta & \Delta & \cdots & 0 & \cdots & \Delta \\ \vdots & \vdots & \ddots & \vdots & \ddots & \vdots \\ \Delta & \Delta & \cdots & 0 & \cdots & \Delta \\ \vdots & \vdots & \ddots & \vdots & \ddots & \vdots \\ \Delta & \Delta & \cdots & 0 & \cdots & \Delta \end{bmatrix}_{q \times \beta} \begin{bmatrix} G_{11} & G_{12} & \cdots & G_{1q} \\ G_{21} & G_{22} & \cdots & G_{2q} \\ \vdots & \vdots & \ddots & \vdots \\ G_{i1} & G_{i2} & \cdots & G_{iq} \\ \vdots & \vdots & \ddots & \vdots \\ G_{\beta 1} & G_{\beta 2} & \cdots & G_{\beta q} \end{bmatrix}_{\beta \times q} \\
\mathbf{k} &= \begin{bmatrix} \square & \square & \cdots & \square & \cdots & \square \\ \square & \square & \cdots & \square & \cdots & \square \\ \vdots & \vdots & \ddots & \vdots & \ddots & \vdots \\ \square & \square & \cdots & \square & \cdots & \square \\ \vdots & \vdots & \ddots & \vdots & \ddots & \vdots \\ \square & \square & \cdots & \square & \cdots & \square \end{bmatrix}_{q \times q}
\end{aligned} \tag{4.1-7}$$

where Δ and \square are generally non-zero values.

The formulation of the example element stiffness matrix so far shows that stress mode i which does not satisfy the equilibrium equations gives no contribution to the element stiffness matrix. The stress matrix in Eq. 4.1-2 is likely to have less stress modes than an ordinary one. Consequently, when the stress matrix consists of insufficient stress modes, this method opens up an opportunity to cause undesirable spurious kinematic deformation modes in the element and may cause failure in the solutions.

To illustrate how the optimization method works, some assumed stress matrices, namely, OPT9EQ, OPT13-1, OPT13-2 and OPT15 are proposed. All of these stress matrices have different stress modes except that only the first 9 stress modes **are the same and in equilibrium**.

$$\mathbf{P}_{\text{OPT9EQ}} = \begin{bmatrix} 1 & y & \cdot & \cdot & \cdot & x & xy & \cdot & \cdot \\ \cdot & \cdot & 1 & x & \cdot & \cdot & \cdot & y & xy \\ \cdot & \cdot & \cdot & \cdot & \cdot & \cdot & \cdot & \cdot & \cdot \\ \cdot & \cdot & \cdot & \cdot & 1 & \cdot & \cdot & \cdot & \cdot \\ \cdot & \cdot & \cdot & \cdot & \cdot & 1 & y & \cdot & \cdot \\ \cdot & \cdot & \cdot & \cdot & \cdot & \cdot & \cdot & 1 & x \end{bmatrix}_{6 \times 9} \tag{4.1-8}$$

$$\mathbf{P}_{\text{OPT13-1}} = \begin{bmatrix} 1 & y & \cdot & \cdot & \cdot & x & xy & \cdot & \cdot & \cdot & \cdot & \cdot & \cdot \\ \cdot & \cdot & 1 & x & \cdot & \cdot & \cdot & y & xy & \cdot & \cdot & \cdot & \cdot \\ \cdot & \cdot & \cdot & \cdot & \cdot & \cdot & \cdot & \cdot & \cdot & \cdot & \cdot & \cdot & \cdot \\ \cdot & \cdot & \cdot & \cdot & 1 & \cdot & \cdot & \cdot & \cdot & \cdot & \cdot & \cdot & \cdot \\ \cdot & \cdot & \cdot & \cdot & \cdot & 1 & y & \cdot & \cdot & 1 & y & \cdot & \cdot \\ \cdot & \cdot & \cdot & \cdot & \cdot & \cdot & \cdot & 1 & x & \cdot & \cdot & 1 & x \end{bmatrix}_{6 \times 13} \quad (4.1-9)$$

$$\mathbf{P}_{\text{OPT13-2}} = \begin{bmatrix} 1 & y & \cdot & \cdot & \cdot & x & xy & \cdot & \cdot & x^2 & \cdot & \cdot & \cdot \\ \cdot & \cdot & 1 & x & \cdot & \cdot & \cdot & y & xy & \cdot & y^2 & \cdot & \cdot \\ \cdot & \cdot & \cdot & \cdot & \cdot & \cdot & \cdot & \cdot & \cdot & \cdot & \cdot & \cdot & \cdot \\ \cdot & \cdot & \cdot & \cdot & 1 & \cdot & \cdot & \cdot & \cdot & \cdot & \cdot & \cdot & \cdot \\ \cdot & \cdot & \cdot & \cdot & \cdot & 1 & y & \cdot & \cdot & \cdot & \cdot & x^2 & \cdot \\ \cdot & \cdot & \cdot & \cdot & \cdot & \cdot & \cdot & 1 & x & \cdot & \cdot & \cdot & y^2 \end{bmatrix}_{6 \times 13} \quad (4.1-10)$$

$$\mathbf{P}_{\text{OPT15}} = \begin{bmatrix} 1 & y & \cdot & \cdot & \cdot & x & xy & \cdot & \cdot & xy & \cdot & x^2 & \cdot & \cdot & \cdot \\ \cdot & \cdot & 1 & x & \cdot & \cdot & \cdot & y & xy & \cdot & xy & \cdot & y^2 & \cdot & \cdot \\ \cdot & \cdot & \cdot & \cdot & \cdot & \cdot & \cdot & \cdot & \cdot & \cdot & \cdot & \cdot & \cdot & \cdot & \cdot \\ \cdot & \cdot & \cdot & \cdot & 1 & \cdot & \cdot & \cdot & \cdot & y & \cdot & xy & \cdot & 1 & 1 \\ \cdot & \cdot & \cdot & \cdot & \cdot & 1 & y & \cdot & \cdot & x & x & \cdot & xy & x^2 & \cdot \\ \cdot & \cdot & \cdot & \cdot & \cdot & \cdot & \cdot & 1 & x & \cdot & y & \cdot & \cdot & \cdot & y^2 \end{bmatrix}_{6 \times 15} \quad (4.1-11)$$

Tests showed that all stress matrices above yield the same results no matter what the second partitioned part of \mathbf{P} is, if that part does not satisfy the equilibrium conditions. This implies that **the optimization by the penalty-equilibrium matrix just simply eliminates those stress modes that are not in equilibrium from the formulation of the element stiffness matrix.**

Nevertheless, this optimization method is still applicable but one should pay attention in choosing the stress matrix. The stress matrix should contain at least m stress modes that satisfy equilibrium equations to guarantee sufficiency of stress modes. See Sec.3.1 for the method of choosing appropriate stress modes.

4.2 Test for Convergence

4.2.1 Rectangular Plate

For the purpose of checking solution convergence, the mesh refinement used was gradually refined. A square plate $2L$ on each side and total thickness t or $2h$ was tested. Only a quadrant of the plate was analyzed due to symmetry of the plate. A quadrant is subdivided into a uniform N_{el} by N_{el} mesh as illustrated in Fig.4.2.1-1.

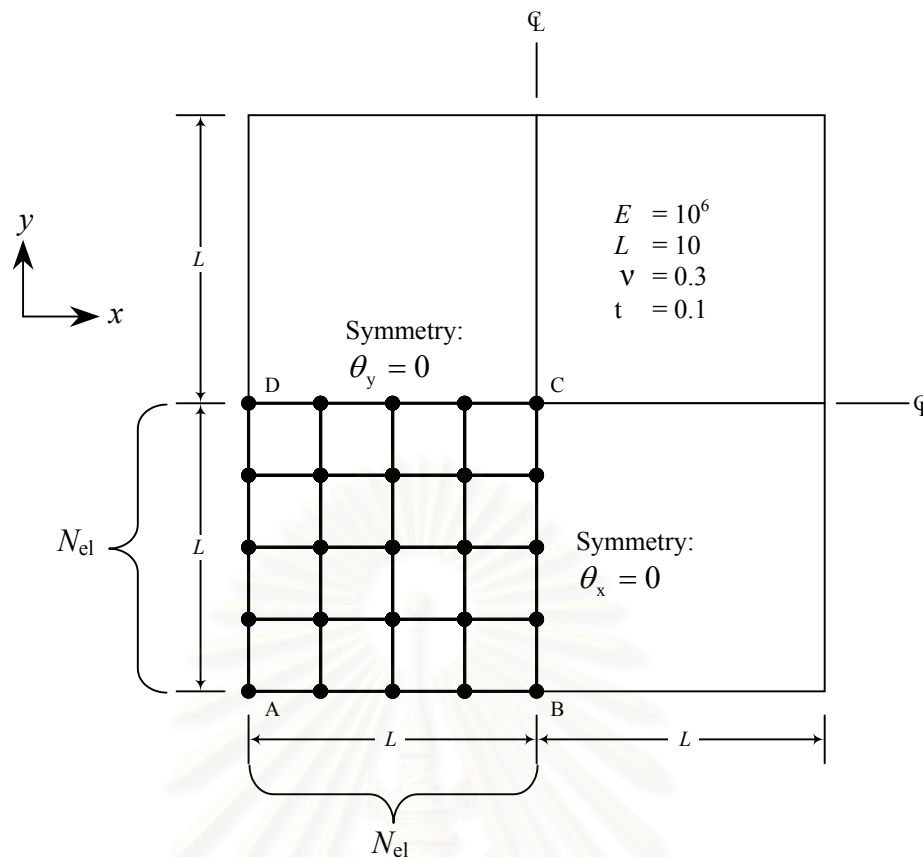


Figure 4.2.1-1 A square plate for convergent tests.

The number of subdivisions N_{el} used in each direction is 2, 4, 6, 8 and 10. Two types of support conditions were considered. The simply supported boundary conditions are denoted by SS1 or SS2 and the clamped boundary conditions are denoted by C. The displacement boundary conditions are tabulated in Table 4.2.1-1.

Table 4.2.1-1 Corresponding constraints of forces and displacements with respect to various edge conditions

Edge Conditions	Boundary conditions on displacements
Free (F)	-
Soft-Simply Supported (SS1)	$w = 0$
Hard-Simply Supported (SS2)	$w = \theta_t = 0$
Clamped (C)	$w = \theta_t = \theta_n = 0$

In addition, two types of loading were applied to the plate. UL denotes the uniformly distributed loads with density q and CL denotes a concentrated load P applied at the center of the plate.

Several cases were tested under various combinations of boundary conditions and loads, namely, SS2-UL, SS2-CL, C-UL and C-CL. For displacement, the analysis results are illustrated in Fig. 4.2.1-2 through Fig. 4.2.1-5. Only the boundary conditions SS2-UL and C-UL were examined for moments and the results are illustrated in Fig.4.2.1-6 and Fig. 4.2.1-7.

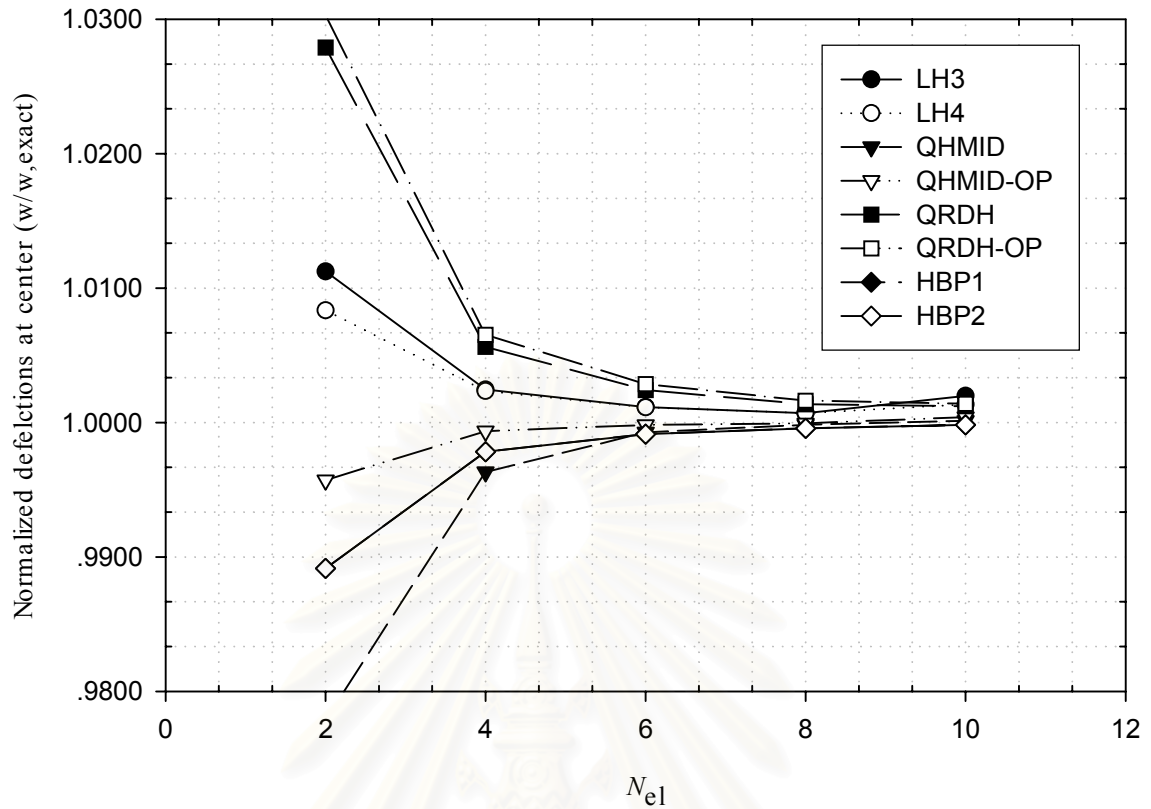


Figure 4.2.1-2 Convergence of central deflections of square plate with SS2-UL.

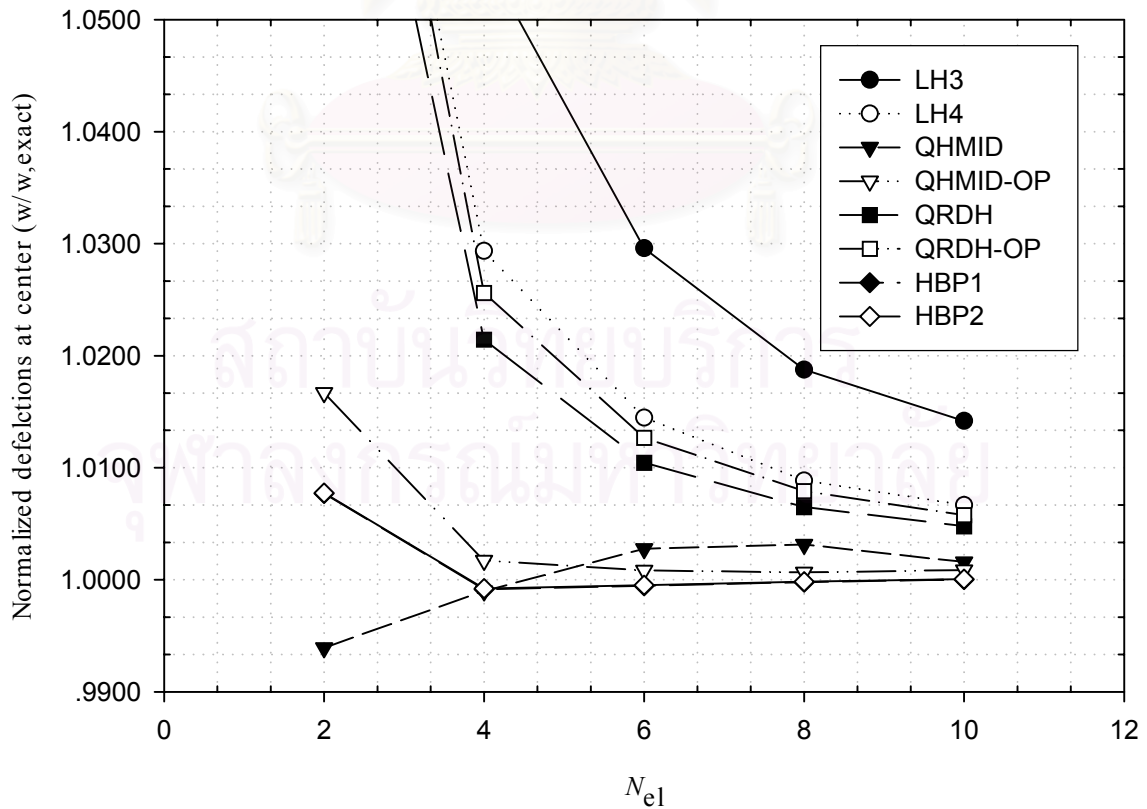


Figure 4.2.1-3 Convergence of central deflections of square plate with SS2-CL.

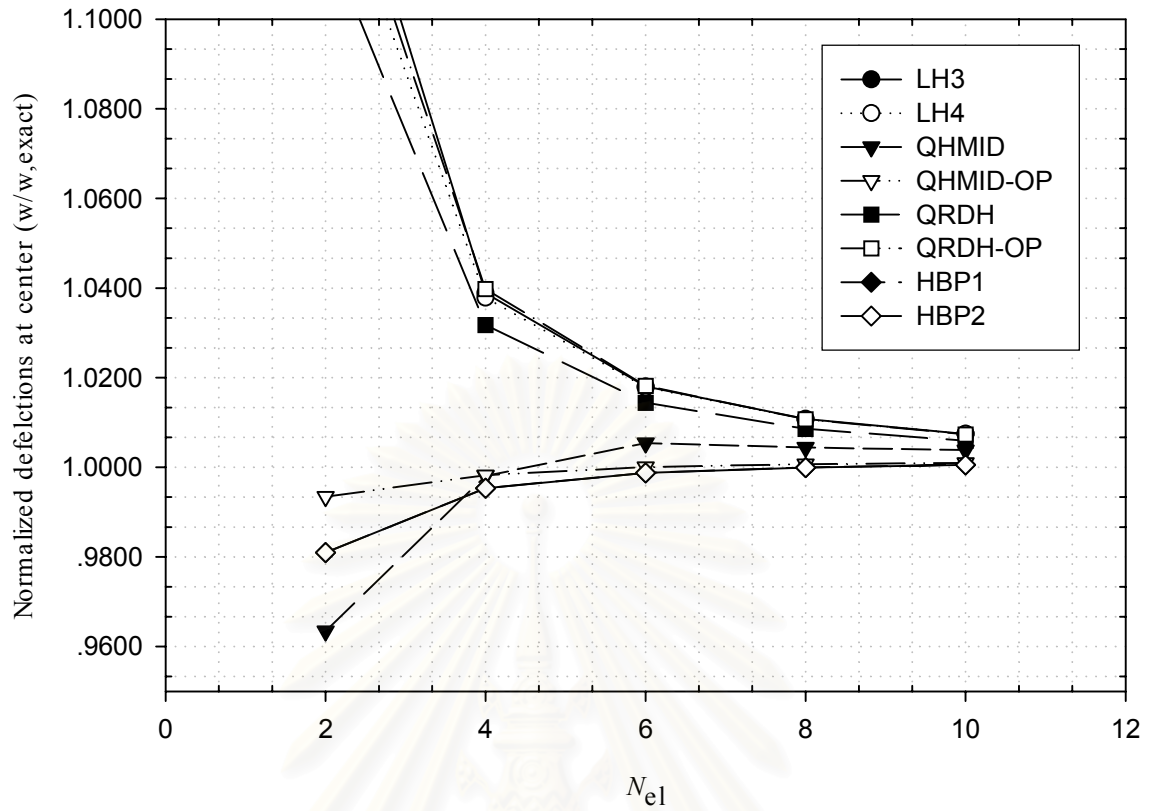


Figure 4.2.1-4 Convergence of central deflections of square plate with C-UL.

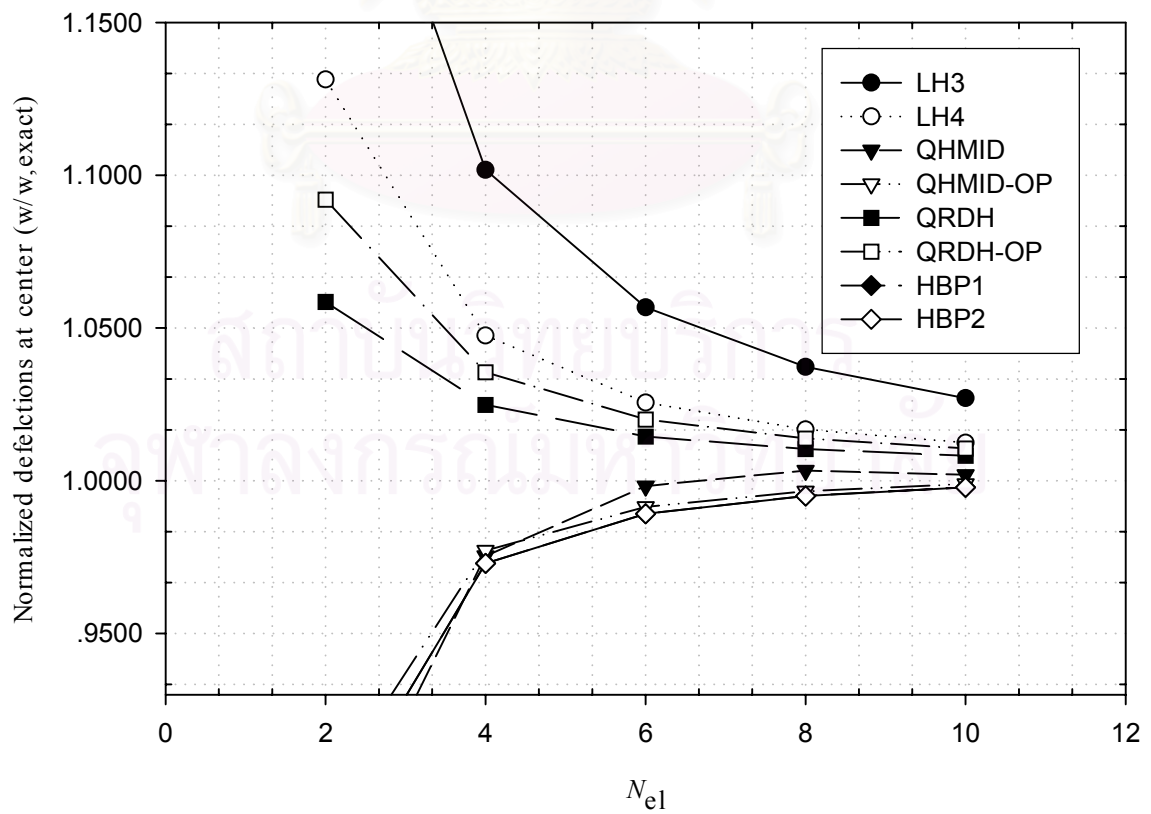


Figure 4.2.1-5 Convergence of central deflections of square plate with C-CL.

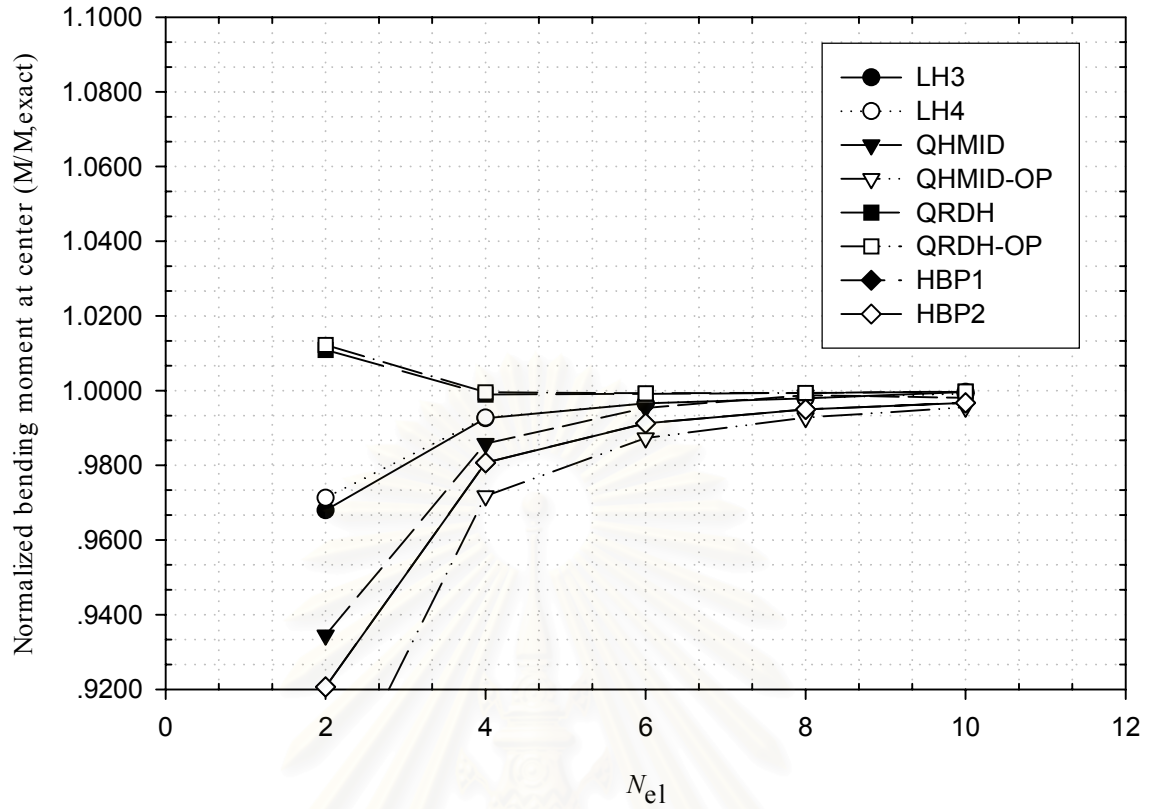


Figure 4.2.1-6 Convergence of central moments of square plate with SS2-UL.

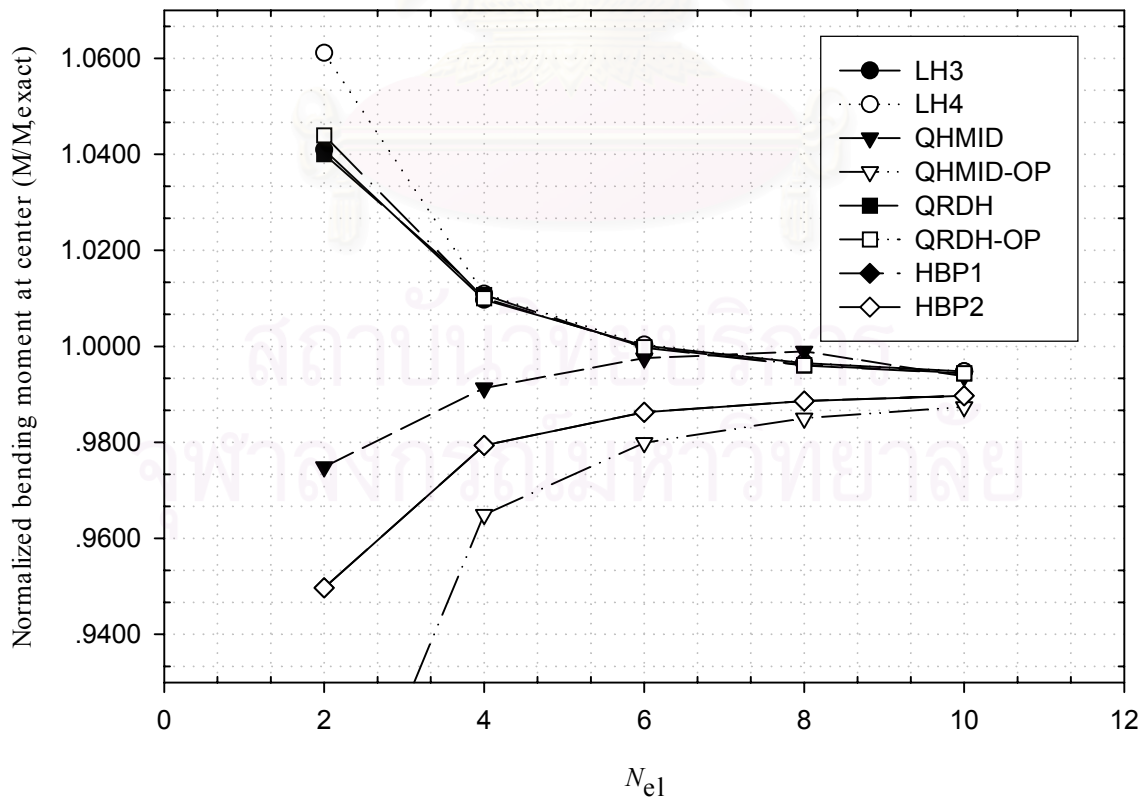


Figure 4.2.1-7 Convergence of central moments of square plate with C-UL.

Tests showed that, unlike the displacement model, hybrid plate elements yield non-monotonic convergence. The element LH4 is the stiffer element than element LH3 in all cases because of the higher number of stress modes used. Most hybrid elements give more than 95 percent accuracy of displacement and moment for $N_{el} \geq 4$. Elements QHMID, QHMID-OP, HBP1 and HBP2 show best convergence of displacement. For $N_{el} = 4$, the deviation of displacement from the exact value is less than 1 percent except in the C-CL case where it is about 3 percent. The element QHMID-OP gives less accuracy on moment than others, particularly in the C-UL case. The results for elements HBP1 and HBP2 differ only slightly. The additional displacements do not affect the element results for this test.

4.2.2 Circular Plate

Convergence study was extended to the circular plate as well. The plate is subjected to either a uniformly distributed load (UL) or a central concentrated load (CL) with two types of boundary conditions, SS1 and C. Due to symmetry of the plate, only a quadrant of the plate was considered. Three different meshes used for the plate are shown in Fig. 4.2.2-1. The analysis results are illustrated in Fig. 4.2.2-2 to Fig. 4.2.2-7.

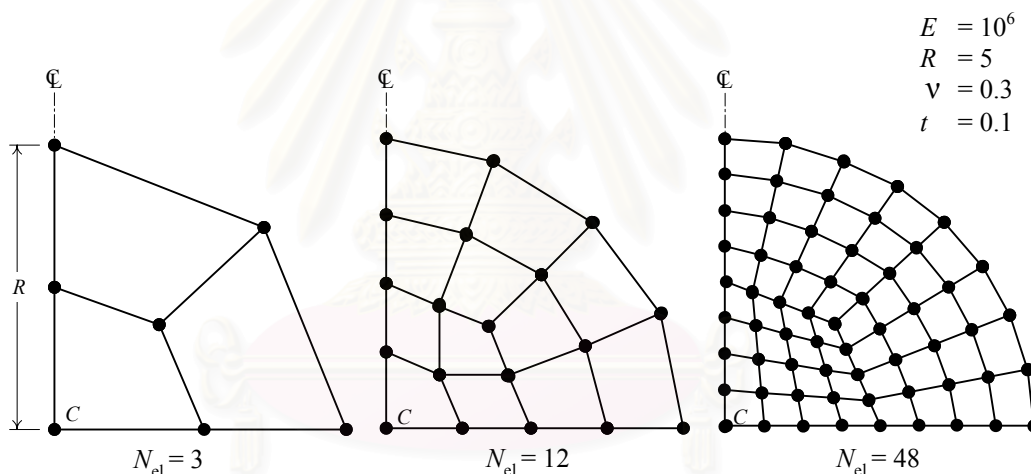


Figure 4.2.2-1 Three meshes for quadrant of a circular plate.

From the results, the elements QHMID, LH3 and HBP2 are considered to be the best elements. It should be noted that elements HBP1 and HBP2 yield different results. Element HBP2 can achieve more accurate results for irregular element geometry than element HBP1.

Almost all elements give the same convergence of moment except element LH4.

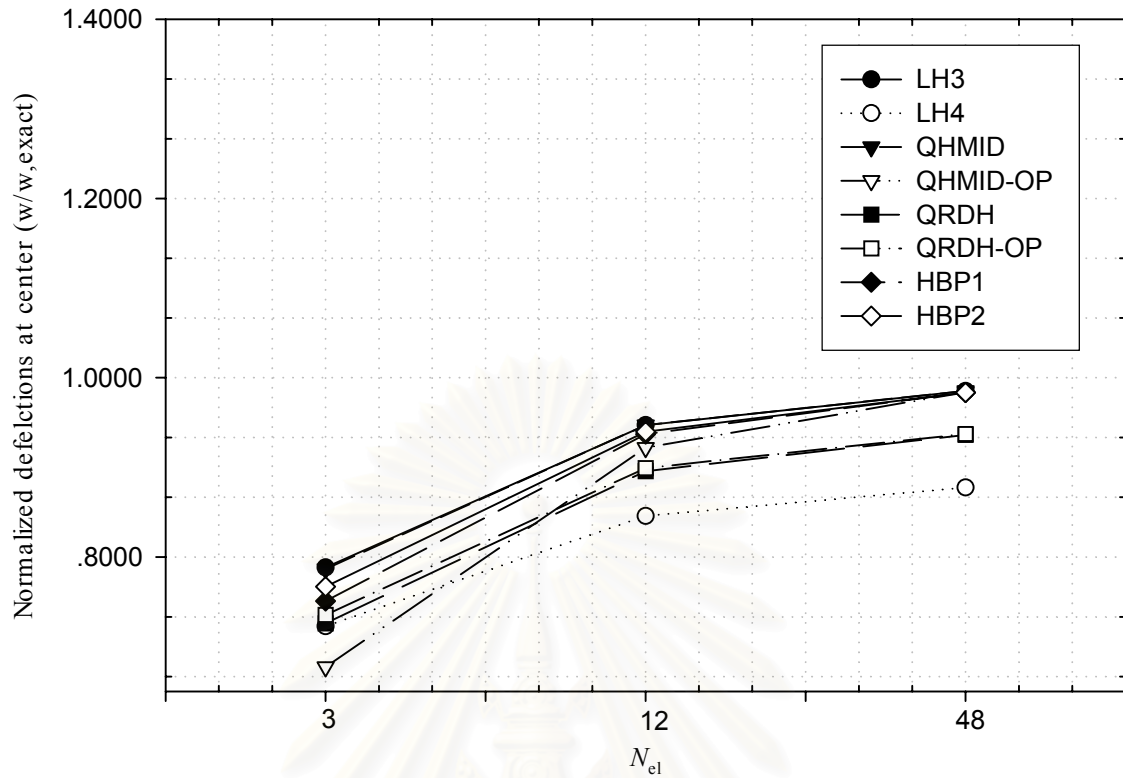


Figure 4.2.2-2 Convergence of central deflections of circular plate with SS1-UL.

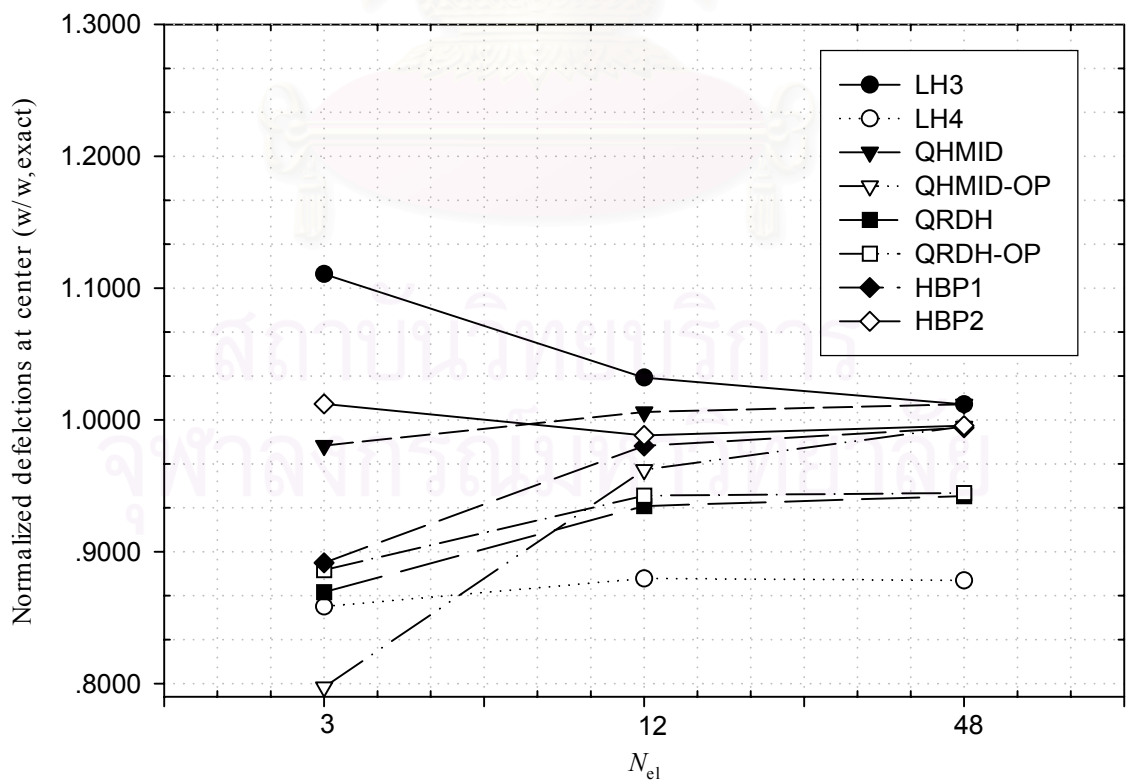


Figure 4.2.2-3 Convergence of central deflections of circular plate with SS1-CL.

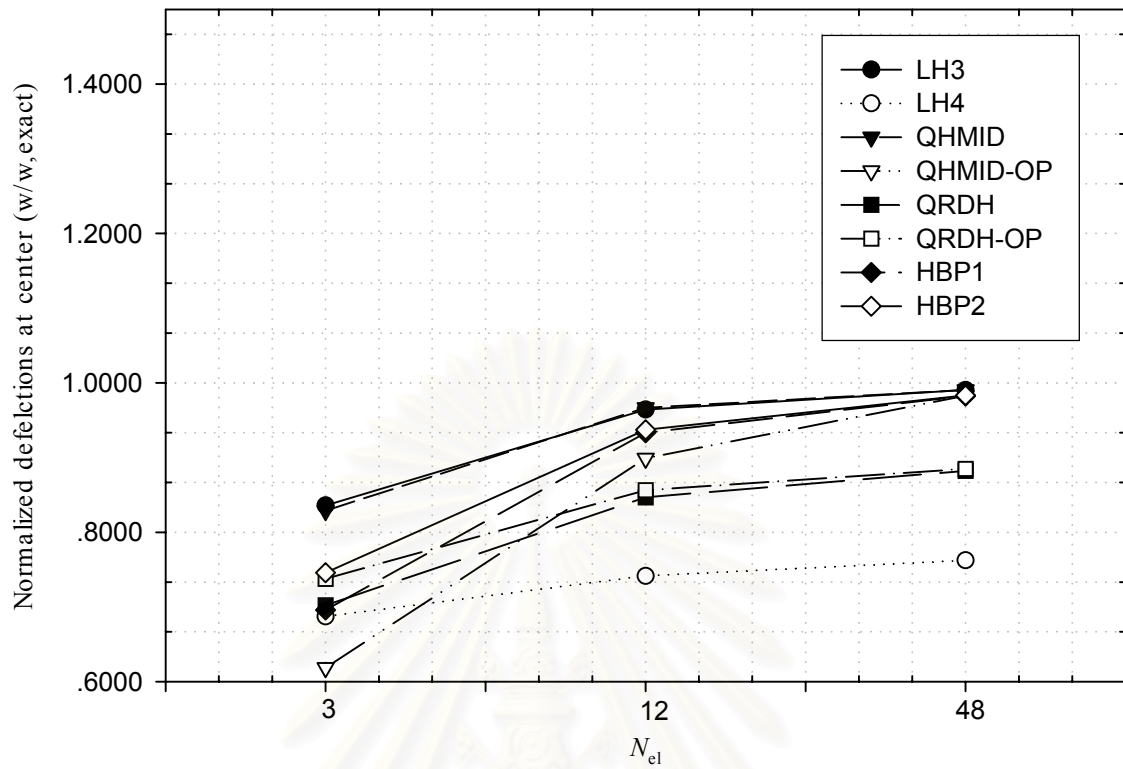


Figure 4.2.2-4 Convergence of central deflections of circular plate with C-UL.

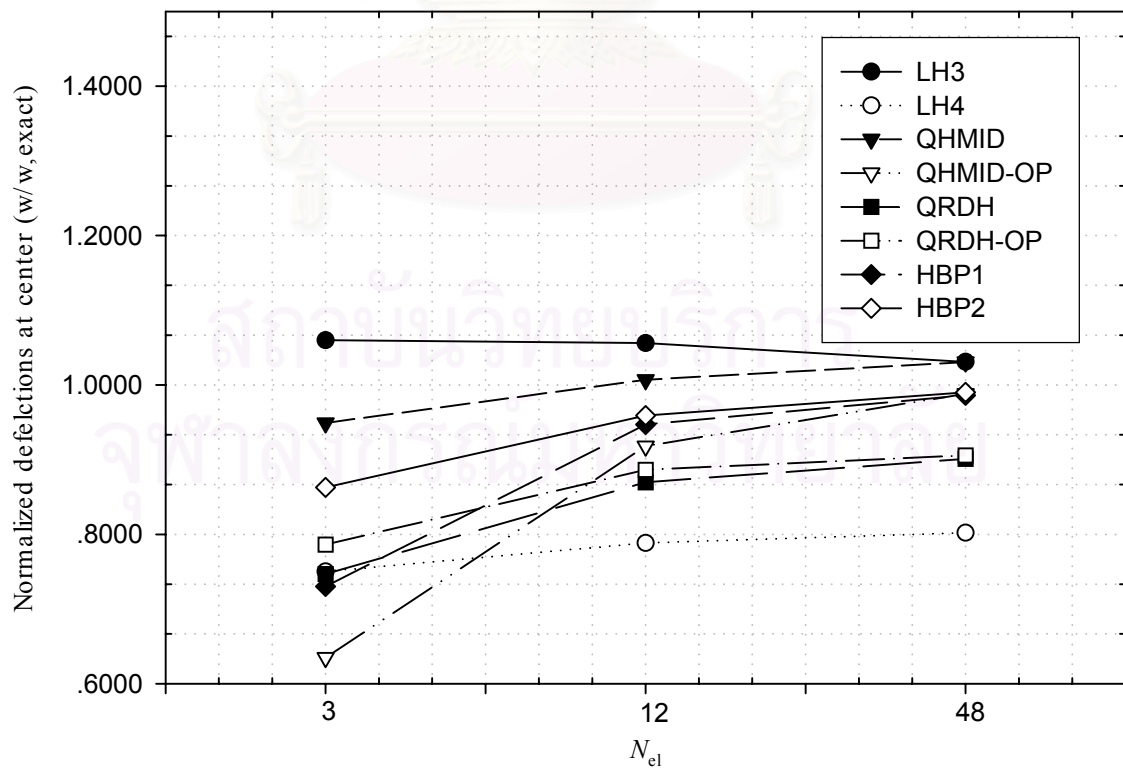


Figure 4.2.2-5 Convergence of central deflections of circular plate with C-CL.

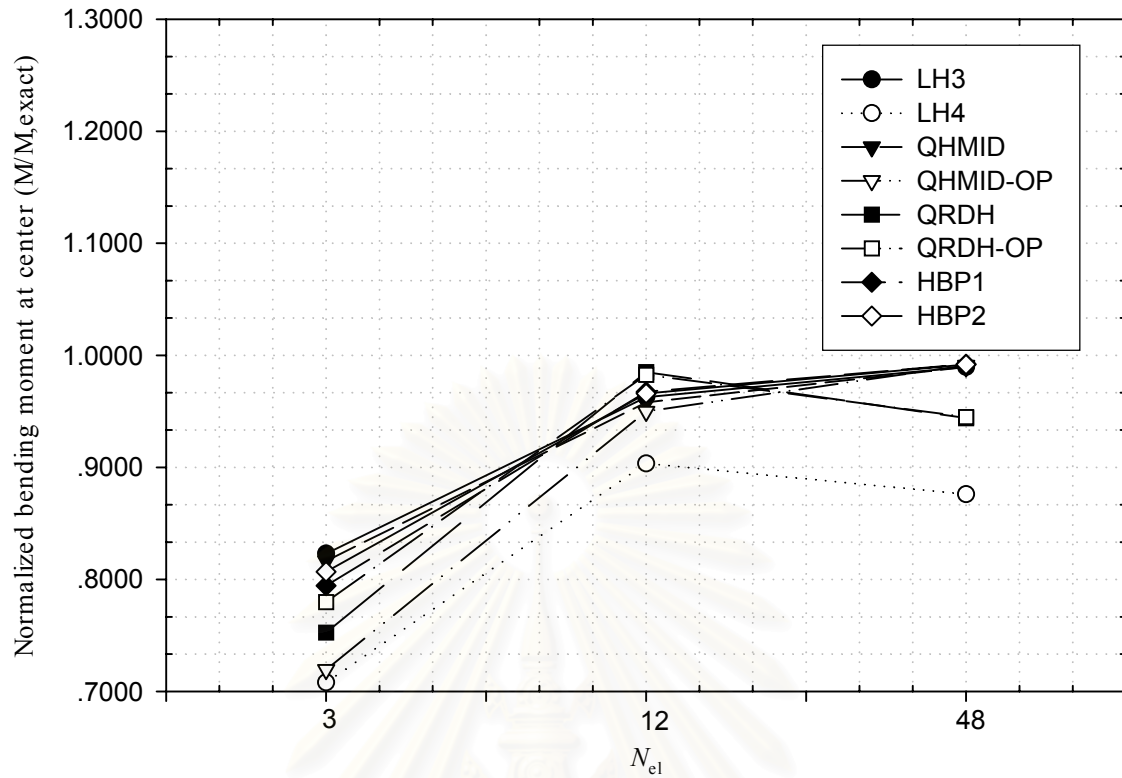


Figure 4.2.2-6 Convergence of central moments of circular plate with SS1-UL.

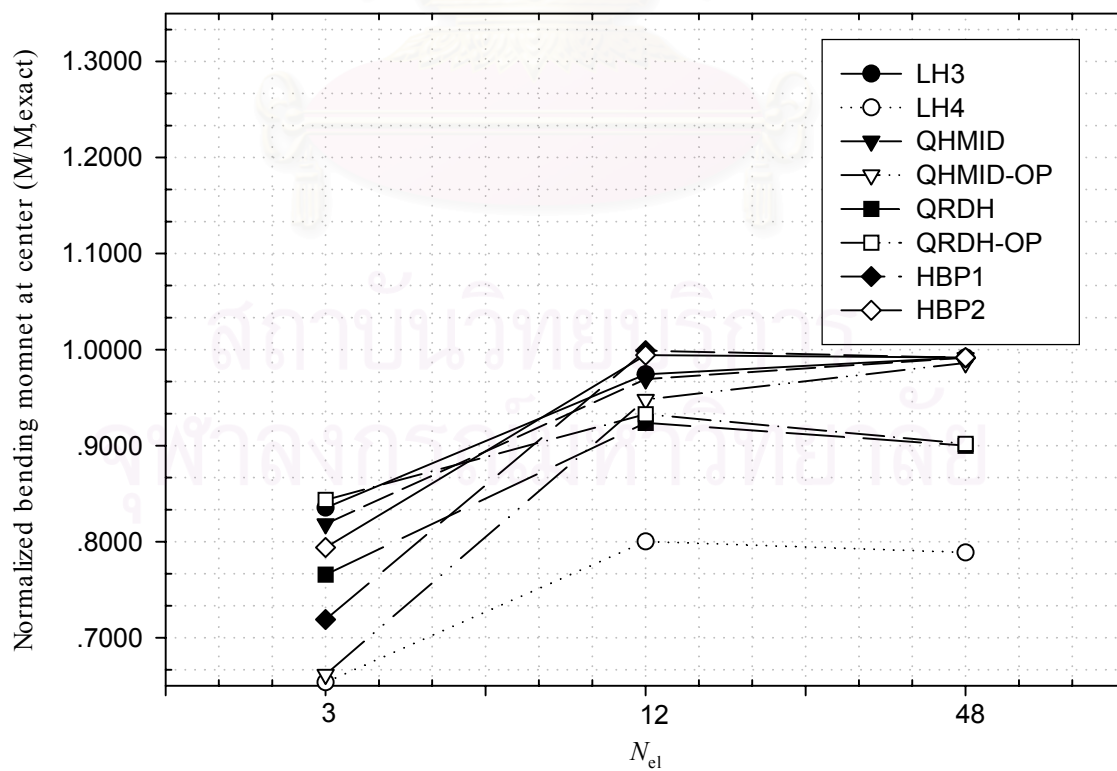


Figure 4.2.2-7 Convergence of central moments of circular plate with C-CL.

4.2.3 Thin Rhombic Plate

A simply supported thin rhombic plate subjected to uniform loading was also analyzed. The mesh, material and geometric constants are given in Fig 4.2.3-1.

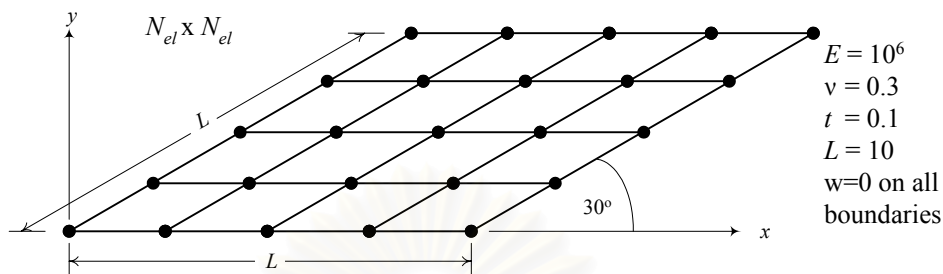


Figure 4.2.3-1 Simply supported thin rhombic plate.

Only the boundary condition SS1 was considered. The normalized deflections and moments at the center of the plate are illustrated in Fig. 4.2.3-2 and Fig. 4.2.3-3, respectively.

For $N_{el} \geq 4$, element QHMID-OP and HBP2 yield stable and accurate displacements. Most elements show the same convergence and accuracy on moment at the center of the plate.

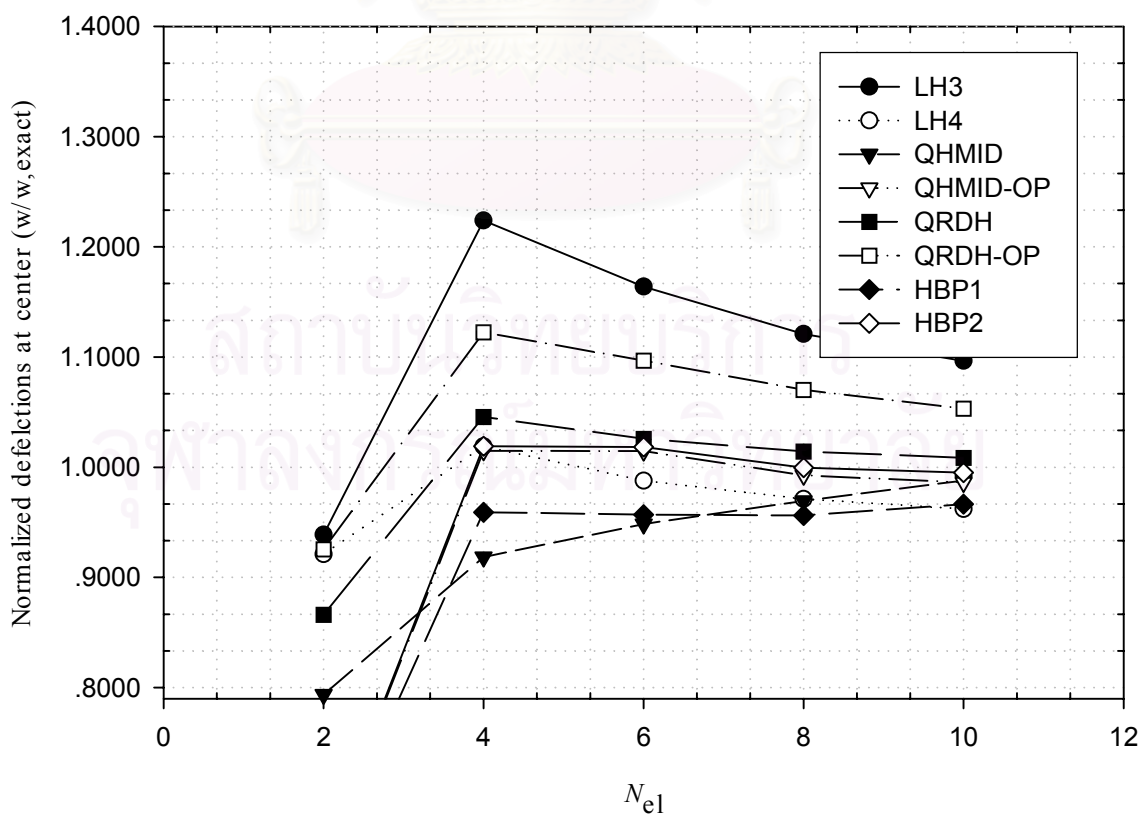


Figure 4.2.3-2 Convergence of central deflections of rhombic plate with SS1-UL.

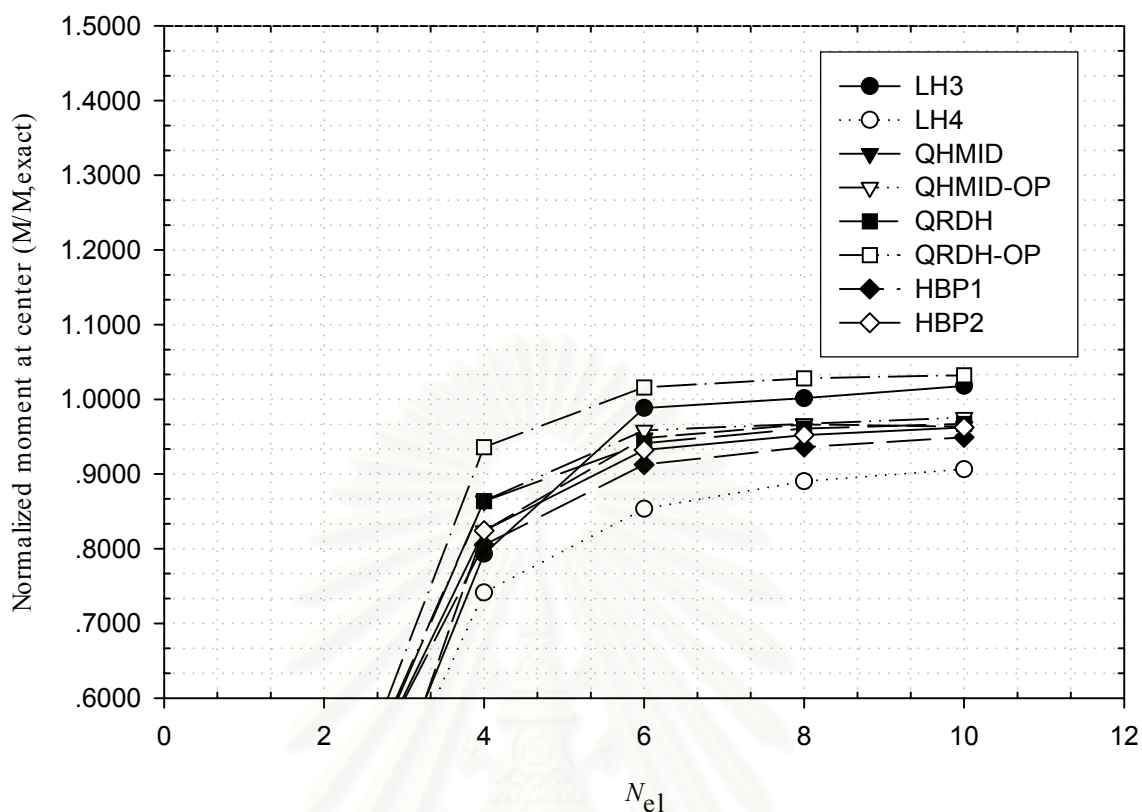


Figure 4.2.3-3 Convergence of central moments of rhombic plate with SS1-UL.

4.2.4 Cantilever Plate

The last test on convergence was conducted on a cantilever plate. The plate dimensions and material properties are given in Fig. 4.2.4-1. This plate is subdivided into N_{el} equal-sided elements. Tip point load and moment are applied to the plate as indicated.

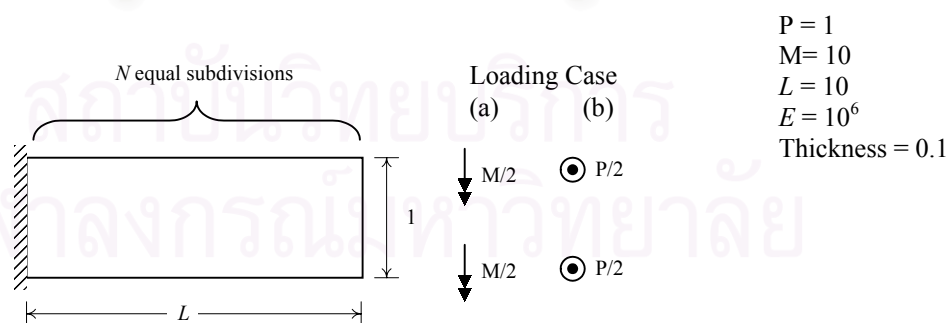


Figure 4.2.4-1 Cantilever plate (beam) subjected to (a) Moment (b) Tip load.

This test concentrates on the convergence of the tip deflection due to the different types of load. The results are illustrated in Fig 4.2.4-2 and Fig 4.2.4-3. All elements give the same behavior in both cases. Among the compared elements, the element QRDH-OP yields the most accuracy for point load at the tip.

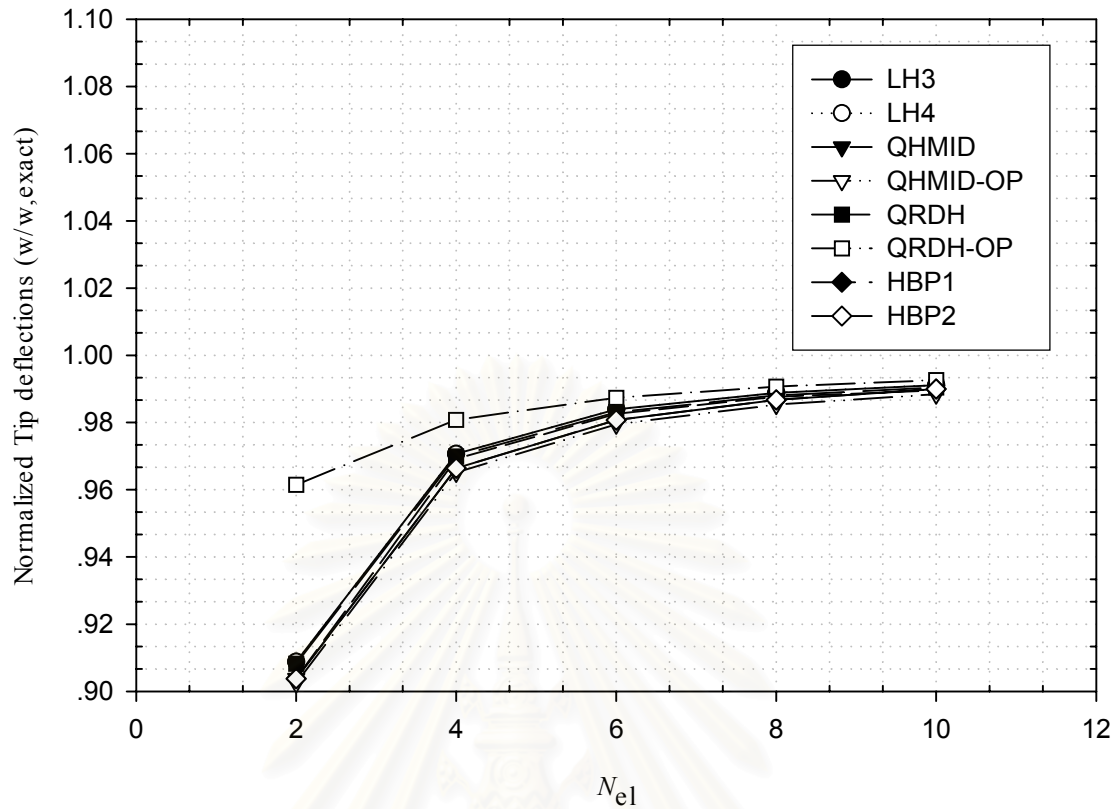


Figure 4.2.4-2 Convergence of tip deflection of cantilever plate subjected to point load.

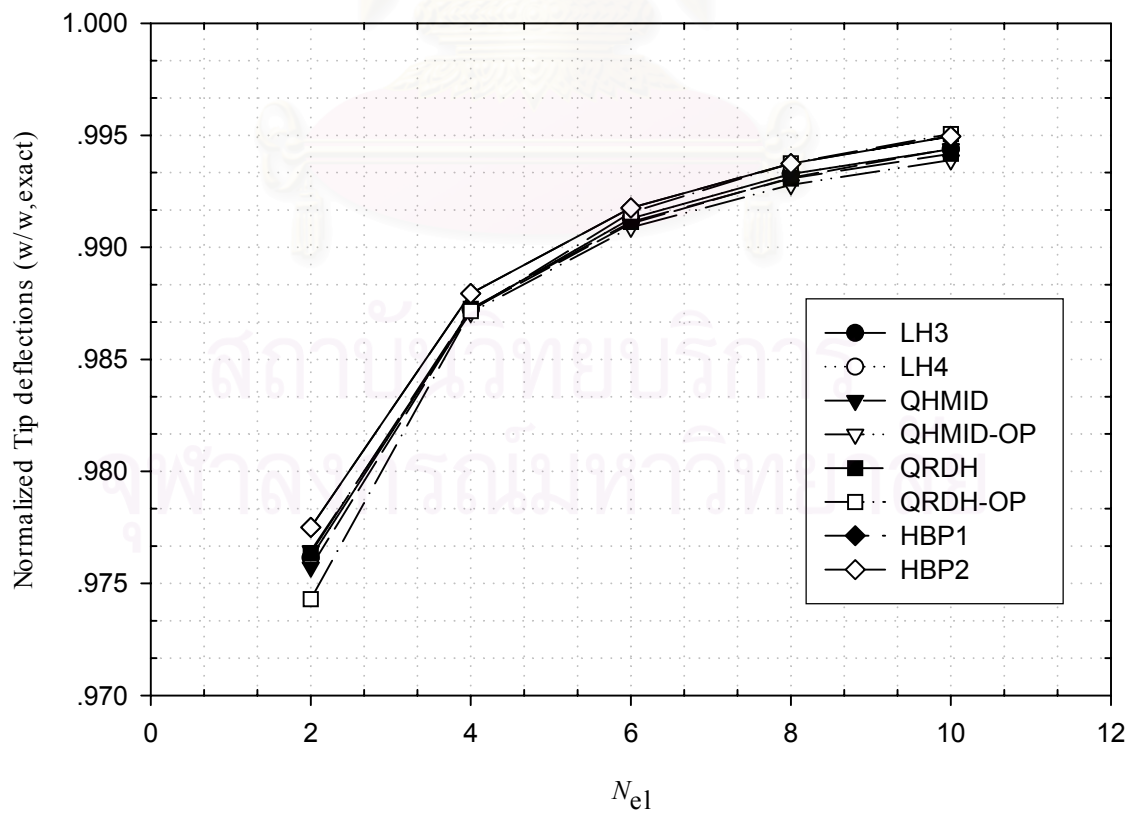


Figure 4.2.4-3 Convergence of tip deflection of cantilever plate subjected to end moment.

4.3 Test for Shear-Locking Effect

This test investigates the effect of plate thickness on the normalized displacement at the plate center. The test employs the same square plate shown in Fig.4.2.1-1 as an example with $N_{el} = 4$. The circular plate shown in Fig.4.2.2-1 with $N_{el} = 48$ was also studied. Plate thickness varies such that L/t ratio is 10, 10^2 , 10^3 , 10^4 , 10^5 and 10^6 for the square plate while $2R/t$ ratio is 10, 10^2 , 10^3 , 10^4 and 10^5 for the circular plate. The results of this test are illustrated in Fig. 4.3-1 to Fig. 4.3-8.

Shear-locking is a serious problem for not only the hybrid element but also the displacement element. A good element must not suffer from this effect. From the results, it can be seen that elements QHMID-OP, HBP1 and HBP2 are the elements that do not suffer from shear-locking in all cases of the square plate. For the circular plate, the element QHMID-OP, on the other hand, fails this test. The elements HBP1 and HBP2, however, are still well-behaved.

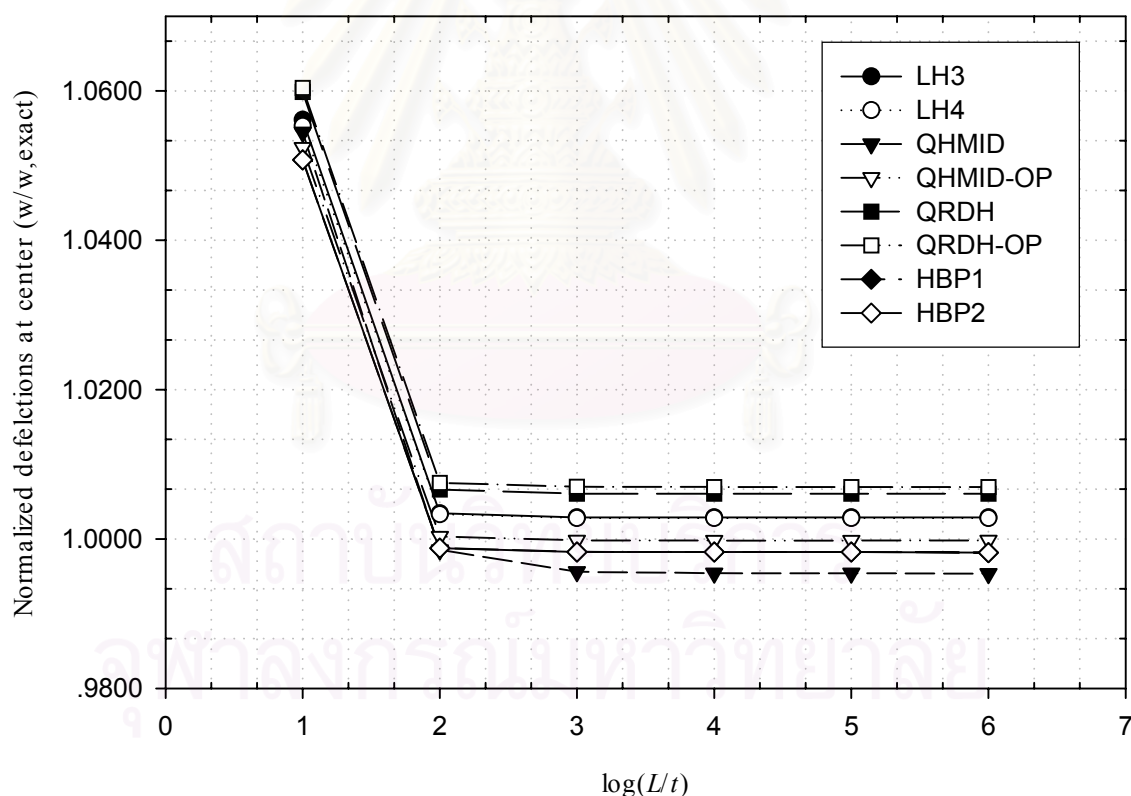


Figure 4.3-1 Effect of plate thickness on center deflection of square plate with SS2-UL ($N_{el} = 4$).

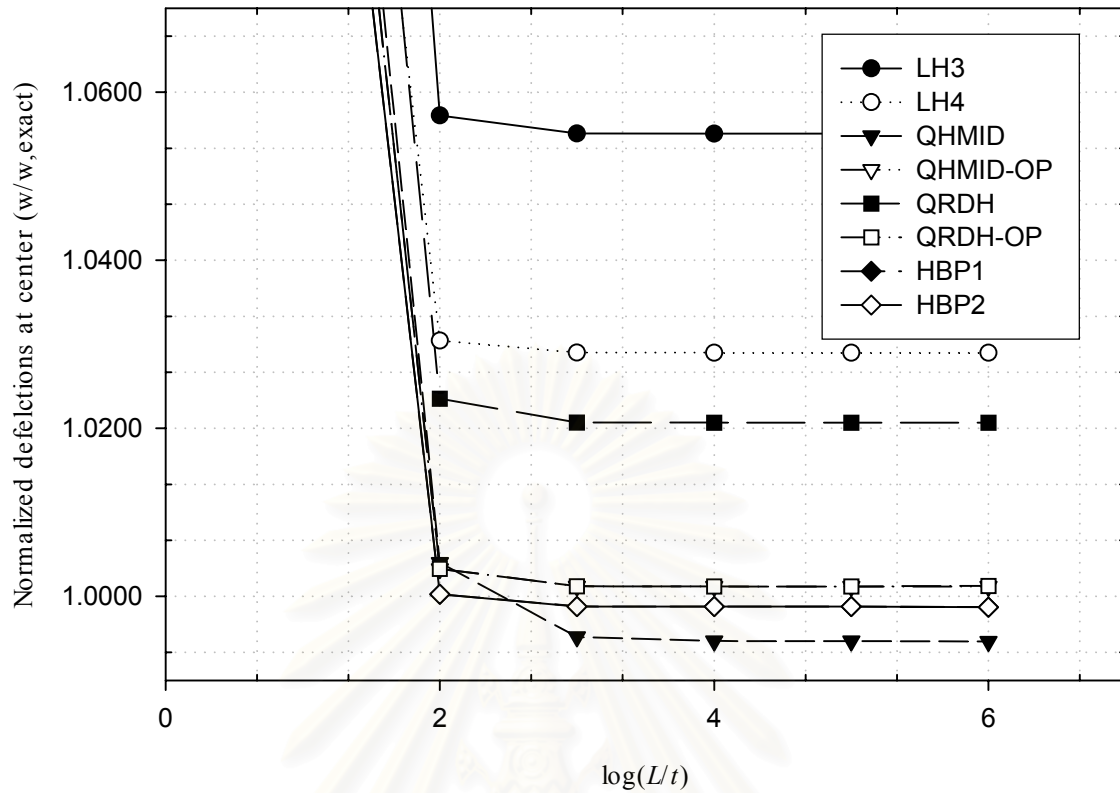


Figure 4.3-2 Effect of plate thickness on center deflection of square plate with SS2-CL ($N_{el} = 4$).

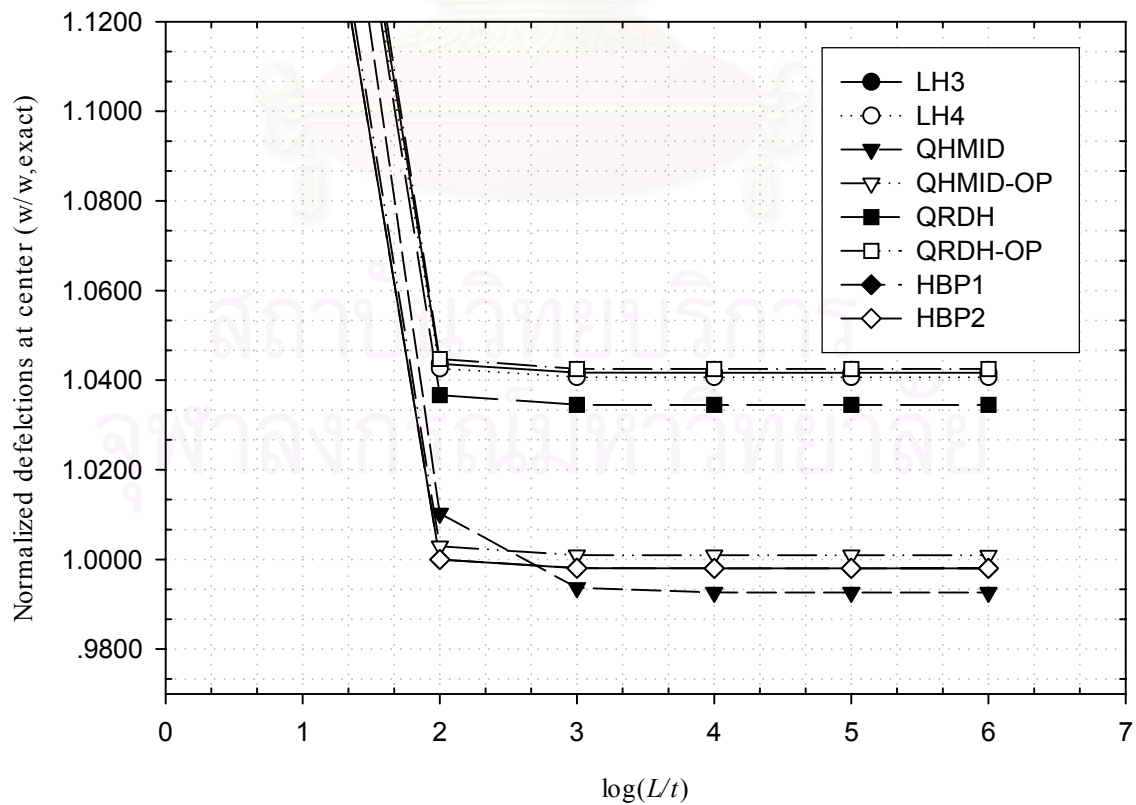


Figure 4.3-3 Effect of plate thickness on center deflection of square plate with C-UL ($N_{el} = 4$).

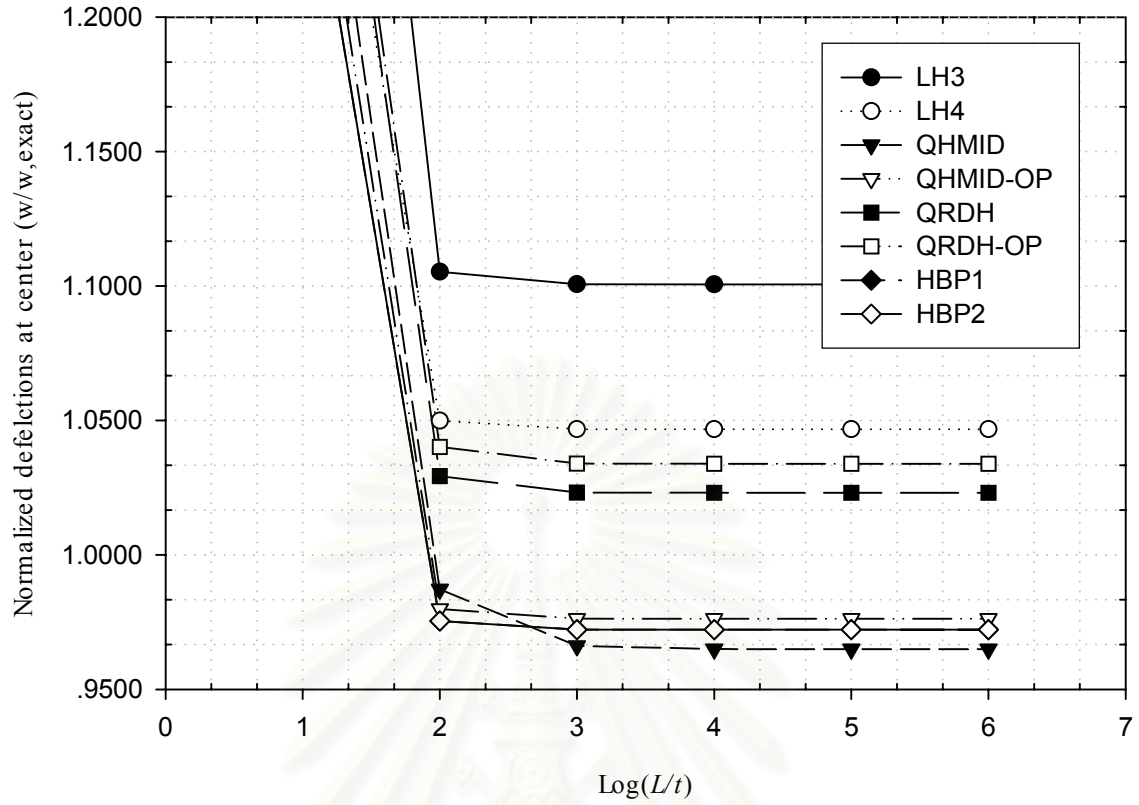


Figure 4.3-4 Effect of plate thickness on center deflection of square plate with C-CL ($N_{el} = 4$).

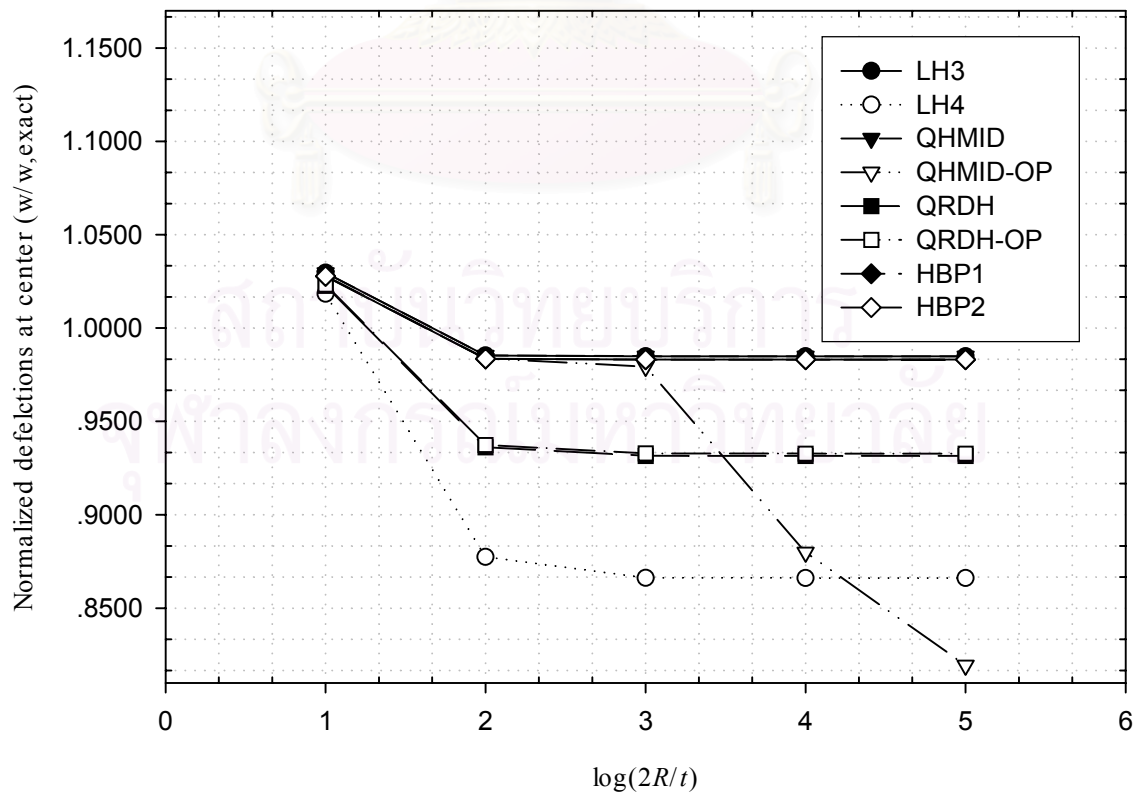


Figure 4.3-5 Effect of plate thickness on center deflection of circular plate with SS1-UL ($N_{el} = 48$).

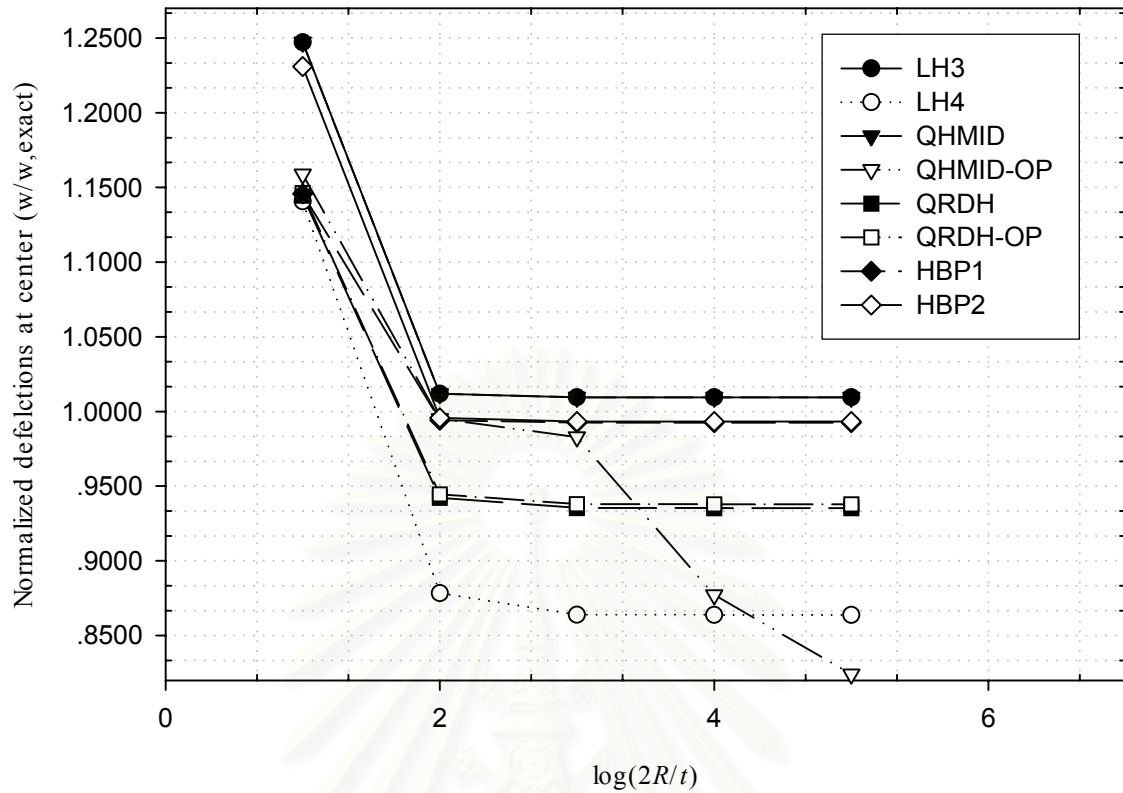


Figure 4.3-6 Effect of plate thickness on center deflection of circular plate with SS1-CL ($N_{el} = 48$).

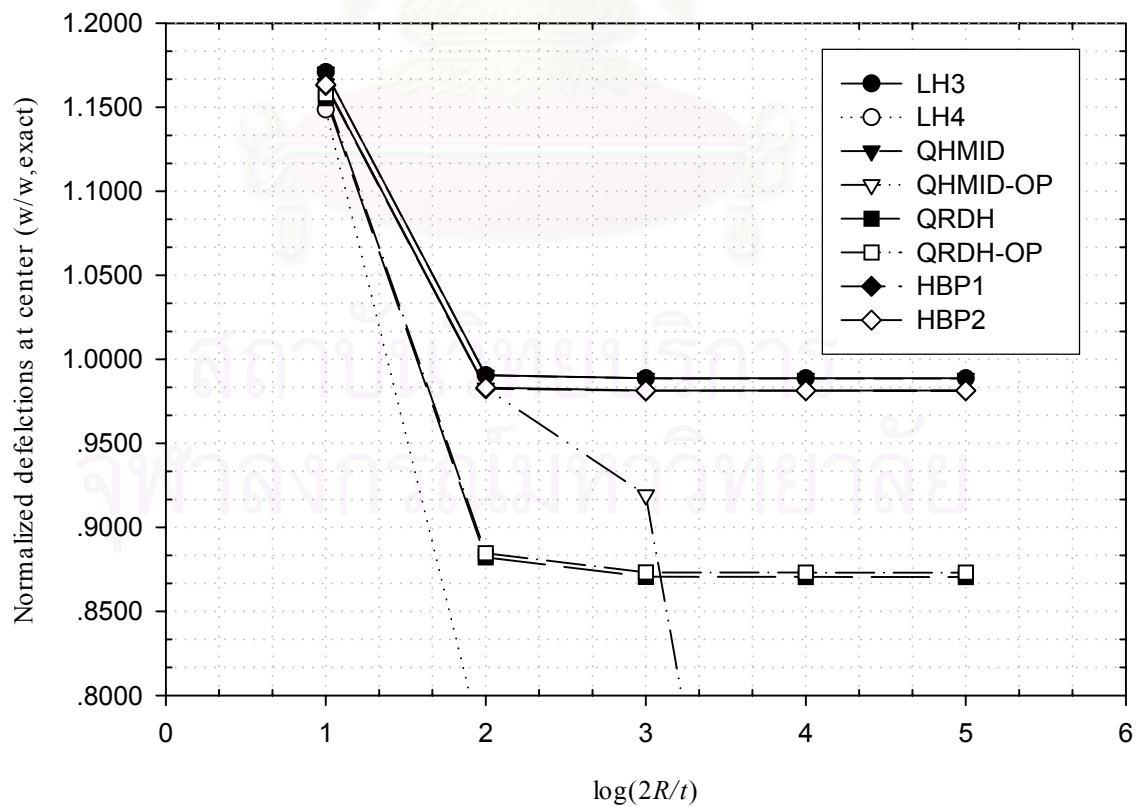


Figure 4.3-7 Effect of plate thickness on center deflection of circular plate with C-UL ($N_{el} = 48$).

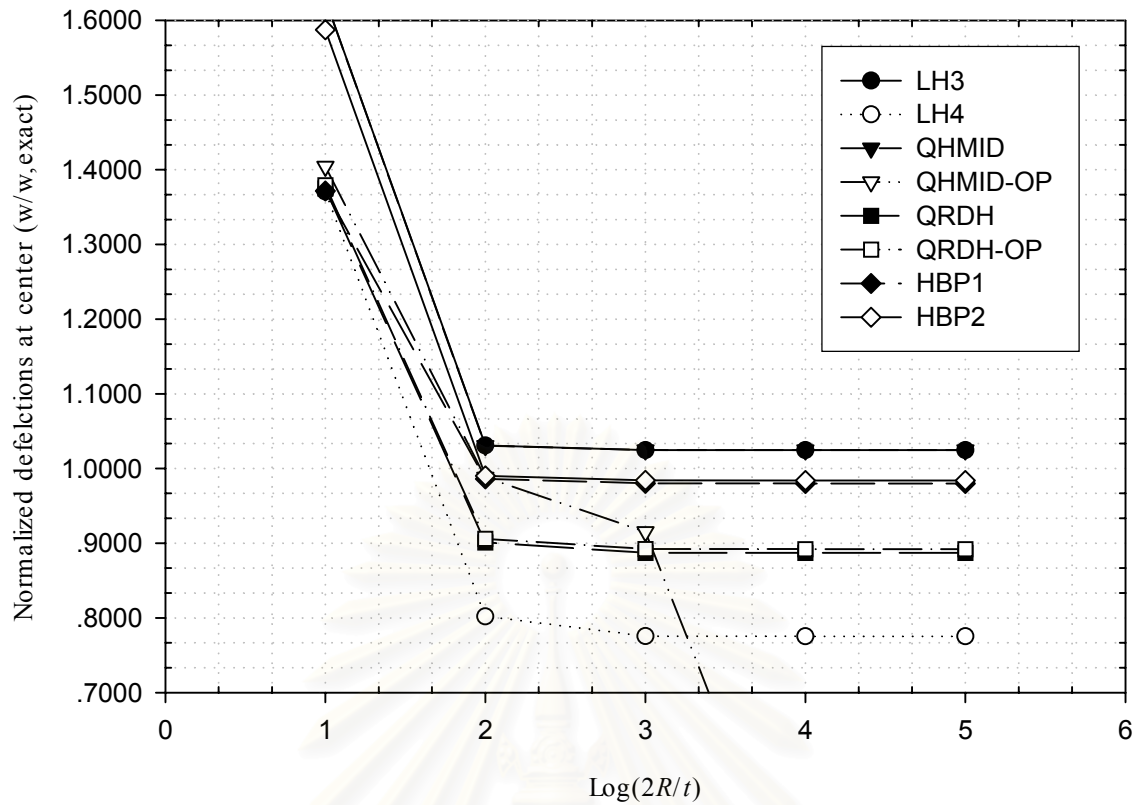


Figure 4.3-8 Effect of plate thickness on center deflection of circular plate with C-CL ($N_{el} = 48$).

4.4 Test on Element Aspect Ratio

The simply supported square plate with $N_{el} = 4$ is employed. The results are illustrated in Fig.4.4-2 and Fig.4.4-3. For SS2-UL, all elements are not much sensitive to the aspect ratio. Deviation from the exact solution is within 1 percent. Only element QRDH-OP suffers from this test for SS2-CL.

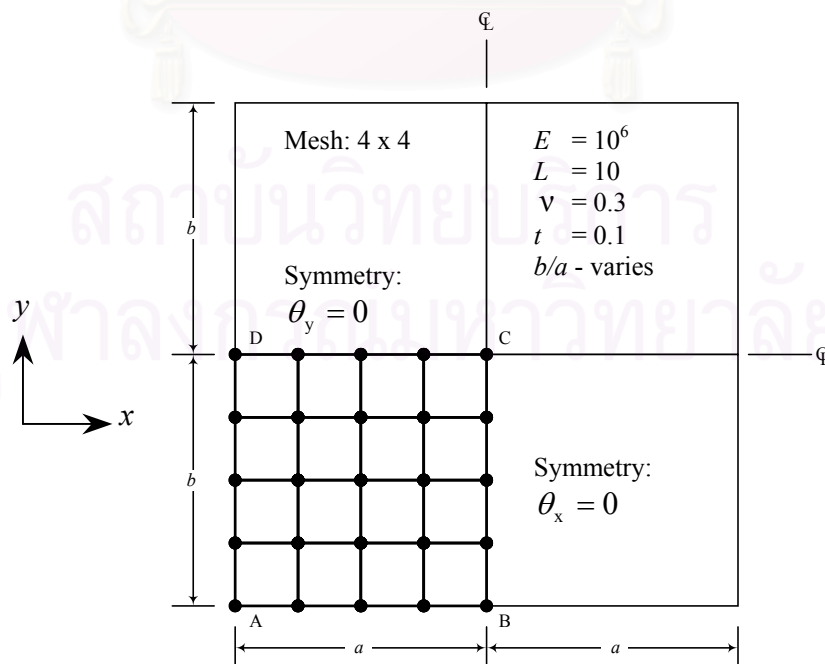


Figure 4.4-1 Square plate for testing on element aspect ratio ($N_{el} = 4$).

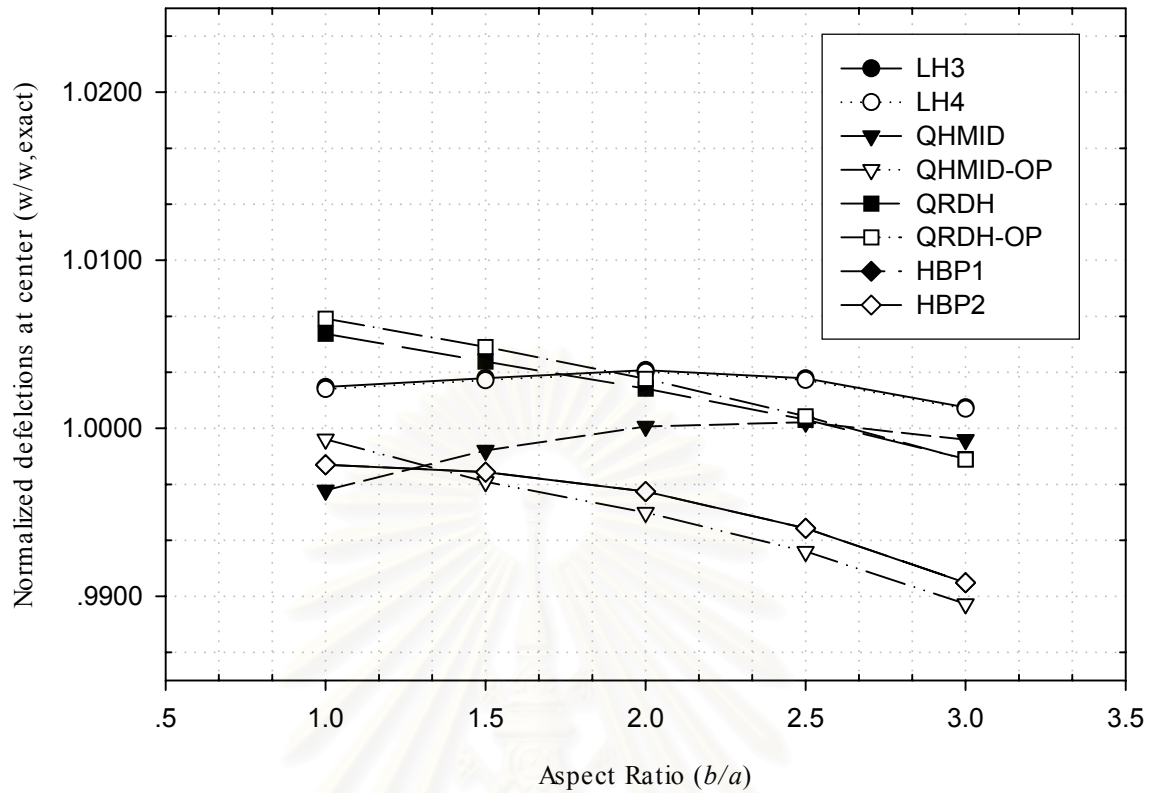


Figure 4.4-2 Effect of aspect ratio on center deflection of square plate with SS2-UL ($N_{el} = 4$).

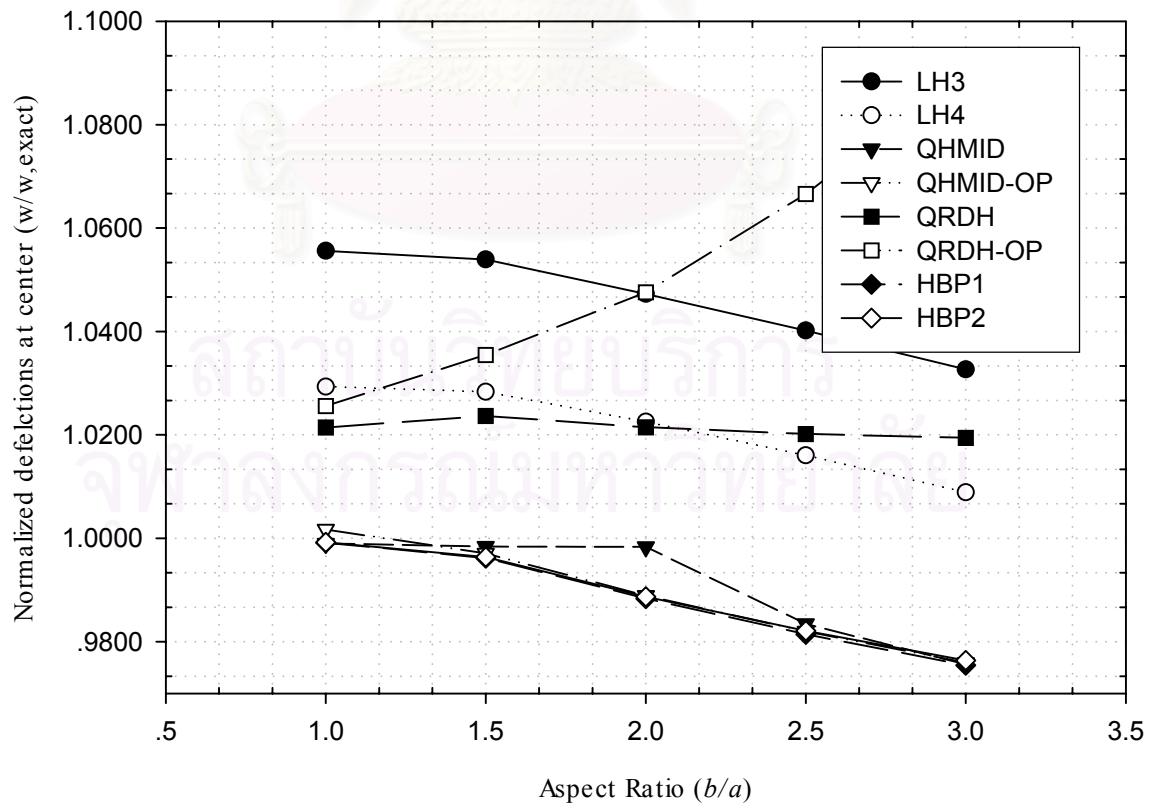


Figure 4.4-3 Effect of aspect ratio on center deflection of square plate with SS2-CL ($N_{el} = 4$).

4.5 Test for Invariance

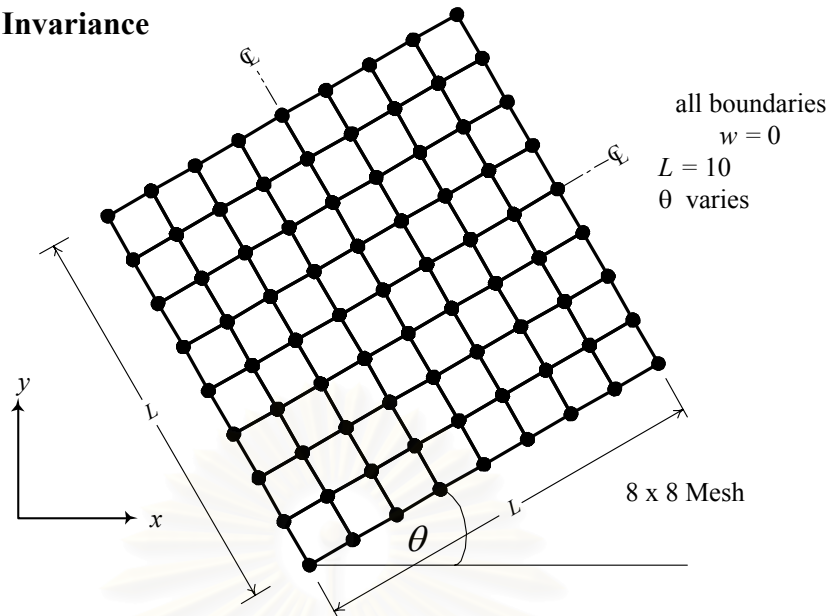


Figure 4.5-1 Mesh for testing invariance of plate with SS2-UL element.

To illustrate the effect of element orientation, the square plate was rotated by an angle θ . The rotations considered were 0, 30, 45, 60, and 90 degrees. Fig.4.5-2 illustrates the percent error of central deflection due to plate orientation. All elements yield an error within 6 percent.

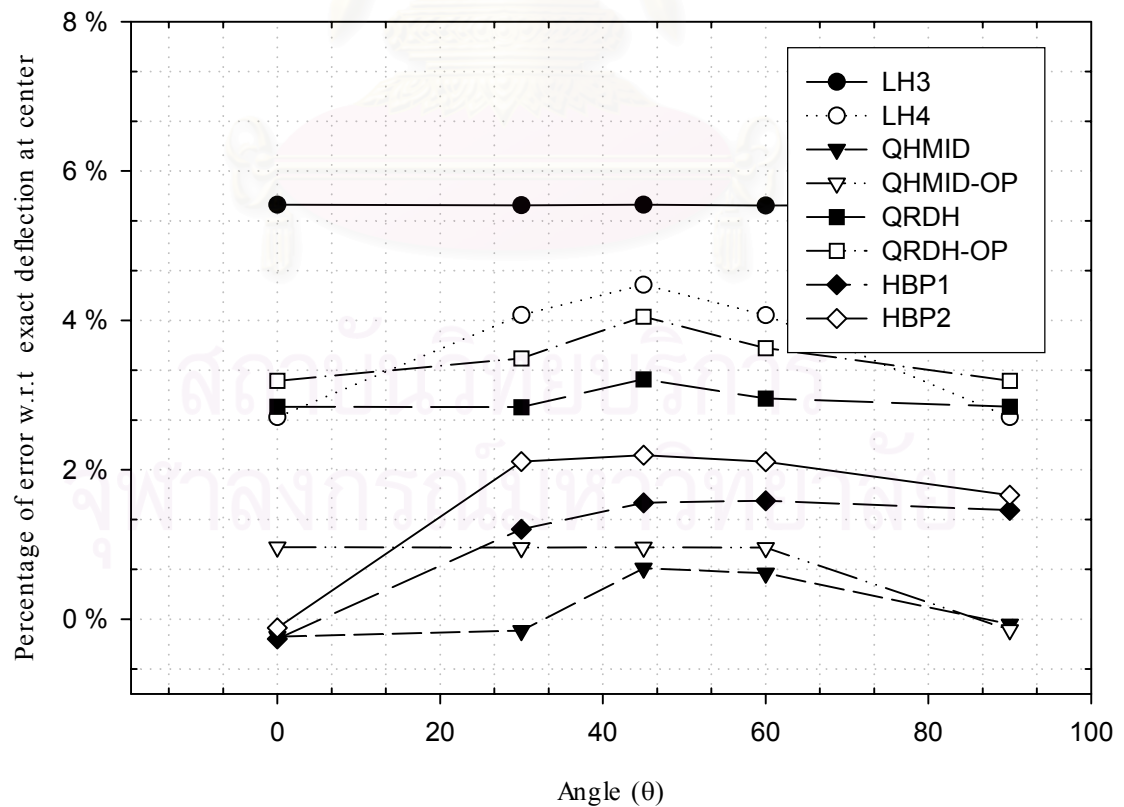


Figure 4.5-2 Effect on mesh orientation with SS1-UL.

Chapter V

Conclusions

In the present study, two hybrid plate elements, namely, HBP1 and HBP2 were constructed by employing the stress classification method as an initial procedure. Then, the proposed elements were expressed in natural reference coordinate system and improved with regard to distortion of element geometry. Eventually, the elements obtained proved to be versatile and fairly robust. Many existing hybrid plate elements as well as the proposed elements were tested and compared. Various tests were conducted so as to verify the performance of each hybrid element.

Based on the results of this study, the following conclusions can be drawn:

1. The optimization method through the penalty-equilibrium matrix has some shortcomings and limitations and should be used with care. This method opens up the possibility of causing undesirable kinematic deformation modes in the element. Proof of the method showed that a penalty constant tends to eliminate the stress modes which do not satisfy the equilibrium equations from the element stiffness formulation, as if those stress modes are not present in the stress matrix. Therefore, the necessary and sufficient conditions for choosing the stress matrix are not satisfied. Consequently, spurious kinematic deformation modes will occur.

2. Some elements having spurious kinematic deformation modes may, nevertheless, give good results. However, these elements are considerably unstable and may cause failure in some element assemblies. The element LH3 is an example of this failure cited in Reference 15.

3. Higher number of stress parameters tend to make an element stiffer, whereas the additional displacement parameters tend to soften the element. However, due to non-monotonic convergence of the general hybrid element, the change in stiffness either way may yet improve the element properties.

4. The stress classification method is considered to be an efficient and systematic procedure as a guideline for obtaining the stress matrix. The necessary and sufficient conditions for choosing the stress matrix can be explained through this method. The stress matrix which is free from kinematic deformation modes in the resulting element stiffness can easily be obtained.

5. Test for accuracy of displacement showed that, for regular element geometry, most of the elements particularly elements QHMID, QHMID-OP, HBP1 and HBP2, give approximately more than 95 percent accuracy for moderate mesh refinement. But among the elements considered superior in convergence when element geometry is irregular, elements QHMID-OP and QHMID give less accuracy than others, as evidenced by the circular plate and rhombic plate examples.

For moment, again, all elements give more than 95 percent accuracy for elements with regular geometry but the accuracy will slightly be lost if distortion of element geometry takes place. Even so, the accuracy on moment is still not less than 90 percent.

6. Shear-locking effect is noticeable when L/t ratio is increase to 10^2 for most elements. For the QHMID element, however, locking does not become apparent until L/t is 10^3 in the square plate or when the ratio $2R/t$ is about 10^2 in the circular plate. For the square plate, elements QHMID, QHMID-OP, HBP1 and HBP2 obviously are the best elements that can overcome severe locking. They give more than 99 percent accuracy on displacement for the SS2-UL, SS2-CL and C-UL cases and more than 96 percent for the C-CL case after locking occurs. For the circular plate, element QHMID-OP seriously fails the test. For all other better elements, the accuracy of displacement averages more than 95 percent.

7. All elements are not much sensitive to element aspect ratio. The discrepancy of displacement from the exact value is within 1 percent for the SS2-UL case and within 3 percent for the SS2-CL case when the aspect ratio is 3.

8. All elements are not invariant. The maximum error takes place when the mesh rotates to an angle of 45 degrees. The results from elements QHMID, QHMID-OP, HBP1 and HBP2 approximately are within 2 percent of those using zero-degree orientation for the mesh.

Comparison of the overall performance of the hybrid elements studied indicates that elements HBP1 and HBP2 are the most efficient among the competing elements. These elements perform very well in all tests especially the shear-locking test.

References

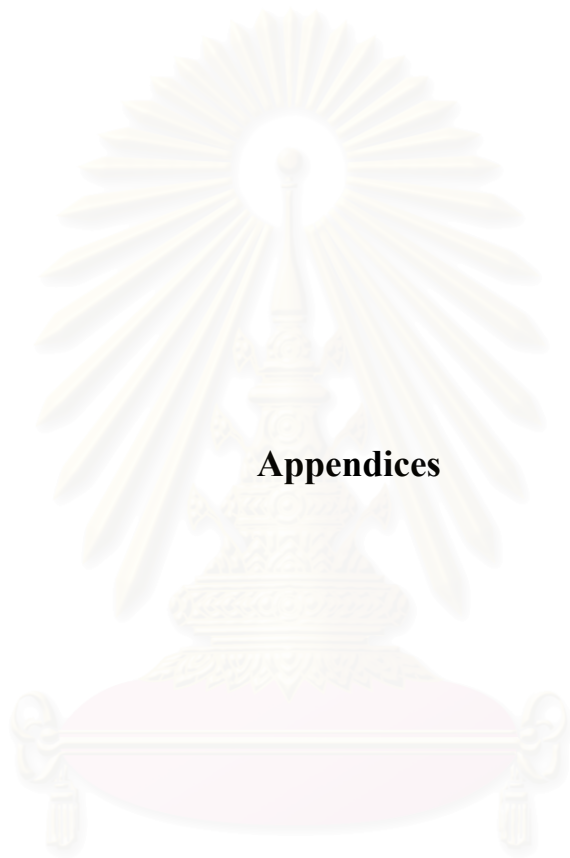
- [1] Pian, T.H.H. and Tong, P. Basis of Finite Element Methods for Solid Continua, *Int. J. Numer. Methods Eng.* **1**, pp. 3-28, 1969.
- [2] Washizu, K. Variational Methods in Elasticity and Plasticity, 3rd ed., Pergamon Press, Oxford, 1982.
- [3] Pian, T.H.H. A Historical Note about Hybrid Elements, *Int. J. Numer. Methods Eng.* **12**, pp. 891-892, 1978.
- [4] Pian, T.H.H. Derivation of Element Stiffness Matrices by Assumed Stress Distributions, *AIAA J.* **2**, pp. 1333-1336, 1964.
- [5] Tong, P. New Displacement Hybrid Finite Element Methods for Solid Continua, *Int. J. Numer. Methods Eng.* **2**, pp. 73-83, 1970.
- [6] Tong, P. An Assumed Stress Hybrid Finite Element Method for an Incompressible and Near-incompressible, *Int. J. Solids Struct.* **5**, pp. 455-461, 1969.
- [7] Tong, P. and Pian, T.H.H. A Variational Principle and the Convergence of a Finite Element Method based on Assumed Stress Distribution, *Int. J. Solids Struct.* **5**, pp. 463-472, 1969.
- [8] Pian, T.H.H. and Chen, D.P. Alternative Ways for Formulation of Hybrid Stress Elements, *Int. J. Numer. Methods Eng.* **18**, pp. 1679-1684, 1982.
- [9] Pian, T.H.H., Chen, D.P. and Kang, D. A New Formulation of Hybrid/Mixed Finite Element, *Comput. Struct.* **16**, pp. 81-87, 1983.
- [10] Pian, T.H.H. and Sumihara, K. Rational Approach for Assumed Stress Finite Elements, *Int. J. Numer. Methods Eng.* **20**, pp. 1685-1695, 1984.
- [11] Pian, T.H.H. Finite Elements Based on Consistently Assumed Stresses and Displacements, *Finite Elements Anal. Des.* **1**, pp. 131-140, 1985.
- [12] Pian, T.H.H. and Wu, C.C. A Rational Approach for Choosing Stress Terms for Hybrid Finite Element Formulations, *Int. J. Numer. Methods Eng.* **26**, pp. 2331-2343, 1988.
- [13] Wu, C.C. and Cheung, Y.K. On Optimization Approaches of Hybrid Stress Elements, *Finite Elements Anal. Des.* **21**, pp. 111-128, 1995.
- [14] Lee, S.W. and Pian, T.H.H. Improvement of Plate and Shell Finite Elements by Mixed Formulations, *AIAA J.* **16**, pp. 23-34, 1978.

- [15] Spilker, R.L. and Munir, N.I. The Hybrid-Stress Model for Thin Plates, *Int. J. Numer. Methods Eng.* **15**, pp. 1239-1260, 1980.
- [16] Spilker, R.L. Invariant 8-node Hybrid-Stress Elements for Thin and Moderately Thick Plates, *Int. J. Numer. Methods Eng.* **18**, pp. 1153-1178, 1982.
- [17] Wanji, C. and Cheung, Y.K. A New Approach for the Hybrid Element Method, *Int. J. Numer. Methods Eng.* **24**, pp. 1697-1709, 1987.
- [18] Pian, T.H.H. and Tong, P. Relation between Incompatible Displacement model and Hybrid Stress Model, *Int. J. Numer. Methods Eng.* **22**, pp. 173-181, 1986.
- [19] Cheung, Y.K. and Wanji, C. Hybrid Quadrilateral Element based on Mindlin/Reissner Plate Theory, *Comput. Struct.* **32**, pp. 327-339, 1989.
- [20] Dong, Y.F., Wu, C.C. and Teixeira de Freitas, J.A. The Hybrid Stress Model for Mindlin-Reissner Plates based on A Stress Optimization Condition, *Comput. Struct.* **46**, pp. 877-897, 1993.
- [21] Dong, Y.F. and Teixeira de Freitas, J.A. A Quadrilateral hybrid Stress Element for Mindlin Plates based on Incompatible Displacements, *Int. J. Numer. Methods Eng.* **37**, pp. 279-296, 1994.
- [22] Pian, T.H.H. and Chen, D.P. On the Suppression of Zero Energy Deformation Modes, *Int. J. Numer. Methods Eng.* **19**, pp. 1741-1752, 1983.
- [23] Feng, W., Hoa, S.V. and Huang, Q. Classification of Stress Modes in Assumed Stress Fields of hybrid Finite Elements, *Int. J. Numer. Methods Eng.* **40**, pp. 4313-4339, 1997.
- [24] Hamhim, B. Comparison of Hybrid Plate Bending Elements(in Thai), *Master Thesis*, Chulalongkorn University, Bangkok, Thailand, 1999.
- [25] Kang, D.S. Present Finite Element Technology from a Hybrid Formulation Perspective, *Comput. Struct.* **35**, pp. 321-327, 1990.
- [26] Pian, T.H.H. State-of-the-art Development of Hybrid/Mixed Finite Element Method, *Finite Elements Anal. Des.* **21**, pp. 5-20, 1995.
- [27] Pian, T.H.H. Some Notes on the Early History of Hybrid Stress Finite Element Method, *Int. J. Numer. Methods Eng.* **47**, pp. 419-425, 2000.
- [28] Chieslar, J.D. and Ghali, A. Computation of Hybrid Element Matrices by Elimination Techniques, *Int. J. Numer. Methods Eng.* **26**, pp. 423-435, 1988.

- [29] Bathe, K.J. *Finite Element Procedures in Engineering Analysis*, Prentice-Hall, 1982.
- [30] Cook, R.D., Malkus, D.S. and Plesha, M.E. *Concepts and Applications of Finite Element Analysis*, 3rd ed., John Wiley & Sons, 1989.
- [31] Timoshenko, K.J. and Woinowsky-Krieger, S. *Theory of Plates and Shells*, 2nd ed., McGraw-Hill, New Jersey, 1959.



สถาบันวิทยบริการ
จุฬาลงกรณ์มหาวิทยาลัย



Appendices

สถาบันวิทยบริการ
จุฬาลงกรณ์มหาวิทยาลัย

Appendix A

Details of Element Stiffness Formulation

A.1 Stress-Strain Approach

(Convention follows Reference 15)

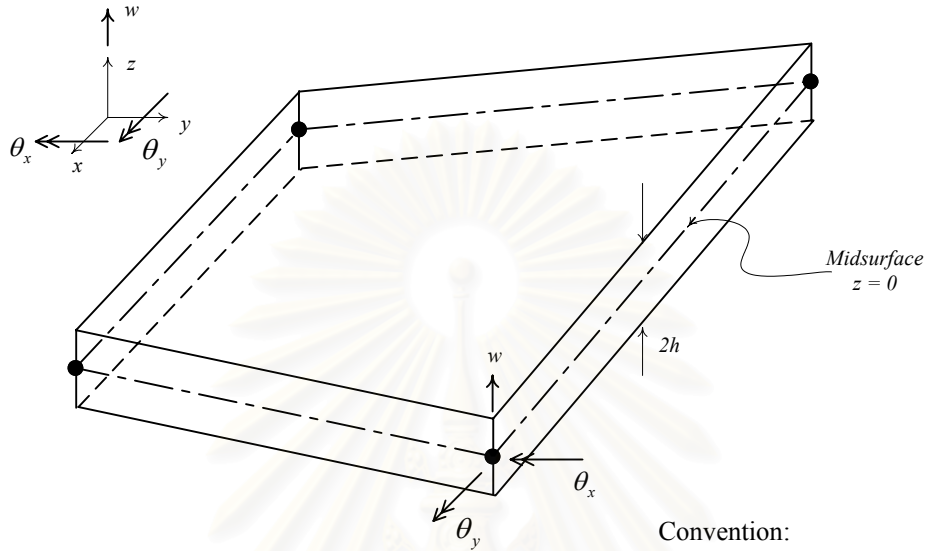


Figure A.1-1 Geometry and degrees of freedom for the four-node quadrilateral plate bending element.

Convention:

$$\mathbf{u} = \begin{Bmatrix} \theta_x \\ \theta_y \\ w \end{Bmatrix}, \quad \boldsymbol{\varepsilon} = \begin{Bmatrix} \theta_{x,x} \\ \theta_{y,y} \\ \cdot \\ \theta_{x,y} + \theta_{y,x} \\ \theta_x - w_{,x} \\ \theta_y - w_{,y} \end{Bmatrix}, \quad \bar{\boldsymbol{\sigma}} = \begin{Bmatrix} \bar{\sigma}_x \\ \bar{\sigma}_y \\ \bar{\sigma}_z \\ \bar{\tau}_{xy} \\ \bar{\tau}_{xz} \\ \bar{\tau}_{yz} \end{Bmatrix}$$

The generalized forces are expressed in terms of 6 stress components varying through a plate of thickness $2h$. By invoking the three-dimensional equilibrium equations, all stress components are

$$\begin{aligned} \sigma_x &= z\bar{\sigma}_x(x, y) \\ \sigma_y &= z\bar{\sigma}_y(x, y) \\ \tau_{xy} &= z\bar{\tau}_{xy}(x, y) \\ \tau_{xz} &= \frac{1}{2}(h^2 - z^2)\bar{\tau}_{xz}(x, y) \\ \tau_{yz} &= \frac{1}{2}(h^2 - z^2)\bar{\tau}_{yz}(x, y) \\ \sigma_z &= \frac{1}{6}(z^3 - 3h^2z - 2h^3)\bar{\sigma}_z(x, y) \end{aligned} \quad (\text{A.1-1})$$

So that the stresses may be assumed as

$$\begin{aligned}
\bar{\sigma}_x &= \beta_1 + \beta_2 x + \beta_3 y + \beta_{10} xy + \frac{1}{2} \beta_{13} x^2 \\
\bar{\sigma}_y &= \beta_4 + \beta_5 x + \beta_6 y + \beta_{11} xy - \frac{1}{2} \beta_{13} y^2 \\
\bar{\tau}_{xy} &= \beta_7 + \beta_8 x + \beta_9 y + \beta_{12} xy \\
\bar{\tau}_{xz} &= (\beta_2 + \beta_9) + (\beta_{12} + \beta_{13})x + \beta_{10} y \\
\bar{\tau}_{yz} &= (\beta_6 + \beta_8) + \beta_{11} x + (\beta_{12} - \beta_{13})y \\
\bar{\sigma}_z &= 2\beta_{12}
\end{aligned}$$

or expressed in matrix form as

$$\begin{Bmatrix} \bar{\sigma}_x \\ \bar{\sigma}_y \\ \bar{\sigma}_z \\ \bar{\tau}_{xy} \\ \bar{\tau}_{xz} \\ \bar{\tau}_{yz} \end{Bmatrix} = \begin{bmatrix} 1 & x & y & \cdot & \cdot & \cdot & \cdot & \cdot & \cdot & xy & \cdot & \cdot & \frac{1}{2}x^2 \\ \cdot & \cdot & \cdot & 1 & x & y & \cdot & \cdot & \cdot & \cdot & xy & \cdot & -\frac{1}{2}y^2 \\ \cdot & \cdot & \cdot & \cdot & \cdot & \cdot & \cdot & \cdot & \cdot & \cdot & \cdot & 2 & \cdot \\ \cdot & \cdot & \cdot & \cdot & \cdot & \cdot & 1 & x & y & \cdot & \cdot & xy & \cdot \\ \cdot & 1 & \cdot & \cdot & \cdot & \cdot & \cdot & 1 & y & \cdot & x & x & \cdot \\ \cdot & \cdot & \cdot & \cdot & \cdot & 1 & \cdot & 1 & \cdot & \cdot & x & y & -y \end{bmatrix} \begin{Bmatrix} \beta_1 \\ \beta_2 \\ \beta_3 \\ \vdots \\ \vdots \\ \beta_{13} \end{Bmatrix} \quad (\text{A.1-2})$$

$$\bar{\sigma} = \mathbf{P}\beta$$

Element LH3 is obtained by setting $\beta_{10} = \beta_{11} = \beta_{12} = \beta_{13} = 0$ whereas $\beta_{12} = \beta_{13} = 0$ is set to obtain element LH4.

The assumed displacements are the same as those for a four-node quadrilateral element varying linearly within the element,

$$\begin{aligned}
\theta_x &= \sum_{i=1}^4 N_i \theta_{xi} \\
\theta_y &= \sum_{i=1}^4 N_i \theta_{yi} \\
w &= \sum_{i=1}^4 N_i w_i
\end{aligned} \quad (\text{A.1-3})$$

where N_i are the bilinear shape functions,

$$N_i = \frac{1}{4}(1 + \xi_i \xi)(1 + \eta_i \eta) \quad (\text{A.1-4})$$

and θ_{xi} , θ_{yi} and w_i are the degrees of freedom at node i . The coordinate transformation is

$$\begin{aligned}
x &= \sum_{i=1}^4 N_i x_i \\
y &= \sum_{i=1}^4 N_i y_i
\end{aligned} \quad (\text{A.1-5})$$

where (x_i, y_i) are the coordinates of node i . The displacements can be expressed in terms of the nodal values as

$$\begin{Bmatrix} \theta_x \\ \theta_y \\ w \end{Bmatrix} = \begin{bmatrix} N_1 & \cdot & \cdot & \cdots & \cdots & N_4 & \cdot & \cdot \\ \cdot & N_1 & \cdot & \cdots & \cdots & \cdot & N_4 & \cdot \\ \cdot & \cdot & N_1 & \cdots & \cdots & \cdot & \cdot & N_4 \end{bmatrix}_{3 \times 12} \begin{Bmatrix} \theta_{x1} \\ \theta_{y1} \\ w_1 \\ \vdots \\ \theta_{x4} \\ \theta_{y4} \\ w_4 \end{Bmatrix}_{12 \times 1} \quad (\text{A.1-6})$$

or

$$\mathbf{u} = \mathbf{Nq}$$

The strain-displacement relations are

$$\begin{aligned} \boldsymbol{\varepsilon} &= \mathbf{D}\mathbf{u} \\ &= \mathbf{D}\mathbf{Nq} \\ &= \mathbf{Bq} \end{aligned}$$

or

where

$$\mathbf{D} = \begin{bmatrix} \partial/\partial x & \cdot & \cdot \\ \cdot & \partial/\partial y & \cdot \\ \cdot & \cdot & \cdot \\ \partial/\partial y & \partial/\partial x & \cdot \\ 1 & \cdot & -\partial/\partial x \\ \cdot & 1 & -\partial/\partial y \end{bmatrix} \quad (\text{A.1-8})$$

The Jacobian matrix is defined by

$$\begin{aligned} \mathbf{J} = \frac{\partial(x, y)}{\partial(\xi, \eta)} &= \begin{bmatrix} \partial x/\partial \xi & \partial y/\partial \xi \\ \partial x/\partial \eta & \partial y/\partial \eta \end{bmatrix} \\ &= \begin{bmatrix} a_1 + a_2\eta & b_1 + b_2\eta \\ a_3 + a_2\xi & b_3 + b_2\xi \end{bmatrix} \end{aligned} \quad (\text{A.1-9})$$

with

$$\begin{bmatrix} a_1 & b_1 \\ a_2 & b_2 \\ a_3 & b_3 \end{bmatrix} = \frac{1}{4} \begin{bmatrix} -1 & 1 & 1 & -1 \\ 1 & -1 & 1 & -1 \\ -1 & -1 & 1 & 1 \end{bmatrix} \begin{bmatrix} x_1 & y_1 \\ x_2 & y_2 \\ x_3 & y_3 \\ x_4 & y_4 \end{bmatrix} \quad (\text{A.1-10})$$

From mechanics of materials, the strain-stress relations are

$$\boldsymbol{\varepsilon} = \mathbf{S}\boldsymbol{\sigma}$$

where

$$\mathbf{S} = \frac{1}{E} \begin{bmatrix} 1 & -\nu & -\nu & \cdot & \cdot & \cdot \\ -\nu & 1 & -\nu & \cdot & \cdot & \cdot \\ -\nu & -\nu & 1 & \cdot & \cdot & \cdot \\ \cdot & \cdot & \cdot & 2(1+\nu) & \cdot & \cdot \\ \cdot & \cdot & \cdot & \cdot & 2(1+\nu) & \cdot \\ \cdot & \cdot & \cdot & \cdot & \cdot & 2(1+\nu) \end{bmatrix} \quad (\text{A.1-11})$$

By integration through the thickness, the first term of Eq. 2.3-4, $\int_V -\frac{1}{2} \boldsymbol{\sigma}^T \mathbf{S} \boldsymbol{\sigma} dV$, becomes

$$\int_A -\frac{1}{2} \bar{\boldsymbol{\sigma}}^T \bar{\mathbf{S}} \bar{\boldsymbol{\sigma}} dA \quad (\text{A.1-12})$$

where

$$\bar{\mathbf{S}} = \frac{1}{E} \begin{bmatrix} 1 & -\nu & \nu \left(\frac{2h^2}{5} \right) & \cdot & \cdot & \cdot \\ -\nu & 1 & \nu \left(\frac{2h^2}{5} \right) & \cdot & \cdot & \cdot \\ \nu \left(\frac{2h^2}{5} \right) & \nu \left(\frac{2h^2}{5} \right) & \frac{52h^4}{105} & \cdot & \cdot & \cdot \\ \cdot & \cdot & \cdot & 2(1+\nu) & \cdot & \cdot \\ \cdot & \cdot & \cdot & \cdot & \frac{4h^2}{5}(1+\nu) & \cdot \\ \cdot & \cdot & \cdot & \cdot & \cdot & \frac{4h^2}{5}(1+\nu) \end{bmatrix} \quad (\text{A.1-13})$$

From Eqs. A.1-2, A.1-7 and A.1-13, we can obtain the matrices shown in Eq. 2.3-13 as

$$\mathbf{H} = \int_A \mathbf{P}^T \bar{\mathbf{S}} \mathbf{P} dA$$

$$\mathbf{G} = \int_A \mathbf{P}^T \mathbf{B} dA$$

or

$$\mathbf{H} = \frac{2h^3}{3} \int_{-1}^1 \int_{-1}^1 \mathbf{P}^T \bar{\mathbf{S}} \mathbf{P} |\mathbf{J}| d\xi d\eta \quad (\text{A.1-14})$$

$$\mathbf{G} = \frac{2h^3}{3} \int_{-1}^1 \int_{-1}^1 \mathbf{P}^T \mathbf{B} |\mathbf{J}| d\xi d\eta$$

Note that integration of the above equation is performed over area only.

Then, the element stiffness matrix is

$$\mathbf{k} = \mathbf{G}^T \mathbf{H}^{-1} \mathbf{G} \quad (\text{A.1-15})$$

To arrive at this step, the equilibrium differential operators for this approach are derived. These operators are denoted by \mathbf{D}^T in Eq.2.3-5 or ∂ in Eq.1.2-4. From Eq. A.1-1 the assumed stresses are

$$\boldsymbol{\sigma} = \mathbf{z}\bar{\boldsymbol{\sigma}} \quad (\text{A.1-16})$$

where $\mathbf{z} = \text{diag}[z \quad z \quad \frac{1}{6}(z^3 - 3h^2z - 2h^3) \quad z \quad \frac{1}{2}(h^2 - z^2) \quad \frac{1}{2}(h^2 - z^2)]$

From Eqs. A.1-2 and A.1-16, the homogeneous equilibrium equations become

$$\begin{aligned} \partial\boldsymbol{\sigma} &= \mathbf{0} \\ &= \partial(\mathbf{z}\bar{\boldsymbol{\sigma}}) \\ &= \partial(\mathbf{z}\bar{\mathbf{P}}\boldsymbol{\beta}) \end{aligned}$$

Let

$$z_1 = z,$$

$$z_2 = \frac{1}{2}(h^2 - z^2),$$

and

$$z_3 = \frac{1}{6}(z^3 - 3h^2z - 2h^3)$$

Therefore,

$$\begin{aligned} \partial\mathbf{P} &= \partial(\mathbf{z}\bar{\mathbf{P}}) \\ &= \begin{bmatrix} \frac{\partial}{\partial x} & \cdot & \cdot & \frac{\partial}{\partial y} & \frac{\partial}{\partial z} & \cdot \\ \cdot & \frac{\partial}{\partial y} & \cdot & \frac{\partial}{\partial x} & \cdot & \frac{\partial}{\partial z} \\ \cdot & \cdot & \frac{\partial}{\partial z} & \cdot & \frac{\partial}{\partial x} & \frac{\partial}{\partial y} \end{bmatrix} \begin{bmatrix} z_1(P_{11} & P_{12} & P_{13} & \cdots & P_{1\beta}) \\ z_1(P_{21} & P_{22} & P_{23} & \cdots & P_{2\beta}) \\ z_3(P_{31} & P_{32} & P_{33} & \cdots & P_{3\beta}) \\ z_1(P_{41} & P_{42} & P_{43} & \cdots & P_{4\beta}) \\ z_2(P_{51} & P_{52} & P_{53} & \cdots & P_{5\beta}) \\ z_2(P_{61} & P_{62} & P_{63} & \cdots & P_{6\beta}) \end{bmatrix} \\ &= \begin{bmatrix} z_1 \frac{\partial P_{11}}{\partial x} + z_1 \frac{\partial P_{41}}{\partial y} + P_{51} \frac{\partial z_2}{\partial z} & z_1 \frac{\partial P_{11}}{\partial x} + z_1 \frac{\partial P_{41}}{\partial y} + P_{51} \frac{\partial z_2}{\partial z} & \cdots \\ z_1 \frac{\partial P_{21}}{\partial y} + z_1 \frac{\partial P_{41}}{\partial x} + P_{61} \frac{\partial z_2}{\partial z} & z_1 \frac{\partial P_{21}}{\partial y} + z_1 \frac{\partial P_{41}}{\partial x} + P_{61} \frac{\partial z_2}{\partial z} & \cdots \\ P_{31} \frac{\partial z_3}{\partial z} + z_2 \frac{\partial P_{51}}{\partial x} + z_2 \frac{\partial P_{61}}{\partial y} & P_{31} \frac{\partial z_3}{\partial z} + z_2 \frac{\partial P_{51}}{\partial x} + z_2 \frac{\partial P_{61}}{\partial y} & \cdots \end{bmatrix} \\ &= \begin{bmatrix} z(\frac{\partial P_{11}}{\partial x} + \frac{\partial P_{41}}{\partial y} - P_{51}) & z(\frac{\partial P_{12}}{\partial x} + \frac{\partial P_{42}}{\partial y} - P_{52}) & \cdots \\ z(\frac{\partial P_{21}}{\partial y} + \frac{\partial P_{41}}{\partial x} - P_{61}) & z(\frac{\partial P_{22}}{\partial y} + \frac{\partial P_{42}}{\partial x} - P_{62}) & \cdots \\ \frac{h^2 - z^2}{2}(\frac{\partial P_{51}}{\partial x} + \frac{\partial P_{61}}{\partial y} - P_{31}) & \frac{h^2 - z^2}{2}(\frac{\partial P_{52}}{\partial x} + \frac{\partial P_{62}}{\partial y} - P_{32}) & \cdots \end{bmatrix} \end{aligned}$$

$$= \begin{bmatrix} z & \cdot & \cdot \\ \cdot & z & \cdot \\ \cdot & \cdot & \frac{h^2 - z^2}{2} \end{bmatrix} \begin{bmatrix} \frac{\partial P_{11}}{\partial x} + \frac{\partial P_{41}}{\partial y} - P_{51} & \frac{\partial P_{12}}{\partial x} + \frac{\partial P_{42}}{\partial y} - P_{52} & \dots \\ \frac{\partial P_{21}}{\partial y} + \frac{\partial P_{41}}{\partial x} - P_{61} & \frac{\partial P_{22}}{\partial y} + \frac{\partial P_{42}}{\partial x} - P_{62} & \dots \\ \frac{\partial P_{51}}{\partial x} + \frac{\partial P_{61}}{\partial y} - P_{31} & \frac{\partial P_{52}}{\partial x} + \frac{\partial P_{62}}{\partial y} - P_{32} & \dots \end{bmatrix}$$

Hence,

$$\partial \mathbf{P} = \mathbf{z}' \bar{\partial} \mathbf{P} \quad (\text{A.1-17})$$

where

$$\mathbf{z}' = \begin{bmatrix} z & \cdot & \cdot \\ \cdot & z & \cdot \\ \cdot & \cdot & \frac{h^2 - z^2}{2} \end{bmatrix}, \quad \bar{\partial} = \begin{bmatrix} \frac{\partial}{\partial x} & \cdot & \cdot & \frac{\partial}{\partial y} & -1 & \cdot \\ \cdot & \frac{\partial}{\partial y} & \cdot & \frac{\partial}{\partial x} & \cdot & -1 \\ \cdot & \cdot & -1 & \cdot & \frac{\partial}{\partial x} & \frac{\partial}{\partial y} \end{bmatrix}$$

Then, by substituting Eq. A.1-17 into Eq. 4.1-3, the penalty-equilibrium matrix in this approach becomes

$$\begin{aligned} \mathbf{H}_p &= \int_V (\partial \mathbf{P})^T (\partial \mathbf{P}) dV \\ &= \int_A (\bar{\partial} \mathbf{P})^T \mathbf{z}'^T \mathbf{z}' (\bar{\partial} \mathbf{P}) dV \\ &= \int_A (\bar{\partial} \mathbf{P})^T \left(\int_{-h}^h \mathbf{z}'^T \mathbf{z}' dz \right) (\bar{\partial} \mathbf{P}) dA \\ &= \int_A (\bar{\partial} \mathbf{P})^T \begin{bmatrix} \frac{2}{3} h^3 & \cdot & \cdot \\ \cdot & \frac{2}{3} h^3 & \cdot \\ \cdot & \cdot & \frac{4}{15} h^5 \end{bmatrix} (\bar{\partial} \mathbf{P}) dA \end{aligned} \quad (\text{A.1-18})$$

Also, from Eq. 2.3-13,

$$\mathbf{R} = \int_V (\partial \mathbf{P})^T \mathbf{N}_\lambda dV,$$

now becomes

$$\begin{aligned} \mathbf{R} &= \int_V (\bar{\partial} \mathbf{P})^T \mathbf{z}'^T \mathbf{N}_\lambda dV \\ &= \int_A (\bar{\partial} \mathbf{P})^T \left(\int_{-h}^h \mathbf{z}'^T dz \right) \mathbf{N}_\lambda dA \\ &= \int_A (\bar{\partial} \mathbf{P})^T \begin{bmatrix} \cdot & \cdot & \cdot \\ \cdot & \cdot & \cdot \\ \cdot & \cdot & \frac{2}{3} h^3 \end{bmatrix} \mathbf{N}_\lambda dA \end{aligned} \quad (\text{A.1-19})$$

A.2 Moment-Curvature Approach

Convention:

$$\mathbf{u} = \begin{Bmatrix} \theta_x \\ \theta_y \\ w \end{Bmatrix}, \quad \mathbf{\kappa} = \begin{Bmatrix} \theta_{x,x} \\ \theta_{y,y} \\ \theta_{x,y} + \theta_{y,x} \\ \theta_x - w_{,x} \\ \theta_y - w_{,y} \end{Bmatrix}, \quad \mathbf{M} = \begin{Bmatrix} M_x \\ M_y \\ M_{xy} \\ Q_x \\ Q_y \end{Bmatrix}$$

The assumed moments are

$$\mathbf{M} = \mathbf{P}\boldsymbol{\beta} \quad (\text{A.2-1})$$

The displacement fields, the interpolation functions and the coordinate transformation are the same as in Eqs. A.1-3, A.1-4 and A.1-5, respectively.

The strain-displacement relations are

$$\begin{aligned} \boldsymbol{\varepsilon} &= \mathbf{D}\mathbf{u} \\ &= \mathbf{D}\mathbf{N}\mathbf{q} \\ &= \mathbf{B}\mathbf{q} \end{aligned} \quad (\text{A.2-2})$$

or
where

$$\mathbf{D} = \begin{bmatrix} \frac{\partial}{\partial x} & \cdot & \cdot \\ \cdot & \frac{\partial}{\partial y} & \cdot \\ \frac{\partial}{\partial y} & \frac{\partial}{\partial x} & \cdot \\ 1 & \cdot & -\frac{\partial}{\partial x} \\ \cdot & 1 & -\frac{\partial}{\partial y} \end{bmatrix} \quad (\text{A.2-3})$$

And the strain-stress relations in this approach are

$$\mathbf{S} = \begin{bmatrix} \frac{12}{Et^3} \begin{bmatrix} 1 & -\nu & \cdot \\ -\nu & 1 & \cdot \\ \cdot & \cdot & (1-\nu)/2 \end{bmatrix} & \mathbf{0} \\ \mathbf{0} & \frac{1.2}{Gt} \begin{bmatrix} 1 & \cdot \\ \cdot & 1 \end{bmatrix} \end{bmatrix} \quad (\text{A.2-4})$$

$$\text{where } G = \frac{E}{2(1+\nu)}$$

From Eqs. A.1-2, A.1-7 and A.1-13, we can obtain the matrices shown in Eq. 2.3-13 as

$$\mathbf{H} = \int_{-1}^1 \int_{-1}^1 \mathbf{P}^T \mathbf{S} \mathbf{P} |\mathbf{J}| d\xi d\eta$$

$$\mathbf{G} = \int_{-1}^1 \int_{-1}^1 \mathbf{P}^T \mathbf{B} |\mathbf{J}| d\xi d\eta$$
(A.2-5)

Note that integration of the above equation is performed over area only.

Then, the element stiffness matrix is

$$\mathbf{k} = \mathbf{G}^T \mathbf{H}^{-1} \mathbf{G}$$
(A.2-6)



สถาบันวิทยบริการ
จุฬาลงกรณ์มหาวิทยาลัย

Appendix B

HybridFE Program

In order to obtain the hybrid finite element results, the program **HybridFE**, which is a hybrid finite element computer program for plate bending, was developed. The program can manipulate any assumed stress matrix. The stress matrix can be input from scratch, imported from a file or imported from a sub-module named **StressClassification**.

The HybridFE program is written such that various element types, element interpolation functions and analysis options can be easily changed. Not only hybrid elements but also conventional elements with assumed displacements can be handled. At this time, five element types, namely, PS, PLATE, PLATE_ALT, PLATE_ACM and PLATE_BFS are provided. PS-type denotes the element used in plane stress problem. PLATE and PLATE_ALT are plate bending elements. The distinction is that PLATE-type is the element formulated in terms of moments and curvatures whereas PLATE_ALT is formulated in terms of stresses and strains. The PLATE_ACM and PLATE_BFS are conventional displacement-based plate elements. The interpolation functions used are those for the four-node quadrilateral element, denoted as Q4, and the eight-node quadrilateral element, denoted as Q8.

In addition to the ordinary hybrid element analysis, the additional displacements and the penalty-equilibrium techniques are optional.

HybridFE incorporates the **OFELI** library in the program code. Some extensions to this library have been made in order to embrace the hybrid version. OFELI is an object-oriented library of C++ class for development of finite element codes. It is not intended as a finite element code itself but as a toolkit of utility functions. For more information on the OFELI, visit the internet website at

<http://www.lma.univ-bpclermont.fr/~touzani/ofeli.html>

B.1 Input File Format

This study utilizes the mesh data file (called MDF file) proposed in OFELI as an input file for HybridFE. An example of a quadrant of a simply supported square plate with 2 x 2 elements is shown below.

```
#MESH!
# A quadrant of Square Plate : 2 x 2 elemetns
Dim 2
Node 1 .000 .000 3 0 0 1
Node 2 5.000 .000 3 0 0 1
Node 3 10.000 .000 3 1 0 1
Node 4 .000 5.000 3 0 0 1
Node 5 5.000 5.000 3 0 0 0
Node 6 10.000 5.000 3 1 0 0
Node 7 .000 10.000 3 0 1 1
Node 8 5.000 10.000 3 0 1 0
Node 9 10.000 10.000 3 1 1 0
Element quad 1 4 1 1 2 5 4
Element quad 2 4 1 2 3 6 5
Element quad 3 4 1 4 5 8 7
Element quad 4 4 1 5 6 9 8
EOF
```

The following explanations of this file format are extracted from the document attached with the library :

The main principle governing the structure of this file is that any information in the file is contained in a line and is defined by a keyword following the rules :

- Any line beginning with a # sign is interpreted as a comment line.
- The first line begins necessarily (at first column) with the string #MESH!
- Keyword Dim starts a line that gives the space dimension. An integer number (between 1 and 3) must follow this keyword.
- Each node must be introduced by a line starting with the keyword Node. This keyword must be followed by the following data :

Variable	Definition	Type
label	Label of node	<i>integer</i>
x[1]	First coordinate of node	<i>real</i>
...
x[dim]	dim-th coordinate of node	<i>real</i>
nb_dof	Code associated to first d.o.f.	<i>integer</i>
code[1]	Code associated to first d.o.f.	<i>integer</i>
...
code[nb_dof]	Code associated to nb_dof-th d.o.f.	<i>integer</i>

- Each element must be introduced by a line starting with the keyword Element. This keyword must be followed by the following data :

Variable	Definition	Type
shape	string defining the element shape	<i>integer</i>
label	Label of element	<i>integer</i>
code	Code associated to element	<i>integer</i>
node[1]	Label of first node of element	<i>integer</i>
...
node[nb_node]	Label of nb_node-th node of element	<i>integer</i>
code[nb_dof]	Code associated to nb_dof-th d.o.f.	<i>integer</i>

- The last line of the MDF file must contain the keyword EOF (as End Of File).

B.2 Element Stiffness Matrix Subroutine

Following is a general procedure to obtain an element stiffness matrix coded in C++ computer language.

```
void CHybridPlateQ4::Stiffness(int Opt)
{
    double c;
    int i, j, k;
    int nPMDim;
    LocalMatrixEx<double> *pP, *pH, *pG, *pB;
    LocalMatrixEx<double> *pdP, *pHp, *pM, *pR;

    pdP = pHp = pM = pR = NULL;

    pP = new LocalMatrixEx<double>(nb_stress_, nb_beta_);
    pH = new LocalMatrixEx<double>(nb_beta_ , nb_beta_);
    pG = new LocalMatrixEx<double>(nb_beta_ , nb_dof_);
    pB = new LocalMatrixEx<double>(nb_stress_, nb_dof_);

    //Loop over each Gauss Points
    for (i=1; i<=gauss_.Order(); i++)
        for (j=1; j<=gauss_.Order(); j++) {
            Point<double> g(gauss_.GP(i),gauss_.GP(j));
            quad_->Local(g);
        }
}
```

```

Point<double> lp = quad_->LocalPoint();

//Transform Coordinates system
if (ePsymb.m_CoordType == XY)
    ePsymb.SetXYValue(lp.x,lp.y);
else
    ePsymb.SetXYValue(g.x,g.y);

eP = ePsymb;

//Evaluate matrix B
for (int k=1; k<=nb_nodes_; k++) {
    eB(1, 3*k-2 ) = quad_->DSh(k).x;
    eB(2, 3*k-1 ) = quad_->DSh(k).y;
    eB(3, 3*k-2 ) = quad_->DSh(k).y;
    eB(3, 3*k-1 ) = quad_->DSh(k).x;
    eB(4, 3*k-2 ) = quad_->Sh(k);
    eB(4, 3*k   ) = -quad_->DSh(k).x;
    eB(5, 3*k-1 ) = quad_->Sh(k);
    eB(5, 3*k   ) = -quad_->DSh(k).y;
}
c = gauss_.W(i)*gauss_.W(j) * quad_->Det();
//Evaluate matrix H
eH += eP.Trn()*eS*eP*c;

//Evaluate matrix G
eG += eP.Trn()*eB*c;
}
nPMDim = nb_dof_+nb_beta_;

if (Opt)
    pdP = new LocalMatrixEx<double>(3, nb_beta_);

if (Opt & HB_LAGRANGEMULT) {
//Evaluate matrix M beware of ambiguity with variable of base class
//FEEqua<> and then evaluate also matrix R

pM = new LocalMatrixEx<double>(3, nb_lambda_);
pR = new LocalMatrixEx<double>(nb_beta_, nb_lambda_);

//Loop over each Gauss Points
for (i=1; i<=gauss_.Order(); i++)
    for (j=1; j<=gauss_.Order(); j++) {
        Point<double> g(gauss_.GP(i),gauss_.GP(j));
        quad_->Local(g);
        Point<double> lp = quad_->LocalPoint();

//Transform Coordinates system
if (ePsymb.m_CoordType == XY) {
    ePsymb.SetXYValue(lp.x,lp.y);
//Differentiate matrix P in XY Coordinates system
for (k=1; k<=nb_beta_; k++) {
        edP(1,k) = ePsymb(1,k).dX()+ePsymb(3,k).dY()-ePsymb(4,k);
        edP(2,k) = ePsymb(2,k).dY()+ePsymb(3,k).dX()-ePsymb(5,k);
        edP(3,k) = ePsymb(4,k).dX()+ePsymb(5,k).dY();
    }
}
else {
    ePsymb.SetXYValue(g.x,g.y);
//Differentiate matrix P in RS Coordinates system
double dP1dr, dP1ds, dP2dr, dP2ds;
double dP3dr, dP3ds, dP4dr, dP4ds, dP5dr, dP5ds;
double dP1dx, dP2dy, dP3dx, dP3dy, dP4dx, dP5dy;
for (k=1; k<=nb_beta_; k++) {
        dP1dr = ePsymb(1,k).dX(); dP1ds = ePsymb(1,k).dY();
        dP2dr = ePsymb(2,k).dX(); dP2ds = ePsymb(2,k).dY();
        dP3dr = ePsymb(3,k).dX(); dP3ds = ePsymb(3,k).dY();
        dP4dr = ePsymb(4,k).dX(); dP4ds = ePsymb(4,k).dY();
        dP5dr = ePsymb(5,k).dX(); dP5ds = ePsymb(5,k).dY();
        c = 1./quad_->Det();

        dP1dx = c*( quad_->j[1][1]*dP1dr-quad_->j[0][1]*dP1ds);
        dP2dy = c*(-quad_->j[1][0]*dP2dr+quad_->j[0][0]*dP2ds);
        dP3dx = c*( quad_->j[1][1]*dP3dr-quad_->j[0][1]*dP3ds);
        dP3dy = c*(-quad_->j[1][0]*dP3dr+quad_->j[0][0]*dP3ds);
        dP4dx = c*( quad_->j[1][1]*dP4dr-quad_->j[0][1]*dP4ds);
        dP5dy = c*(-quad_->j[1][0]*dP5dr+quad_->j[0][0]*dP5ds);

```

```

        edP(1,k) = dP1dx + dP3dy - ePsymb(4,k);
        edP(2,k) = dP2dy + dP3dx - ePsymb(5,k);
        edP(3,k) = dP4dx + dP5dy;
    }
}
if (eMsymb.m_CoordType == XY)
    eMsymb.SetXYValue(lp.x,lp.y);
else
    eMsymb.SetXYValue(g.x,g.y);

eM = eMsymb;//eP = ePsymb;

c = gauss_.W(i)*gauss_.W(j) * quad_>Det();
//Evaluate matrix R
eR += edP.Trn()*eM*c;
}
nPMDim += nb_lambda_;
}
else
    nb_lambda_ = 0;

if (Opt & HB_PENALTYMTX) {
//Evaluate matrix Hp beware of ambiguity with var. of base class FEEqua<>
pHp = new LocalMatrixEx<double>(nb_beta_, nb_beta_);

//Loop over each Gauss Points
for (i=1; i<=gauss_.Order(); i++)
    for (j=1; j<=gauss_.Order(); j++) {
        Point<double> g(gauss_.GP(i),gauss_.GP(j));
        quad_>Local(g);
        Point<double> lp = quad_>LocalPoint();

//Transform Coordinates system
if (ePsymb.m_CoordType == XY) {
    ePsymb.SetXYValue(lp.x,lp.y);
//Differentiate matrix P in XY Coordinates system
for (k=1; k<=nb_beta_; k++) {
        edP(1,k) = ePsymb(1,k).dX()+ePsymb(3,k).dY()-ePsymb(4,k);
        edP(2,k) = ePsymb(2,k).dY()+ePsymb(3,k).dX()-ePsymb(5,k);
        edP(3,k) = ePsymb(4,k).dX()+ePsymb(5,k).dY();
    }
}
else {
    ePsymb.SetXYValue(g.x,g.y);
//Differentiate matrix P in RS Coordinates system
double dP1dr, dP1ds, dP2dr, dP2ds, dP3dr, dP3ds;
double dP4dr, dP4ds, dP5dr, dP5ds;
double dP1dx, dP2dy, dP3dx, dP3dy, dP4dx, dP5dy;
for (k=1; k<=nb_beta_; k++) {
        dP1dr = ePsymb(1,k).dX(); dP1ds = ePsymb(1,k).dY();
        dP2dr = ePsymb(2,k).dX(); dP2ds = ePsymb(2,k).dY();
        dP3dr = ePsymb(3,k).dX(); dP3ds = ePsymb(3,k).dY();
        dP4dr = ePsymb(4,k).dX(); dP4ds = ePsymb(4,k).dY();
        dP5dr = ePsymb(5,k).dX(); dP5ds = ePsymb(5,k).dY();
        c = 1./quad_>Det();

        dP1dx = c*( quad_>j[1][1]*dP1dr-quad_>j[0][1]*dP1ds);
        dP2dy = c*(-quad_>j[1][0]*dP2dr+quad_>j[0][0]*dP2ds);
        dP3dx = c*( quad_>j[1][1]*dP3dr-quad_>j[0][1]*dP3ds);
        dP3dy = c*(-quad_>j[1][0]*dP3dr+quad_>j[0][0]*dP3ds);
        dP4dx = c*( quad_>j[1][1]*dP4dr-quad_>j[0][1]*dP4ds);
        dP5dy = c*(-quad_>j[1][0]*dP5dr+quad_>j[0][0]*dP5ds);

        edP(1,k) = dP1dx + dP3dy - ePsymb(4,k);
        edP(2,k) = dP2dy + dP3dx - ePsymb(5,k);
        edP(3,k) = dP4dx + dP5dy;
    }
}

c = gauss_.W(i)*gauss_.W(j) * quad_>Det();

//Evaluate matrix Hp : Penalty Equilibrium Matrix
eHp += edP.Trn()*edP*c;
}
eHp *= (penalty_const_/E_);
eH += eHp;

```

```

}

if (pP) { delete pP; pP = NULL; }
if (pB) { delete pB; pB = NULL; }
if (pHp) { delete pHp; pHp = NULL; }
if (pM) { delete pM; pM = NULL; }
if (pdP) { delete pdP; pdP = NULL; }

//Partitioned Matrix which to be eliminated to obtain matrix K
LocalMatrixEx<double> PM(nPMDim, nPMDim);

PM.Copy(eG      ,1,1, nb_dof_+nb_lambda_+1, 1);
PM.Copy(eG.Trn(),1,1, 1, nb_dof_+nb_lambda_+1);

if (Opt & HB_LAGRANGEMULT) {
    eR *= -1.0;
    PM.Copy(eR      ,1,1, nb_dof_+nb_lambda_+1, nb_dof_+1);
    PM.Copy(eR.Trn(),1,1, nb_dof_+1, nb_dof_+nb_lambda_+1);
}

eH *= -1.0;
PM.Copy(eH      ,1,1, nb_dof_+nb_lambda_+1, nb_dof_+nb_lambda_+1);

if (pH) { delete pH; pH = NULL; }
if (pG) { delete pG; pG = NULL; }
if (pR) { delete pR; pR = NULL; }

PM.GEliminate(-nb_dof_);

// Copy element stiffness to based class variable DMatrix<double> *M
for (i=1; i<=nb_dof_; i++)
    for (j=1; j<=nb_dof_; j++)
        eMat(i,j) = PM(i,j);

// Solve for stress recovery matrix by backward substitution
/* K K 0 0 0
   K K 0 0 0
   A A B 0 0 <---- Paradigm of partitioned matrix PM
   A A B B 0
   A A B B B
*/
//Process backward substitution
for (j=1; j<=nb_dof_; j++) {
    PM(nb_dof_+1,j) /= -PM(nb_dof_+1,nb_dof_+1);
    for (i=2; i<=nb_lambda_+nb_beta_; i++) {
        PM(nb_dof_+i,j) = -PM(nb_dof_+i,j);
        for (k=1; k<=i-1; k++)
            PM(nb_dof_+i,j) -= PM(nb_dof_+i,nb_dof_+k) * PM(nb_dof_+k,j);
        PM(nb_dof_+i,j) /= PM(nb_dof_+i,nb_dof_+i);
    }
}

// *** Store 'SubMtxA' to Recovery Matrix ***
for (j=1; j<=nb_dof_; j++) {
    for (i=1; i<=nb_lambda_; i++)
        eLambdaRCV(i,j) = PM(nb_dof_+i,j); // for additional displacement parameters
    for (i=1; i<=nb_beta_; i++)
        eBetaRCV(i,j) = PM(nb_dof_+nb_lambda_+i,j); // for stress parameters
}
}

```


B.3 Main Fragment of Code in Analysis Task

```

void CHybridFEDoc::Analysis(void)
{
...
    // Global Stiffness matrix
    SkMatrix<double> a(m_Mesh);

    if (m_pDisplacement) delete m_pDisplacement;
    m_pDisplacement = new Vect<double>(m_Mesh.NbDOF());
    ASSERT(m_pDisplacement);
...
    Element *el;
    GenericMaterial MyMaterial;
    MyMaterial.Young(m_dYoung);
    MyMaterial.Poisson(m_dPoisson);

    if (m_pMatrixP) m_pMatrixP->m_CoordType = m_CoordType;
    if (m_pMatrixM) m_pMatrixM->m_CoordType = m_CoordType;

// Loop over elements
// -----
    Info( _T("Looping over elements ... \r\n") );

    for (m_Mesh.TopElement(); (el=m_Mesh.GetElement());) {
        el->Mat(&MyMaterial);
        el->MatName("MyMaterial");
        el->Thickness(m_dThickness);

        switch (m_ElShape) {
        case Q4 : {
            switch(m_ElType) {
            case PS : {
                m_nNbDOFperNode = 2;
                m_nNbForces = 3;
                CHybridPSQ4 eq(el, m_pMatrixP,m_pMatrixM);
                eq.PenaltyConst(m_dPenaltyConst);
                eq.GaussOrder(m_iQOrder);
                eq.Stiffness(m_Options);
                a.Assembly(el,eq.A());
                SaveRCVMatrix(stream,eq.BetaRCV());
                break;
            }
            case PLATE : {
                m_nNbDOFperNode = 3;
                m_nNbForces = 5;
                CHybridPlateQ4 eq(el, m_pMatrixP,m_pMatrixM);
                eq.PenaltyConst(m_dPenaltyConst);
                eq.GaussOrder(m_iQOrder);
                eq.Stiffness(m_Options);
                a.Assembly(el,eq.A());
                SaveRCVMatrix(stream,eq.BetaRCV());
                break;
            }
            case PLATE_ALT : {
                m_nNbDOFperNode = 3;
                m_nNbForces = 6;
                CHybridPlateQ4Alt eq(el, m_pMatrixP,m_pMatrixM);
                eq.PenaltyConst(m_dPenaltyConst);
                eq.GaussOrder(m_iQOrder);
                eq.Stiffness(m_Options);
                a.Assembly(el,eq.A());
                SaveRCVMatrix(stream,eq.BetaRCV());
                break;
            }
            case PLATE_ACM : {
                m_nNbDOFperNode = 3;
                m_nNbForces = 3;
                CPlateACM eq(el);
                eq.GaussOrder(m_iQOrder);
                eq.Stiffness();
                a.Assembly(el,eq.A());
                break;
            }
        }
    }
}

```

```

        case PLATE_BFS : {
            m_nNbDOFperNode = 4;
            m_nNbForces = 3;
            CPlateBFS eq(el);
            eq.GaussOrder(m_iQOrder);
            eq.Stiffness();
            a.Assembly(el,eq.A());
            break;
        }
    }
    break;
}
case Q8 : {
    switch(m_ElType) {
        case PS : {
            m_nNbDOFperNode = 2;
            m_nNbForces = 3;
            CHybridPSQ8 eq(el, m_pMatrixP,m_pMatrixM);
            eq.PenaltyConst(m_dPenaltyConst);
            eq.GaussOrder(m_iQOrder);
            eq.Stiffness(m_Options);
            a.Assembly(el,eq.A());
            SaveRCVMatrix(stream,eq.BetaRCV());
            break;
        }
        case PLATE : {
            m_nNbDOFperNode = 3;
            m_nNbForces = 5;
            CHybridPlateQ8 eq(el, m_pMatrixP,m_pMatrixM);
            eq.PenaltyConst(m_dPenaltyConst);
            eq.GaussOrder(m_iQOrder);
            eq.Stiffness(m_Options);
            a.Assembly(el,eq.A());
            SaveRCVMatrix(stream,eq.BetaRCV());
            break;
        }
        case PLATE_ALT : {
            m_nNbDOFperNode = 3;
            m_nNbForces = 6;
            CHybridPlateQ8Alt eq(el, m_pMatrixP,m_pMatrixM);
            eq.PenaltyConst(m_dPenaltyConst);
            eq.GaussOrder(m_iQOrder);
            eq.Stiffness(m_Options);
            a.Assembly(el,eq.A());
            SaveRCVMatrix(stream,eq.BetaRCV());
            break;
        }
    }
    break;
}
} //End switch (m_ElShape)
} //End Loop over elements

//Assemble External Applied Loads
AssemblyLoad();

Info( _T("Imposing boundary conditions ...\r\n") );
a.Constraint(m_Mesh /*,RHS,bc*/);

int ret = a.Factor();
if ( ret ) {
    CString strErr;
    strErr.Format(_T("Error in matrix factorization : %d-th pivot\r\n is too small =
%f"),ret,a(ret,ret));
    AfxMessageBox(strErr);
    return;
}
Info( _T("Solving ... ") );
a.Solve(RHS);
Info( _T("done\r\n") );
// Recovery for stresses
BetaRecovery(stream);
...
//////////
// Output Results //
//////////
}

```

Biography

Supatana Hengyotmark was born on July 16, 1977 in Burirum, Thailand. He graduated from Trium Udom Suxsa Secondary School in 1994. He was enrolled in Chulalongkorn University, Faculty of Engineering, where he obtained his B.Eng. degree in Civil Engineering in 1998. He continued his study toward the M.Eng. degree in Civil Engineering (Structures) at the same university and graduated in 2001.



สถาบันวิทยบริการ
จุฬาลงกรณ์มหาวิทยาลัย